

EFFECT OF THE FLEXURAL AND THE HORIZONTAL
SHEAR REINFORCEMENTS UPON THE STRENGTH
OF DEEP REINFORCED CONCRETE BEAM

A Thesis

by

MOHAMMAD ABDUR RASHID



Submitted to the Department of Civil Engineering of Bangladesh
University of Engineering and Technology, Dhaka in partial
fulfillment of the requirements for the degree

of

MASTER OF SCIENCE IN CIVIL ENGINEERING



March, 1993

624483
1993
MOH

EFFECT OF THE FLEXURAL AND THE HORIZONTAL
SHEAR REINFORCEMENTS UPON THE STRENGTH
OF DEEP REINFORCED CONCRETE BEAMS

A Thesis

by

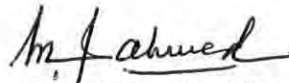
MOHAMMAD ABDUR RASHID

Approved as to style and content by :



Chairman of
the committee

Dr. Ahsanul Kabir
Associate Professor
Department of Civil Engineering
BUET.



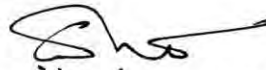
Member

Dr. M. Feroze Ahmed
Professor and Head
Department of Civil Engineering
BUET.



Member

Dr. Md. Alee Murtuza
Professor
Department of Civil Engineering
BUET.



Member
(External)

Mr. A. S. M. Abdul Hamid
Senior Structural Engineer
Development Design Consultants Ltd.
New Eskaton Road, Dhaka.

ACKNOWLEDGMENT

This research was carried out under the supervision of Dr. Ahsanul Kabir, Associate Professor, Department of Civil Engineering, BUET, Dhaka. The author expressed his heartfelt gratitude and profound indebtedness to Dr. Kabir for his valuable suggestions, encouragement and constant supervision at all stages of this research.

The author wishes to thank Dr. Alamgir Mujibul Hoque, Professor of Civil Engineering, BUET, and Dr. M. Feroze Ahmed, Professor and Head of the Department of Civil Engineering, BUET, for their kind co-operation at different stages of this research.

Sincere appreciation is expressed to acknowledge the valuable service rendered by Messrs. Malek, Hamid, Bhuiyan, Barkat, Barek, Zulhash, Karim, Rozario, Rabbani and other members of different laboratories and workshops of BUET, Dhaka.

The author is also grateful to his family members and his colleagues for their considerate attitude and profuse inspiration without which this study could have never been materialized.

ABSTRACT

A total of fourteen brick aggregate reinforced concrete deep beams have been tested in this study in order to investigate the effect of the flexural and the horizontal shear reinforcements on the strength of such beams. The test beams were single span and simply supported type. The beams were divided into two series according to their span to depth ratio ($L/D = 1$ and 2). The first beam of each series was designed and detailed as per the recommendations of ACI Building Code (ACI 318-89). In the other six beams of each series, the amount of either the flexural or the horizontal web reinforcement or both were increased in relation to those of first beam of the corresponding series.

The nominal cross section of the first series of test beams was 6"x21" and that of the second series was 6"x12". The effective span lengths for two different series of beams were 21" and 24" respectively.

The test beams were subjected to uniformly distributed loads. The effects of the variations of different horizontal reinforcements (flexural and web reinforcements) and span to depth ratio on the cracking load, ultimate load, crack pattern, and the mode of failure were investigated.

It was observed in the study that the amount of both the flexural and the horizontal web reinforcements influenced to some extent the diagonal cracking load and the ultimate load capacity of test beams. It was also found that the change in the amount of either the flexural or the horizontal web reinforcement alone could not bring about a significant change in the load carrying capacity of test beams.

Certain modifications are suggested in five of the several available formulas (e.g. ACI 318-89 ; Singh, Ray and Reddy ; Ramakrishnan and Ananthanarayana ; Selvam and Kuruvilla ; and Mau and Hsu) in order to compute the ultimate load of deep reinforced brick aggregate concrete beams. It was shown that all of the five formulas with the suggested changes can be used efficiently to estimate the ultimate load capacity of deep beams.

CONTENTS

	Page
ACKNOWLEDGEMENT	ii
ABSTRACT	iii
LIST OF TABLES	x
LIST OF FIGURES	xii
NOTATIONS	xiv
CHAPTER 1 : INTRODUCTION	
1.1 General	1
1.2 Need for Study	1
1.3 Objective of the Study	3
1.4 Scope and Limitations of the Study	4
CHAPTER 2 : REVIEW OF LITERATURE	
2.1 General	5
2.2 Deep Beams with Brick Aggregate Concrete	5
2.2.1 Brief Descriptions of Tests	5
2.2.2 Findings of the Studies	6
2.2.2a Cracking Strength of Deep Beams	6
2.2.2b Ultimate Strength of Deep Beams	7
2.2.2c Moment Characteristics of Beams	7
2.2.2d Deflection of Beams	8
2.2.2e Stresses in Reinforcements	8
2.2.2f Cracking Pattern and Mode of Failure	8

2.3 Strength and Behavior of Stone Aggregate R C Deep Beam	8
2.3.1 Study of de Paiva and Siess	9
2.3.2 Study of Fritz Leonhardt	10
2.3.3 Study of Ramakrishnan and Ananthanarayana	10
2.3.4 Study of Kong, Robins, and Cole	11
2.3.5 Study of Manuel, Slight, and Suter	11
2.3.6 Study of Singh, Ray, and Reddy	12
2.3.7 Study of Smith and Vantsiotis	13
2.3.8 Study of Barry and Ainso	14
2.3.9 Study of Rogowsky, MacGregor, and Ong	15
2.3.10 Study of Selvam and Kuruvilla	15
2.3.11 Study of Mau and Hsu	16

CHAPTER 3 : AVAILABLE THEORIES AND DESIGN METHODS

3.1 General	17
3.2 Stress Pattern in Deep Beams	17
3.3 Distribution of Stresses in Deep Beams (Other Approaches)	20
3.3.1 Heino Ainso and J.E. Berry's Approach	20
3.3.2 Krishna Raju Approach	20
3.3.3 Coker and Filon Approach	20
3.3.4 Leonhardt Approach	25
3.4 Ultimate Strength and Behavior of Deep Beams	25
3.4.1 Ultimate Strength of Deep Beams, ACI Bldg. Code Approach	27
3.4.2 Ramakrishnan and Ananthanarayana Approach	31

	Page
3.4.3 Singh, Ray, and Reddy Approach	31
3.4.4 Kong, Robins, and Cole Approach	33
3.4.5 de Paiva and Siess Approach	33
3.4.6 Selvam and Kuruvilla Approach	34
3.4.7 Mau and Hsu Approach	35
3.5 Mechanism of Shear Resistance in RC Deep Beams	36
3.5.1 Role of Shear Reinforcements	37
3.5.2 Role of Main Flexural Reinforcements	37
3.6 Mode of Shear Failure	39
3.6.1 Beam Action Failure	39
3.6.2 Shear Compression Failure	39
3.6.3 Diagonal Tension or Diagonal Compression Failure	40
 CHAPTER 4 : EXPERIMENTAL INVESTIGATIONS	
4.1 General	41
4.2 Properties of the Constituents of Reinforced Concrete	41
4.2.1 Cement	42
4.2.2 Fine Aggregate	42
4.2.3 Coarse Aggregate	42
4.2.4 Reinforcements	43
4.3 Design of Concrete Mix	44
4.4 Preparation of Test Beams	47
4.4.1 Preparation of Moulds	47
4.4.2 Prelude to the Test Beams	47

4.4.3 Fabrication of the Test Beams	49
4.5 Testing Operations	57
4.5.1 Testing of Beams	57
4.5.2 Testing of Control Cylinders	61
CHAPTER 5 : TEST RESULTS	
5.1 General	62
5.2 Summary of the Test Results	62
5.3 Load Deflection Records	63
5.4 Stresses in Reinforcements	66
5.5 General Crack Pattern	66
CHAPTER 6 : ANALYSIS AND DISCUSSIONS OF TEST RESULTS	
6.1 General	85
6.2 Strains in Reinforcements	85
6.3 Shear Characteristics of Test Beams	86
6.3.1 The Cracking Load and the Shear Capacity of Test Beams	88
6.3.2 Nominal Shear Stress at Failure	95
6.4 Ultimate Load Capacity of Test Beams	100
6.4.1 Variation of Ultimate Load Capacity with the Horizontal Reinforcements	100
6.4.2 Estimate of Ultimate Load Capacity using Different Methods	103
6.4.3 Suggested Modifications of Different Methods for Determination of Ultimate Load Capacity	108
6.5 Moment Characteristics of Test Beams	113
6.6 Load Deflection Characteristics of Test Beams	115

6.7 Crack Pattern and Mode of Failure	118
6.7.1 Cracking Pattern	118
6.7.2 Mode of Failure	120
CHAPTER 7 : CONCLUSIONS AND RECOMMENDATIONS FOR FUTURE STUDY	
7.1 Conclusions	121
7.2 Recommendations for Future Study	123
LIST OF REFERENCES	125
APPENDIX-A : Design of Test Beam DB-P1	128
APPENDIX-B : Sample Calculations for Ultimate Load Capacity of Test Beam DB-P1 by Various Methods	132
APPENDIX-C : Derivation of Formula for Deflection	139
APPENDIX-D : Observed Strain Values in Reinforcements	143

LIST OF TABLES

Table		Page
4.1	Grading of Fine Aggregate	43
4.2	Grading of Coarse Aggregate	44
4.3	Physical Properties of Reinforcements used in Test Beams	46
4.4	Contents of Concrete-mix Batch	46
5.1	Properties of Test Beams	64
5.2	Observed Cracking and Ultimate Loads of Test Beams	65
5.3	Observed Maximum Deflections (at mid-span) of Test Beams	67
6.1	Checking for the Arch-action Mechanism in Test Beams	87
6.2	Observed Cracking and Ultimate Loads for different Percentage of Flexural and Horizontal Shear Reinforcements	89
6.3	Diagonal Cracking Shear Stress Properties of Test Beams	90
6.4	Observed Diagonal Cracking Stress Variation	94
6.5	Comparison of Measured and Suggested Estimate of Diagonal Cracking Stress	96

6.6	Nominal Ultimate Shear Stress Properties of Test Beams	97
6.7	Comparison of Measured and Suggested Estimate of the Ultimate Shear Stress	99
6.8	Variation of Ultimate Load Capacity with the Variation of Horizontal Reinforcements	101
6.9a	Ultimate Load Capacity of Test Beams Computed by Various Methods	104
6.9b	Ultimate Load Capacity of Test Beams Computed by Various Methods	105
6.10	Ultimate Load Capacity of Test Beams Computed by Mau and Hsu Method	106
6.11	Comparison of Observed Ultimate Loads and Computed Ultimate Loads by Various Methods	107
6.12	Comparison of Observed Ultimate Loads with Ultimate Loads Computed by Various Methods after Suggested Modifications	114
6.13	Moment Characteristics of Test Beams	116
6.14	Cracking Load Characteristics of Test Beams	119
C.1	Computed Maximum Deflections (at mid-span) of Test Beams at Different Load Levels	142
D.1-D.14	Observed Strain Values in Reinforcements of Test Beams at Different Load Levels	143-156

LIST OF FIGURES

Figure		Page
3.1	Distribution of Flexural Stresses in Homogeneous Simply Supported Beam	19
3.2-3.6	Stresses in Deep Beam according to Heino Ainso and J.E. Barry	21-23
3.7	Flexural Stresses in Deep Beam according to K. Raju	24
3.8	Principal Stress Trajectories of the Uncracked State of Deep Beam under Concentrated Load	24
3.9-3.11	Deep Beam Properties according to Leonhardt	26
3.12-3.15	Deep Beam Properties according to ACI 318-89 Code Provision	30
3.16	Diagonal Tension Cracks in Shallow and Deep Beams	38
3.17	Shear Transfer by Tied-Arch Mechanism	38
4.1	Stress-Strain Diagram of 7/8" dia Steel Bar	45
4.2	Flexural Steel Assembly with Anchor Plates	48
4.3-4.18	Reinforcement Arrangement of Test Beams	50-56

4.19-4.22	Test Set-up for Loading	59-60
5.1-5.2	Load vs. Deflection Diagram of Beams of DB-P Series	68-69
5.3-5.4	Load vs. Deflection Diagram of Beams of DB-Q Series	70-71
5.5-5.18	Cracking Pattern of Test Beams	72-77
5.19-5.32	Mode of Failure and Crack Pattern of Test Beams	78-84
6.1	Shear Force Diagram (near support) for the Test Beam of DB-P Series	110
6.2	Shear Force Diagram (near support) for the Test Beam of DB-Q Series	110
A.1	Test Beam DB-P1 under Uniform Loading	130
C.1	An Uniformly Distributed Loaded Beam	139

NOTATIONS

A_s	= Cross sectional area of flexural steel
A_v	= Cross sectional area of individual vertical web steel
A_{vh}	= Cross sectional area of individual horizontal web steel
A_w	= Cross sectional area of individual inclined web steel
a, x	= Clear shear span (unless otherwise specified)
a'	= Equivalent rectangular stress block
α	= Inclination of the web steel with the horizontal (unless otherwise specified)
b	= Width of beam
β	= Angle of inclination of potential diagonal crack with the horizontal (unless otherwise stated)
c	= Cohesion of concrete
C	= Co-efficient of variation in percent
D	= Overall depth of beam
d	= Effective depth of beam
E	= Modulus of elasticity of steel
E_c	= Modulus of elasticity of concrete
σ_x	= Normal stress in the direction of length of beam
σ_y	= Stress in the direction perpendicular to the length of the beam
f'_c	= Compressive strength of standard cylinder specimen
f'_{sp}	= Split cylinder strength of concrete
f_t	= Tensile stress in concrete
f_y	= Yield stress of flexural steel
f_{hy}	= Yield stress of horizontal web steel
f_{vy}	= Yield stress of vertical web steel
G	= Shear modulus of concrete
I	= Moment of inertia of concrete section
K	= Splitting coefficient
L	= Effective span of beam
M_{cr}	= Moment developed at the critical section of the beam at the initiation of diagonal crack

- M_u = Maximum moment developed in the beam at failure
 M_{uf} = Flexural capacity of the beam
 n = Modular ratio = E_s/E_c
 p_f = Flexural steel ratio
 p_h = Horizontal web steel ratio
 p_v = Vertical web steel ratio
 P_a = Measured load at the initiation of arch-action
 P_{cr} = Measured load corresponding to diagonal cracking
 P_f = Measured load corresponding to flexural cracking
 P_u = Measured ultimate load of beam
 Q_u = Resisting shear force after Singh, Ray, and Reddy
 s = Spacing of the vertical web steel
 s_2 = Spacing of horizontal web steel
 V_c = Contribution of concrete on ultimate shear
 V_{cr} = Nominal shear force at the critical section at the initial diagonal cracking
 v_{cr} = Critical shear stress at the initial diagonal cracking
 V_u = Ultimate shear force at the section of M_u
 v_u = Ultimate shear stress
 ϕ_h, θ_h = Multiplying factor for contribution of total (flexural plus web) horizontal steel on ultimate load
 ϕ_v, θ_v = Multiplying factor for contribution of vertical web steel on ultimate load
 τ_1, μ_s, μ_v = Empirical constants
 w = Applied load per unit length upon the beam
 δ = Total deflection at mid-span of beam
 δ_m = Deflection of beam at mid-span due to bending only

CHAPTER 1

INTRODUCTION

1.1 GENERAL

Some concrete members have depth much greater than normal in relation to their span, while the thickness in the perpendicular direction is much smaller than either span or depth. The main loads and reactions act in the plane of the member, and a state of plane stress in the concrete is approximated. Members of this type are called deep beams. They can be defined as beams having a ratio of span to depth of about 5 or less, or having a shear span less than about twice the depth and which are loaded at the top or compression face only⁽¹⁾.

According to CEB⁽²⁾, when span to depth ratio of simply supported beams is less than 2, or less than 2.5 for any span of a continuous beam, it is customary to define these beams as deep beams.

Deep beam structures are encountered in transfer girders, foundation walls, parapet walls, raft beams, walls of rectangular tanks and bins, hoppers, floor diaphragms and shear walls, as well as in folded plate roof structures. The behavior of a deep beam is significantly different from that of a beam of more normal proportions, requiring special consideration in analysis, design and detailing of reinforcements.

1.2 NEED FOR STUDY

Cement concrete is one of the seemingly simple but actually complex material. Many of its complex behaviors are yet to be identified to employ this material advantageously and economically. ASCE-ACI shear committee report⁽³⁾ gave a selective

list of about 200 recent papers on shear which indicates clearly the intensive research effort in this regard during the last two decades. Yet, the progress in the understanding and quantitative assessment of the behavior of members subjected to flexure and shear has been less spectacular. This has been acknowledged by the ACI-ASCE Committee 426⁽⁴⁾ in their concluding remarks as, "It has been emphasized that the design procedures proposed are empirical because the fundamental nature of shear and diagonal tension strength is not yet clearly understood. Further basic research should be encouraged to determine the mechanism which results in shear failures of reinforced concrete members".

There are quite a good number of research papers on the stresses and behaviors of stone aggregate reinforced concrete deep beams. On the other hand, only a limited study has been directed to understand the stresses and nature of such beams when made of brick aggregate concrete. Brick aggregate concrete is widely used in Bangladesh and it is generally felt that studies are needed to understand the behavior of structural members including deep beams made of such concrete both in working and ultimate load level. Attempts should be made to correlate their behavior with those made from stone aggregate concrete.

No accurate theory exists for predicting ultimate shear strength of deep reinforced concrete beams. The greater number of parameters affecting beam strength has led to a limited understanding of shear failure. These parameters include the proportions and shape of the beam, loading and support conditions, amount and arrangement of tensile, compressive and web reinforcements, as well as the concrete and steel properties.

In Bangladesh, only a few series of test have been carried out so far to investigate the important properties of brick aggregate concrete deep beams. All the variables mentioned earlier can not be included in a single test program. Therefore it is

instructive to study systematically the effect of a few variables at a time on the ultimate strength of deep reinforced concrete members made with brick aggregate concrete.

1.3 OBJECTIVE OF THE STUDY

The basic objective of this research was to investigate the strength and behavior of brick aggregate reinforced concrete deep beams by varying the amount of flexural and the horizontal shear reinforcements. The results of this investigation may help in preparing the proper Code provisions for the flexural and the horizontal shear reinforcements in brick aggregate concrete deep beams.

The main objectives of this research work on brick aggregate reinforced concrete deep beams subjected to uniformly distributed load are as follows :

- (a) To investigate the influence of the amount of the longitudinal flexural reinforcement on the shear strength of deep reinforced concrete beam.
- (b) To investigate the influence of the amount of the longitudinal shear reinforcement upon the shear strength of deep beams.
- (c) To investigate the initiation and subsequent propagation pattern of cracks.
- (d) To investigate the nature of failure at ultimate load.
- (e) To study the load-deflection characteristics of deep reinforced concrete beam.

- (f) To correlate the findings of the present study with the behavior of conventional aggregate concrete deep beams and to suggest, if needed, the necessary modifications in the design procedures.

1.4 SCOPE AND LIMITATIONS OF THE STUDY

In this study the amounts of flexural & horizontal shear reinforcements, and the span to depth ratio (L/D) were varied and these are the two among the large number of variables affecting deep beam strength. The maximum span length (24") and maximum depth (21") of test beams were provided considering the dimension of the anvil and the vertical space for loading respectively of the universal testing machine used. To make the test beam simply supported, one of it's end was rested upon roller support while the other end-support (considered as hinge) was a 3" wide, 1" thick steel plate covering the width of beam. This is not an ideal hinge mechanism. But considering practical situations, it is believed that the width of support would provide little resistance to rotation at this end.

The uniform loading was achieved with a four-point loading system where the gap between two point loads was small enough compared to the width of loading plates. The yield strengths of steel used in test beams were different for different bar sizes. This variation was unintentional. The concrete strengths varied between 2510 psi and 2930 psi.

CHAPTER 2

REVIEW OF LITERATURE

2.1 GENERAL

A review of literature reveals that significant attempts have been made to investigate the behavior and strength of deep reinforced concrete beams in shear. Most of these efforts, however, concern deep beams having crushed stones as coarse aggregates and having subjected to concentrated loads. A very few number of studies were performed on deep beams either having brick chips as coarse aggregates or having subjected to uniformly distributed loads during tests.

2.2 DEEP BEAMS WITH BRICK AGGREGATE CONCRETE

Two studies concerning the behaviors of deep beams made of brick aggregate concrete were performed in Bangladesh. All of the beams of these researches were single span and simply supported. The study done by Kabir⁽⁵⁾ was with the beams subjected to mid-span concentrated load and that of Ali⁽⁶⁾ was related to the deep beams under uniformly distributed load. The above mentioned two studies and the findings are described in brief in the following :

2.2.1 Brief Descriptions of Tests

In 1982, Kabir reported the results of investigations on the shear strength of deep reinforced concrete simply supported beams with crushed brick as coarse aggregate. In this study two sets of beams, five in each set were investigated. One set had span to depth ratio (L/D) of 1 and the other had L/D ratio of 2. The applied load was a midpoint concentrated load in all the cases. In each set of beams, only the amount and arrangement of web reinforcements (both vertical and horizontal) were varied.

In 1985, Ali reported the results of investigations on ten brick aggregate reinforced concrete deep beams having span to depth ratios of 1 and 2. The applied load was a uniformly distributed load for all the beams. In all of the beams the flexural reinforcements were kept the same but the amounts of web reinforcements were varied.

2.2.2 Findings of the Studies

From the test results both Kabir⁽⁵⁾ and Ali⁽⁶⁾ made some remarks and then gave some suggestions on some specific properties of deep reinforced brick aggregate concrete beams. But their findings and suggestions were not verified by further study till now. These findings are as follows :

2.2.2a Cracking Strength of Deep Beams

In his study Kabir found that the different web reinforcement arrangements had no appreciable effect on the formation of initial diagonal crack in a deep beam under mid-span concentrated load. The observed diagonal cracks were usually the first cracks in the clear shear span of a deep beam, on some occasions they were simultaneously accompanied by flexural cracks. He also mentioned that the Diaz de Cosio⁽⁷⁾ equation for predicting the nominal shear stress at initial diagonal cracking may be used fairly reliably for deep beams under mid-span concentrated loading.

Ali reported that diagonal cracks develop first in relatively deeper beams ($L/D=1$) and flexural cracks develop first in the shallower deep beams ($L/D=2$) subjected to uniformly distributed load. He also commented that the ACI 318-77 Code⁽⁸⁾ underestimated the diagonal cracking shear stress. However, the upper limit of shear stress causing diagonal crack set by ACI 318-77 Code was in conformity with his test results. He said that the Diaz de Cosio⁽⁷⁾ equation was unconservative for calculating

diagonal shear stress for deep beams having lower span to depth ratio.

2.2.2b Ultimate Strength of Deep Beams

Kabir reported that the difference in web steel spacings had no significant influence over the ultimate shear strength of deep beams and the percentage of flexural reinforcement had some positive bearing upon the nominal stress at failure. He presented that the ACI 318-77 Code provisions for determination of ultimate shear strength was conservative and he suggested that the limit of $\sqrt{f'_c}$ for maximum shear stress as suggested in the Code might be raised to $10\sqrt{f'_c}$. He also said that the Singh, Ray and Reddy⁽⁹⁾ method of computing ultimate shear of deep beams could be used effectively providing the contribution of dowel force be limited to one-fourth of the total tension force developed in the flexural steel at yielding. He suggested to raise the splitting coefficient 'K' of Ramakrishnan and Ananthanarayana,⁽¹⁰⁾ formula for a better prediction of ultimate load of deep R.C. brick aggregate concrete beams.

Ali published that the upper limit of $8\sqrt{f'_c}$ for the ultimate shear stress suggested by ACI 318-77 Code was a fairly conservative estimate for brick aggregate concrete deep beams and the upper limit of $6\sqrt{f'_c}$ for the contribution of concrete in ultimate shear stress was also conservative for deep beams subjected to uniformly distributed load.

2.2.2c Moment Characteristics of Beams

In his report Kabir mentioned that the maximum moment at mid-span was about 50% of the ultimate flexural capacity of the test beams when the diagonal cracks first appeared.

2.2.2d Deflection of Beams

In his report Ali stated that the deflections of beams with span to depth ratio of 2 was fairly accurately predicted by the ordinary shallow beam formula using uncracked section. For the lower values of span to depth ratio ($L/D=1$) this formula grossly underestimated the actual deflections of beams. It was also mentioned that the ordinary shallow beam theory using cracked sections predicted the deflections of all the test beams fairly accurately.

2.2.2e Stresses in Reinforcements

Ali published that ordinary shallow beam theory as well as Holmes and Meson's⁽¹¹⁾ approach predicted the stresses in vertical and horizontal web reinforcements properly. Also steel stresses in flexural steel was predicted fairly accurately by the ordinary shallow beam theory using cracked section only when the load level is close to the ultimate load capacity of the deep beam.

2.2.2f Cracking Pattern and Mode of Failure

For deep beams under mid-span concentrated load Kabir stated that the principal mode of failure in the beams having adequate web steel was the diagonal tension cracking and the concrete 'strut' between two parallel diagonal cracks might sometime be formed but in general, the failure of a deep beam was not due to the compression failure by crushing of such a 'strut'.

But in Ali's study shear compression failure was found in relatively shallower deep beams ($L/D=2$) whereas in the deeper beams ($L/D=1$) diagonal tension failure was predominant.

2.3 STRENGTH AND BEHAVIOR OF STONE AGGREGATE R C DEEP BEAMS

The behavior and strength of deep flexural

members exhibit certain differences in failure mechanism and this has drawn attention of some researchers in this field. The length to total depth ratio (L/D) of a member is used as an index of its deepness. Flexural members having L to D ratio below 2 are usually considered deep and L to D ratio between 2 and 8 are considered moderately deep members⁽²⁾. The behaviors of deep beams under different types of loading as were found by some researchers are stated below :

2.3.1 Study of de Paiva and Siess⁽¹²⁾

In 1965, de Paiva and Siess reported the results of tests on nineteen simply supported deep beams. They asserted that there is a gradual transition from shallow beam behavior to deep beam behavior. The transition range appears to be span-depth ratio between two to six. The major variables involved in the study were the amount of tension reinforcement, the concrete strength, the amount of web reinforcement, and the span-depth ratio. In all the beams reported, well developed inclined cracks were observed at failure and the beams behaved essentially as tied arch. They have designated the failure of "tied arch" as a flexure failure either by crushing of concrete rib at the "crown" or by rupture of the tension bar. Such type of failure was usually accompanied by large inelastic deformation. For the beams that failed in shear, a second inclined crack was formed, which extended from the load point to the support outside the first inclined crack giving the beam a 'strut like' appearance. The failure of this strut in compression was accompanied by the shearing of the unloaded part of the beam outside load block and unbonding of the tension steel over the support. Some of the test beams failed in a manner identical to that described for shear failure but had undergone extensive deformation like flexural failure before its final collapse. Such failures are described as flexure-shear by the authors.

During their investigation de Paiva and Siess observed that concrete strength had a negligible effect on the flexural capacity of the beams but can have significant influence on modes of failure of beams failing in shear. Some of their test beams changed from flexure-shear mode of failure to flexure as concrete strength was increased. Increasing the percentage of tension steel increased the moment capacity of beams and tended to change the mode of failure from flexure to shear. In their concluding remarks they have said " The addition of vertical and inclined stirrups have no effect on the formation of inclined cracks and seemed to have little effect on the ultimate strength of beams failing in either flexure or shear."

2.3.2 Study of Fritz Leonhardt⁽¹³⁾

In 1966 Fritz Leonhardt in his paper titled " Strength and Behavior of Deep Beam in Shear" made some remarks upon the properties of deep beams. He reported, with the help of the principal stress trajectories of deep beams with span to depth ratio equal to one ($L/D=1$), that a distribution of horizontal tie bars over approximately $1/5$ to $1/10$ of the depth from the bottom of the beam will be helpful against the propagation of inclined cracks. He also presented that the beam with $L/D < 2$ always failed because of the concrete crushing near the bearing where the principal compression stress became critical giving the upper limit of carrying capacity, if the tie bars were well anchored and distributed.

2.3.3 Study of Ramakrishnan and Ananthanarayana⁽¹⁰⁾

In 1968 Ramakrishnan and Anathanarayana reported the results of the investigations on 26 single span rectangular deep beams. Depth-span ratio and type of loading were the main variables considered. Effect of both single concentrated load and distributed load were investigated. Based on the observed behaviors

and strengths of beams they presented an equation for predicting the ultimate shear strength of deep beams. They presented that the mode of shear failure in deep beams were nearly the same as those in shallow beams under lower shear span-depth ratio ($a/D < 2$) and this type of failure in deep beam was always initiated by splitting action of concrete without any sliding action.

2.3.4 Study of Kong, Robins, and Cole⁽¹⁴⁾

In 1970 Kong, Robins, and Cole investigated the effects of various types of web reinforcements on ultimate and cracking strengths, crack widths, crack spacing and deflections. 35 simply supported deep beams of span-depth ratio (L/D) ranging from 1 to 3 and shear span - depth ratio (a/D) from 0.23 to 0.7 with seven different types of web reinforcements were tested. The loads applied were two point loading applied at top or compression face of test beams. They reported that for the control of deflections and crack widths the preferred arrangement of web reinforcement depended very much on the span to depth ratio and shear span to depth ratio, and only horizontal web reinforcement placed near the bottom at a fairly close spacing was effective. Where L/D ratio is higher than 1.5 and a/D ratio higher than 0.35 vertical stirrups could be used and where L/D was 3 and a/D was 0.7, vertical stirrups were preferable to others.

They concluded that in general, the primary cause of failure was diagonal cracking ; crushing of concrete at the bearing blocks was usually only a secondary effect, and failure in compression of the concrete 'strut' between diagonal cracks occurred a few times only.

2.3.5 Study of Manuel, Slight, and Suter⁽¹⁵⁾

In the year 1971, Manuel, Slight, and Suter reported the

effect of the variation of span to depth and shear span to depth ratios on the behavior of deep beams. They investigated 12 reinforced concrete deep beams in which the variables a/D and L/D were systematically varied and other major variables were kept constant. The effects of changes in a/D and L/D on failure, diagonal cracking, steel strains at the supports, maximum crack widths, and mid-span deflections were observed. They published that the ultimate strength of reinforced concrete deep beams were influenced significantly by a/D ratio and insignificantly by L/D ratio. And the value of a/D ratio influenced the mode of failure.

They also reported that the diagonal cracking capacity of deep beams was not influenced significantly by L/D ratio; there was an overall tendency for the diagonal cracking capacity to increase with an increase in a/D ratio from 0.3 to 1.0. The extent of arch action for beams of constant shear span at any load level was reduced as the length of beam increased. The effect of a/D ratio on the extent of arch action at any load level was not apparent.

They concluded that the maximum flexural and diagonal crack widths were not influenced by a/D ratio, but were reduced slightly with the increase in L/D ratio for a constant a/D ratio. They also suggested to consider the influence of diagonal racking for the deflection computations.

2.3.6 Study of Singh, Ray, and Reddy⁽⁹⁾

In 1980 Singh, Ray and Reddy developed a somewhat rational equation for the shear strength of deep reinforced concrete beams. The results of 11 reinforced concrete deep beams tested under four-point loading condition simulating approximately the distributed loading, were reported.

The proposed equation is based on the identity of the

states of stresses in diagonal cracking mode of failure and rupture phenomenon in Mohr-Coulomb fracture criterion. It was assumed that the diagonal mode of failure, frequently encountered in problems involving deep beams was a state of failure akin to the rupture phenomenon in the Mohr-Coulomb failure criterion with straight line envelopes. Equilibrium equations involving cohesion c , and tangent of angle of internal friction $\tan\phi$ of the Mohr diagram had been developed with normal and tangential forces acting on the ruptured inclined plane at failure of the beam.

In its simple final form the ultimate shear force at failure had been shown to be made up of contributions from three distinct shear resistance mechanisms. The first term represents the contribution of concrete, the second represents the contribution of tensile steel while the third represents the contribution of inclined web reinforcement to the ultimate shear strength of the beam. Certain modifying factors were proposed to account for the shear-span to depth ratio and other web opening parameters. Finally, using there proposed formula, the ultimate loads were computed for deep beams reported in the recent literature and a good correlation between the computed loads and the observed loads were shown.

2.3.7 Study of Smith and Vantsiotis⁽¹⁶⁾

In the year 1982 Smith and Vantsiotis reported the results of tests on 52 deep reinforced concrete beams under symmetrically placed two equal point loads. The objectives of the investigation were to study the effect of vertical and horizontal web reinforcements and shear span to effective depth ratio (a/D) on inclined cracking shear, ultimate shear strength, mid-span deflection, tension reinforcement strain, and crack width.

They reported that cracking patterns were essentially

the same for beams with or without web reinforcement. However, less damage at failure was observed in beams with web reinforcements. Presence of a minimum amount of vertical and horizontal reinforcement (0.18% and 0.23% respectively) as was found to considerably reduce crack widths and deflections after inclined cracking. Inclined cracking loads were considerably lower than ultimate loads for beams with or without web reinforcement. Test results show that inclined cracking loads vary between 40 and 50 percent of the ultimate loads.

They also concluded that the presence of vertical (ranging 0.18% to 1.25%) and horizontal (ranging 0.23% to 0.91%) web reinforcements had no effect on inclined cracking load. But the presence of vertical web steel increased ultimate shear strength of deep beams. However, the effectiveness of vertical stirrups seemed to diminish for beams with $a/D < 1$. Horizontal web steel appears to have had little influence on the ultimate shear strength but its influence was more noticeable in beams with $a/D < 1$.

2.3.8 Study of Barry and Ainso⁽¹⁷⁾

In 1983 J.E. Barry and Heino Ainso in the paper titled "Single Span Deep Beams" used the multiple Fourier technique to compare the stress fields in single span deep beams due to uniform loading at the top edge and at the bottom edge. It was believed that the multiple Fourier method could be effectively used to handle the analysis of a single span deep beam. Nothing inherent in the method would prevent the extension of the analysis to cover deep beams with different load configurations or deep beams extending over two or three bays. They suggested that when the span to depth ratio (L/D) was equal to 2, the bending stress distribution was reasonably well with that predicted by ordinary bending theory. This might be considered as a limiting span to depth ratio so that ordinary bending theory

might be used to obtain the bending stress distribution. However, the shear stress distribution near the interior face of the support would be significantly different than that predicted by ordinary bending theory at this span to depth ratio.

2.3.9 Study of Rogowsky, MacGregor, and Ong⁽¹⁸⁾

In 1986 the tests on the behaviors of 7 simply supported and 17 two-span deep beams were reported by Rogowsky, MacGregor, and Ong. The behavior ranged from brittle for beams without vertical web reinforcement to ductile for beams with large amounts of vertical web reinforcements. They observed that the horizontal web reinforcement had no effect on the capacity.

They found that beams without stirrups or with minimum stirrups approached tied arch action at failure. This was true regardless of the amount of horizontal web reinforcement present. These failures were sudden with little or no plastic deformation. On the other hand beams with large amounts of stirrups failed in a ductile manner.

2.3.10 Study of Selvam and Kuruville⁽¹⁹⁾

In 1987 Selvam and Kuruville tested 24 single span and simply supported deep beams with span to depth ratio (L/D) varying from 0.89 to 3.0 and subjected to two point loading. They studied the mode of failure and for computing the ultimate load capacity in shear, two equations were proposed.

They reported that the ultimate load carrying capacity of deep beam in the shear compression mode was very high. There was no sign of flexural distress in the crushing mode which was purely a localized one. Failure in crushing mode was found to occur at a load very much lower than the shear capacity of the beams.

2.3.11 Study of Mau and Hsu⁽²⁰⁾

In the year 1989, S. T. Mau and T. C. Hsu gave a rational formula for the shear strength of deep beams. Using the three equilibrium equations from the truss model theory, this explicit formula was derived. The constants in the formula were calibrated utilizing test data available in the literature. The formula is dimensionless and contains four variables that express the horizontal and vertical reinforcement ratios, the concrete strength, and the shear span ratio.

The above mentioned formula has four nondimensionalized variables. It gives accurate predictions in the range where the horizontal shear steel ratio is less than 0.009, vertical shear steel ratio is less than 0.0245, and span to depth ratio is less than 3.3.

CHAPTER 3

AVAILABLE THEORIES AND DESIGN METHODS

3.1 GENERAL

The stresses in a deep beam differ radically from stresses predicted by the ordinary theory of beam bending for shallow beams. The behavior of ordinary shallow beams under both service and ultimate load conditions are relatively more well understood as compared to deep beams. Numerous text books on reinforced concrete design give theories for analysis and design of shallow beams. But, the provision of empirical methods of design for deep beams in the available Code of practice is a relatively recent development. Some of the theories and design practices available in the literature are presented in this chapter.

3.2 STRESS PATTERN IN DEEP BEAMS

The usual methods developed for stress analysis for shallow beams are neither suitable nor adequate to determine the strength of reinforced concrete deep beams. The stresses in isotropic homogeneous deep beams before cracking can be studied using the methods of two dimensional elasticity, photoelasticity, or finite element analysis. Such studies confirm that the usual hypothesis, "plane sections before bending remain plane after bending", does not hold good for deep beams. Significant warping of the cross section occurs because of high shear stresses. Consequently, flexural stresses are not linearly distributed, even in the elastic range.

Deep beam is rather sensitive with respect to the loading at the boundaries. The length of the bearing surfaces of the beam in fig. 3.1 would affect the principal stresses, which can be very critical in the immediate vicinity of these supports.

Similarly, stiffening ribs, cross walls or, extended columns at the supports would markedly influence the stress patterns. One of the most significant aspects of stress analysis would be the manner of application of the load, which is uniformly distributed in the case depicted in fig. 3.1 .

It was found that smaller the span/depth ratio (i.e. less than 2.5) the more pronounced the deviation of the stress pattern from that of Bernouli and Navier. Fig. 3.1 shows the distribution of horizontal flexural stresses at the mid-span of simply supported beams having different span/depth (L/D) ratios, when carrying a uniformly distributed load of intensity w per unit length. The mid-span moment being $wL^2/8$, the usual extreme fiber stress at mid-span would be -

$$f_t = f_c = \frac{6M}{bD^2} = 0.75 \frac{wL^2}{bD^2} \text{ and which becomes } 0.75w/b \text{ for}$$

a square panel beam i.e. $L/D=1.0$.

But fig. 3.1 indicates that the tensile stresses at the bottom fiber are more than twice this intensity. Similar deviations occur in the distribution of shear stresses.

It is interesting to note that the internal lever arm is not greatly affected by span/depth ratio and the tension zone in the bottom is relatively small. The internal lever arm for very deep beams does not appear to increase greatly after cracking and for design purpose the following approximation for the internal lever arm z may be made⁽²¹⁾.

$$z = 0.2 (L + 2D) \quad \text{when } 1 \leq L/D \leq 2$$

$$z = 0.6 L \quad \text{when } L/D < 1$$

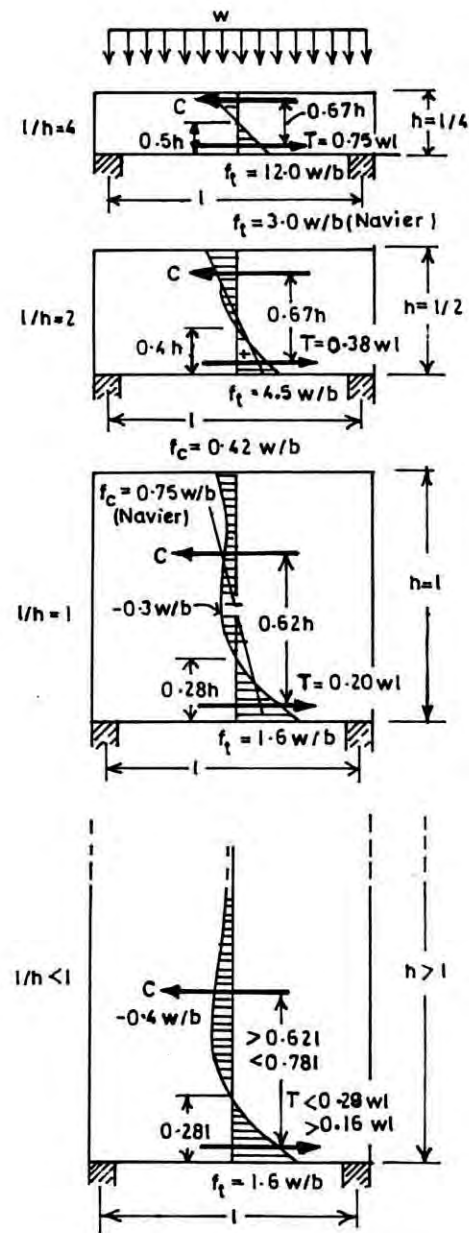


Fig 3.1 Distribution of flexural stresses in homogeneous simply supported beams⁽²¹⁾..

3.3 DISTRIBUTION OF STRESSES IN DEEP BEAMS (OTHER APPROACHES)

3.3.1 Heino Ainso and J. E. Barry's⁽¹⁷⁾ Approach

A multiple fourier technique was used to compare the stress fields in single span deep beams due to uniform loading at the top edge. The method involves the superposition of three stress functions. The first stress function is used to satisfy the boundary conditions on the upper and lower edges of the beam. The second and third stress functions are used to satisfy the boundary conditions on the vertical edges of the beam. The deep beam they analyzed is shown in fig. 3.2 .

Letters a, b, c, h, p have the meanings exactly as shown in fig. 3.2 . Some of the findings are shown in fig. 3.3 through fig. 3.6 .

3.3.2 Krishna Raju⁽²²⁾ Approach

Fig. 3.7 shows the flexural stress at mid-span of a simply supported single span deep beam subjected to uniformly distributed loads and for different ratios of β (a function of L/D) having values of 0.5, 0.67 and 1.0. As β increases from 0.5 to 1.0, the compressive stress decreases rapidly at the top and the neutral axis moves towards the soffit of the beam.

3.3.3 Coker and Filon⁽²³⁾ Approach

For the simply supported single span deep beam subjected to mid-span concentrated load, Coker and Filon presented the principal stress trajectories of the uncracked state of the beam. They used photoelasticity and their finding is shown in fig. 3.8.

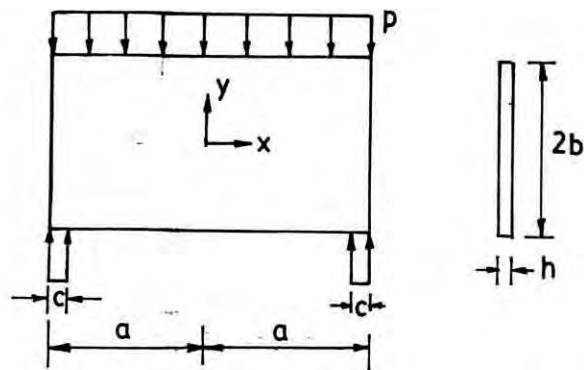


Fig. 3.2 Single span deep beam subjected to uniformly distributed load⁽¹⁷⁾

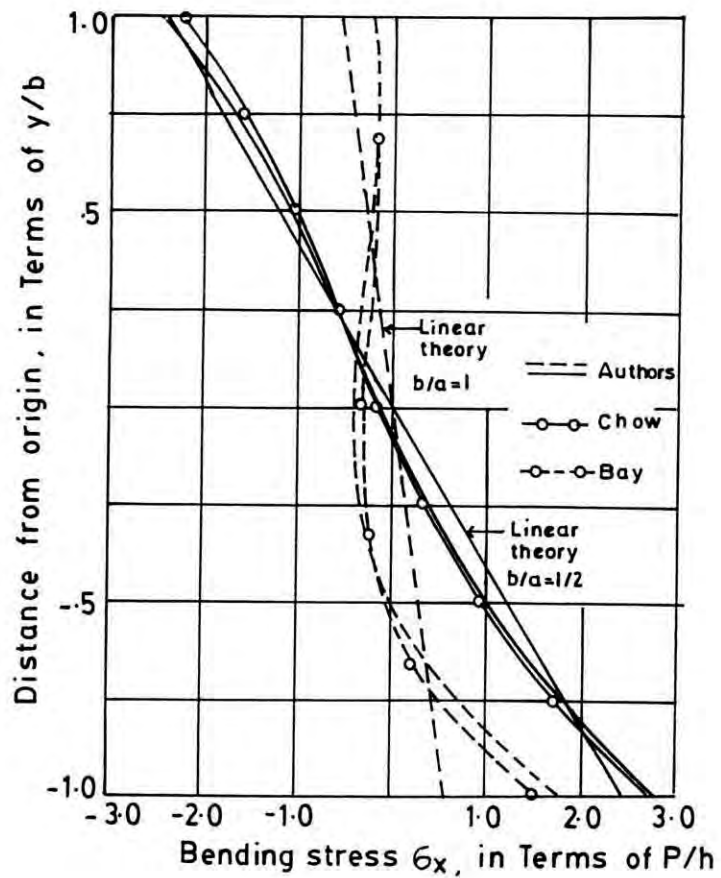


Fig. 3.3 Bending stress at Midspan⁽¹⁷⁾

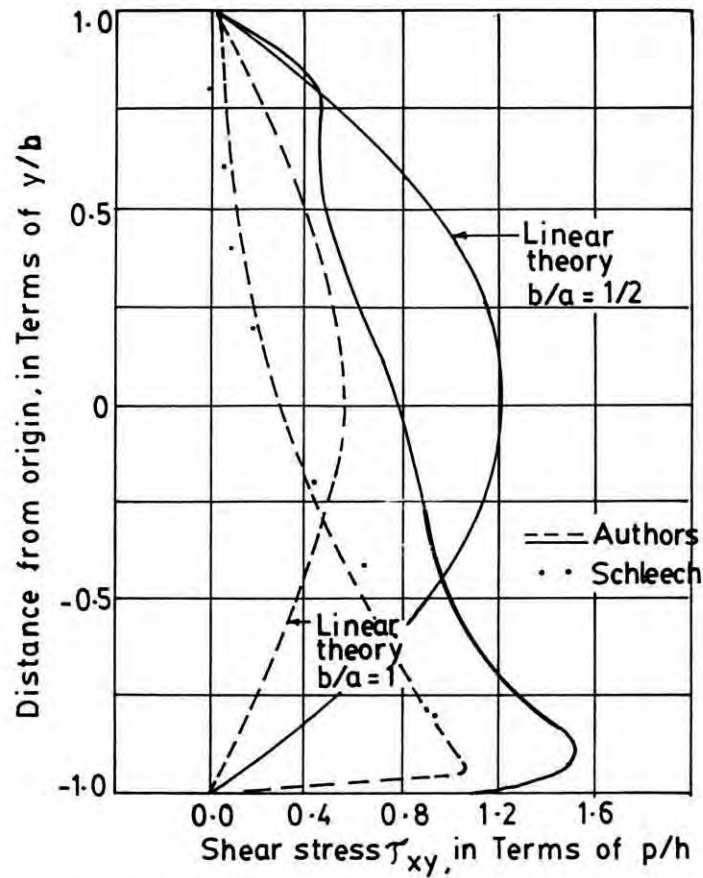


Fig. 3.4 Shear Stress at $x = 4a/5$ (Face of Support)⁽¹⁷⁾

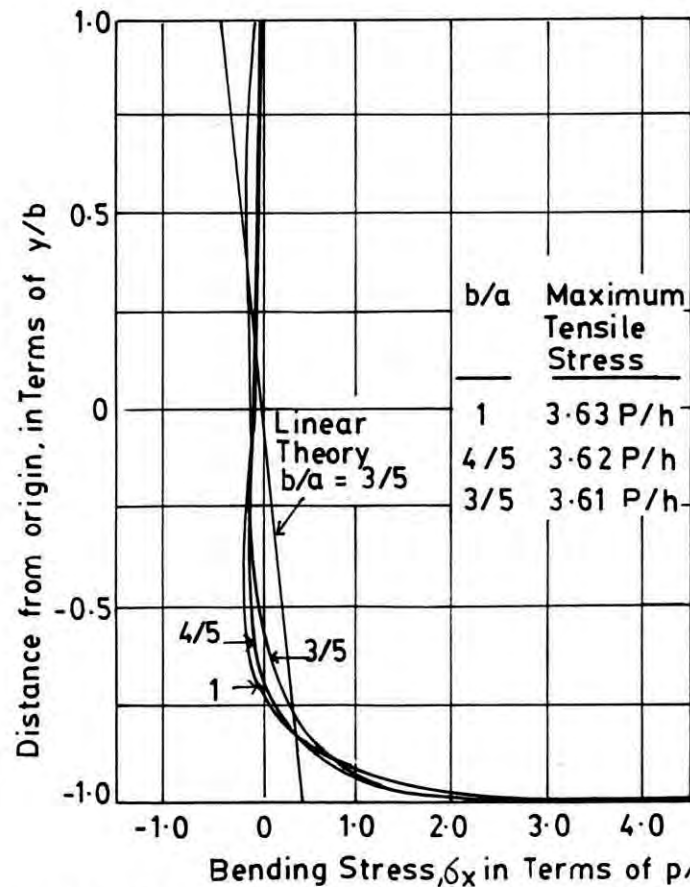


Fig. 3.5 Maximum Bending Stress at $x = .77a$ ⁽¹⁷⁾

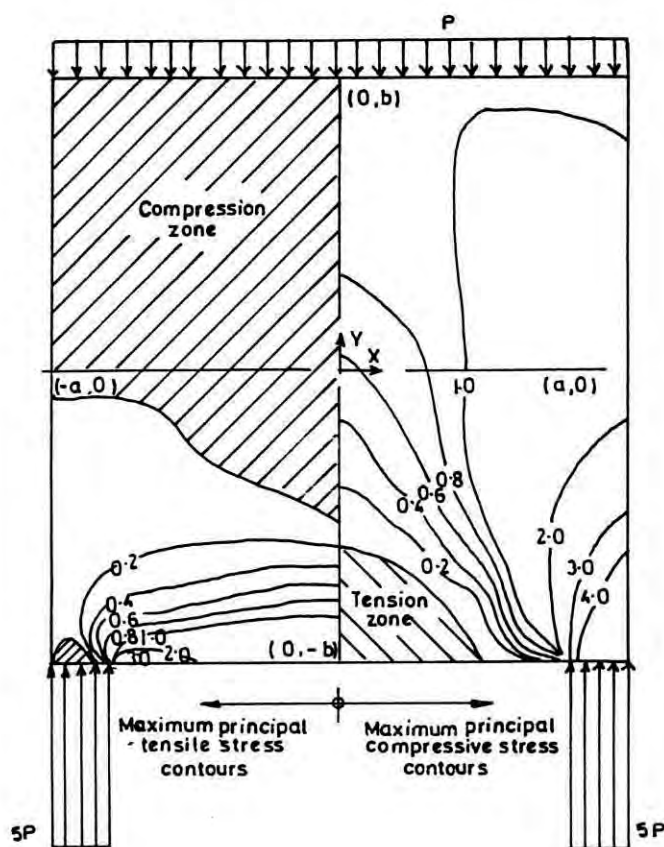


Fig. 3-6 Maximum principal stress contours in terms of P/h for top loaded beams (17)

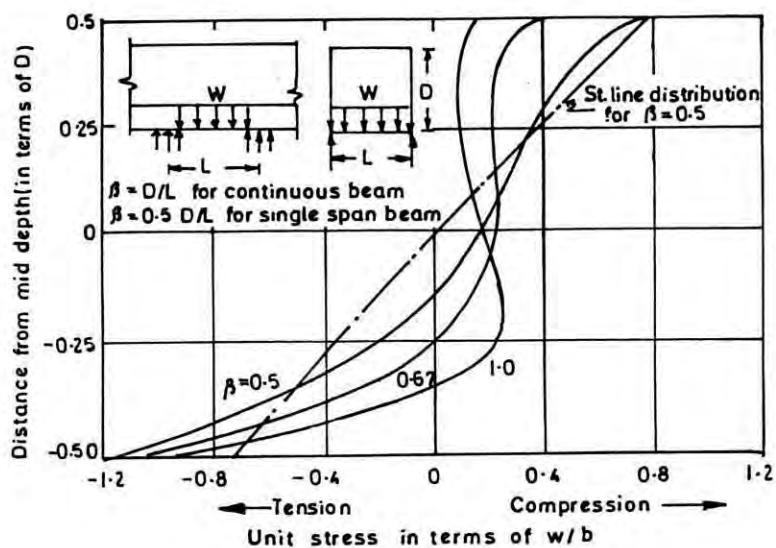


Fig. 3.7 Flexural stresses in simply supported single span deep beam(22)

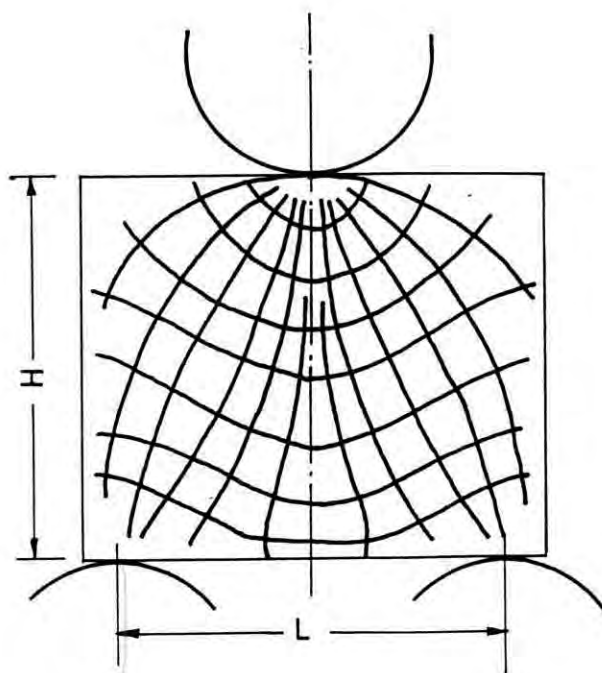


Fig. 3.8 Principal stress trajectories of the uncracked state of deep beam under concentrated load(23)

3.3.4 Leonhardt⁽¹³⁾ Approach

The principal stress trajectories of single span and simply supported deep beam under uniformly distributed load were reported by Fritz Leonhardt which is presented here in fig. 3.9 .

3.4 ULTIMATE STRENGTH AND BEHAVIOR OF DEEP BEAMS

Because of the proportions of deep beams, they are likely to have strength controlled by shear. On the other hand, their shear strength is likely to be significantly greater than predicted by the usual equations for shallow beams. Internal forces are redistributed before failure, and develop mechanisms of force transfer quite different from beams of common proportions. Special design methods are needed to account for these differences.

F. Leonhardt⁽¹³⁾ presented that the usual type of shear reinforcement does not increase the strength of deep beams. A shear stress indicates only that the principal stresses are not parallel to the system of coordinates on which the bending analysis is based. The direction of such principal stresses are influenced by σ_x and σ_y . In shallow beams, the directions of the principal stresses at the depth of the neutral axis ($\sigma_x = \sigma$) is 5° , in deep beams this inclination is much smaller, mainly because of σ_y , the vertical component of stresses (fig.3.10). The necessary amount of shear reinforcement with vertical or inclined stirrups under 45° to 60° decreases, with decreasing inclination of the principal tensile stress.

If the truss analogy for the cracked state is considered, then the necessary amount of tension bars between the chord members decreases mainly by the inclination of the corresponding chord, which increases with decreasing slenderness ratio (fig. 3.10). This inclination of the compression chord of the truss corresponds to the arching effect. The truss analogy

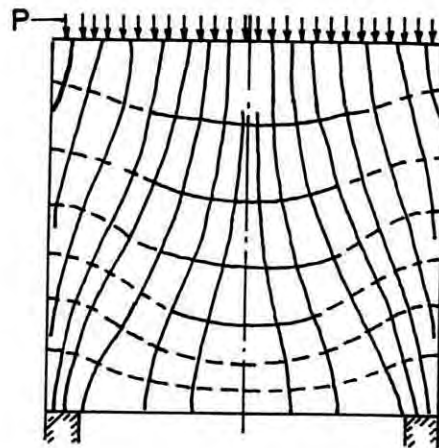


Fig. 3-9 Principal stress trajectories of single span deep beam under uniform loading(13)

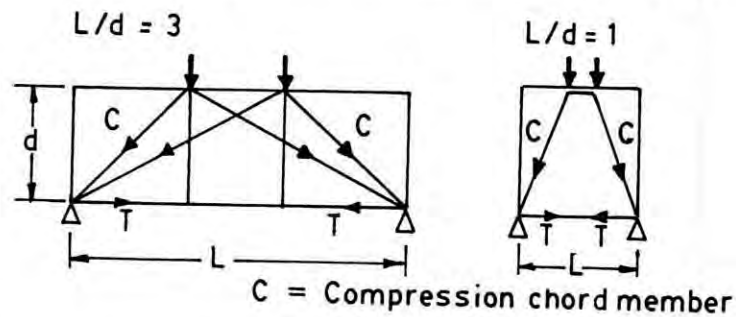


Fig. 3-10 Truss analogy for the cracked state of deep beam(13)

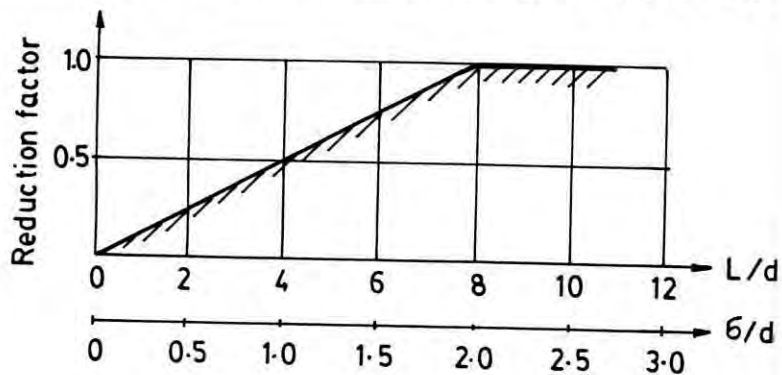


Fig. 3-11 Reduction of the shear reinforcement in deep beam(13)

helps to show that the usual shear reinforcement is practically useless in deep beams with $L/D = 1.0$; the necessary quantity of shear reinforcement can be decreased proportionately to L/D as shown in fig. 3.11 beginning with a span/depth ratio $L/D = 8.0$.

The principal stress trajectories of a deep beam with $L/D = 1.0$ (fig. 3.10) indicates that a distribution of the horizontal tie bars over approximately $1/5$ th to $1/10$ th of the depth will be helpful against the propagation of inclined cracks.

3.4.1 Ultimate Strength of Deep Beam, ACI Bldg. Code⁽¹⁾ Approach

The ACI 318-89 code makes some special provisions for deep beams loaded at the compression face only. If the loads are applied at the sides or bottom of a member, design provisions for ordinary beams apply. The code considers the effects on the web, in terms of nominal shear stresses and shear reinforcement only.

As usual, the design basis is that

$$V_u < \phi V_n$$

where, $\phi = 0.85$ for shear, and

$$V_n = V_c + V_s$$

Regardless of the amount of reinforcement provided, the nominal shear strength V_n is not to be taken greater than the following -

$$\text{For } L/D < 2 \quad : \quad V_n = 8 \sqrt{f'_c} \, bd \quad \text{--- (3.1a)}$$

$$\text{For } 2 \leq L/D \leq 5 \quad : \quad V_n = \frac{2 (10 + L/D) \sqrt{f'_c} \, bd}{3} \quad \text{--- (3.1b)}$$

The variation of the maximum permissible V_u , as a function of L/D , is shown in fig. 3.12 .

The critical section for shear is to be taken a distance $0.15L$ from face of the supports for uniformly distributed loads and $0.5a$ for beams with concentrated loads, but not to exceed a distance d (effective depth) from the support face in either case. Shear reinforcement required by calculation or other ACI code provision at the critical section is to be used throughout the span.

Shear strength capacity increase considerably for deep beams due to tied-arch action. The concrete contribution to shear strength can be computed from :

$$V_c = \left(3.5 - \frac{2.5 M_u}{V_u d} \right) \left(1.9 \sqrt{f'_c} + 2500 \frac{p V_u d}{M_u} \right) bd \quad \text{--- (3.2)}$$

Where the multiplier $(3.5 - 2.5 M_u/V_u d)$ is used to account for the increased shear resistance of deep beams. However, this multiplier has the restrictions that it must not exceed 2.5 and that V_c must not be taken greater than $6 \sqrt{f'_c} bd$. Here M_u and V_u are the moment and shear force, at factored load, occurring simultaneously at the critical section. Fig. 3.13 shows the value of the multiplier in eqn.(3.2) as a function of the parameter $M_u/(V_u d)$.

When the shear force V_u at , factored loads exceeds the design shear strength of the concrete ϕV_c , shear reinforcement must be provided to carry the excess shear. The contribution of the web steel V_s is to be calculated from -

$$V_s = \left\{ \frac{A_v}{s} \times \left(\frac{1 + L/D}{12} \right) + \frac{A_{vh}}{s_2} \times \left(\frac{11 - L/D}{12} \right) \right\} f_y d \quad \text{--- (3.3)}$$

in which A_v is the area of shear reinforcement perpendicular to the main flexural steel within a distance s and A_{vh} is the area of shear reinforcement parallel to the main flexural steel within a distance s_2 (fig. 3.14).

So the expression for the required shear reinforcement for deep beams is -

$$\left\{ \frac{A_v}{s} \times \left(\frac{1 + L/D}{12} \right) + \frac{A_{vh}}{s_2} \times \left(\frac{11 - L/D}{12} \right) \right\} = \frac{V_u - \phi V_c}{\phi f_y d} \quad \text{--- (3.4)}$$

The relative amounts of horizontal and vertical web steel that are used, based on eqn.(3.4), may vary within the following restrictions :

The area A_v must not be less than $0.0015bs$ and s must not exceed $d/5$ or, 18 inches. The area A_{vh} must not be less than $0.0025bs_2$, and s_2 must not exceed $d/3$ or, 18 inches.

The coefficients in parentheses in eqn.(3.4) are weighting factors for the relative effectiveness of the vertical and horizontal web steel. From fig. 3.15, it is seen that, for very deep beams with small L/D , the horizontal steel A_{vh} is dominantly effective, and the addition of vertical web steel A_v will have little effect in increasing strength. As the ratio L/D increases the effectiveness of the vertical steel tends to increase, until at $L/D = 5$, vertical and horizontal steel taken to be equally effective. Thus for very deep beams it is more efficient to add web steel, if needed, in the form of horizontal bars, while satisfying the minimum requirements for vertical steel.

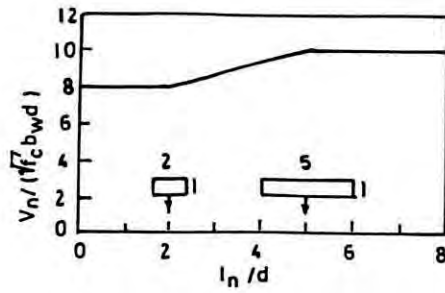


Fig. 3.12 ACI Code limitation on total nominal shear strength V_n for deep beams (1)

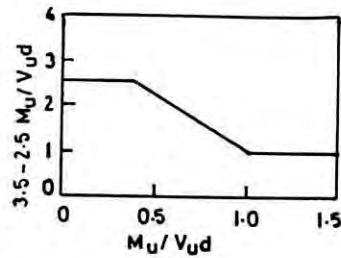


Fig. 3.13 Shear strength multiplier for deep beams (1)

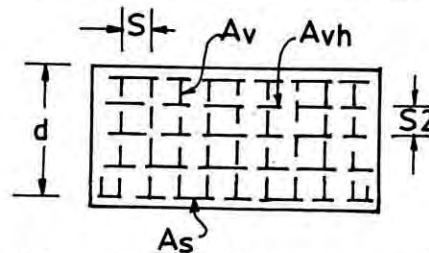


Fig. 3.14 Deep beam reinforcement pattern (1)

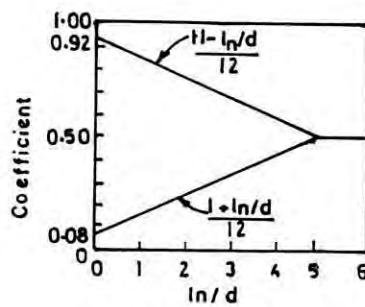


Fig. 3.15 Effectiveness coefficients for vertical and horizontal web reinforcement in deep beams (1)

3.4.2 Ramakrishnan and Ananthanarayana⁽¹⁰⁾ Approach

The equation for predicting the ultimate load of deep beams from the similarity of diagonal tension splitting along the potential crack with that of a cylinder under diametral compression. It is one of the simplest formula available at present to assess the ultimate shear strength of deep beams. The equation in its general form is -

$$P_u = \beta K f'_{sp} b d$$

where, β = a coefficient for shear span and loading condition effect.

K = splitting coefficient which is 1.57 for cylinder splitting and 1.12 suggested by them for deep beams.

For deep beams under uniformly distributed load, it is reduced to

$$P_u = 2.24 f'_{sp} b d \quad \text{--- (3.5)}$$

3.4.3 Singh, Ray, and Reddy⁽⁹⁾ Approach

Singh, Ray and Reddy have estimated the ultimate shear capacity of deep beams by assuming that the diagonal tension mode of failure is similar to the rupture phenomenon in the Mohr-Coulomb failure criterion with straight line envelopes. Equilibrium equations involving cohesion of concrete 'c' and the angle of internal friction ' ϕ ' of the Mohr-diagram have been developed with the normal and tangential forces acting on the ruptured diagonal crack plane at failure of the beam. On simplification of the equilibrium equations, the ultimate shear strength equation is developed as -

$$Q_u = \frac{c b D}{\{\sin\beta \cos\beta (\tan\beta + \tan\phi)\}} + \frac{A_s f_y (\tan\beta \tan\phi - 1)}{\tan\beta + \tan\phi}$$

$$+ \Sigma A_w f_{wy} \left[\frac{\sin\alpha \cot\beta + \cot\alpha}{\{(\tan\beta + \tan\phi) / (\tan\beta \tan\phi)\}} \right]$$

$$- \frac{\cos\alpha}{\{(\tan\beta + \tan\phi) / (1 - \tan\alpha \tan\beta)\}}$$

where, α = inclination of the web steel with horizontal.
 β = angle of inclination of potential diagonal crack with the horizontal.

When the web steels are placed in horizontal and vertical directions only, the equation reduces to

$$Q_u = P_c(\tau_1) + \mu_s P_s + \mu_w P_w \quad \text{--- (3.6)}$$

where, $P_c = \frac{c b D}{\sin\beta \cos\beta (\tan\beta + \tan\phi)}$

$$\tau_1 = \left(1 - \frac{X_u}{3 D}\right) \quad \text{for } X/D \leq 1$$

$$P_s = \frac{A_s f_y (\tan\beta \tan\phi - 1)}{\tan\beta + \tan\phi}$$

$$P_w = P_{wv} + P_{wh}$$

and $P_{wv} = \Sigma A_v f_{vy} \left(\frac{\tan\phi}{\tan\beta + \tan\phi}\right)$

$$P_{wh} = \Sigma A_{vh} f_{hy} \left(\frac{\tan\beta \tan\phi - 1}{\tan\beta + \tan\phi} \right)$$

$$\mu_s = 1.0 \quad \text{for solid beams}$$

$$\mu_w = 0.5 \quad \text{for solid beams}$$

τ_1 , μ_s , and μ_w are proposed factors to account for the shear span/depth ratio and other web opening parameters.

3.4.4 Kong, Robins, and Cole⁽¹⁴⁾ Approach

A formula that also uses the concrete cylinder splitting strength was proposed in 1972 with the contribution of steel included as follows :

$$V_n = C_1 \left(1 - \frac{0.35 x}{h} \right) f_{sp} bd + C_2 \Sigma A \frac{n y}{h} (\sin\alpha)^2 \quad - - - - (3.7)$$

where C_1 is 1.4 for normal weight concrete, C_2 is 18900 psi (130 MPa) for plain round bars and 43500 psi (300 MPa) for deformed bars, n is the number of all the steel bars crossing a straight line connecting the edges of the supporting plate and the loading plate through the clear span, A is the area of each bar, y is the vertical distance from the top of the beam to the intersection point of the straight line and the bar axis, and the angle α is the angle between the straight line and the bar axis.

This formula was calibrated for x/D between 0.23 and 0.70.

3.4.5 de Paiva and Siess⁽¹²⁾ Approach

This formula is a modification of an earlier one due to

Laupa, Siess, and Newmark. The de Paiva and Siess formula was intended to be a lower bound to the actual shear strength -

$$V = 0.8bh\left(1 - \frac{0.6x}{h}\right)\left(200 + 0.188f'_c + 21300 \times \frac{A_s}{bh}\right) \quad \text{--- (3.8)}$$

where, A_s = the total cross-sectional area of horizontal steel.

3.4.6 Selvam and Kuruville⁽¹⁹⁾ Approach

V.K. Manicka Selvam and Kuruville Thomas proposed an equation for computing the ultimate load capacity of deep beams in shear. They also proposed a guideline for the quantity of main flexural reinforcement to be used so that shear mode of failure is effected in deep beams, eliminating flexural failure.

The quantity of reinforcement to be used in deep beams for bringing about shear mode of failure is established in the form of the following equation :

$$p \geq \frac{1}{2\beta} \quad \text{--- (3.9)}$$

where,

$p = 100 A_s / (bD) =$ steel index.

$A_s =$ Area of main flexural reinforcement.

$b =$ Thickness of the beam.

$D =$ Total depth of beam.

$\beta =$ Deep beam parameter = D/L

$L =$ Effective span of beam.

They suggested the following empirical equation for the computation of ultimate load capacity of deep beams :

$$P_u = [2.2 \alpha^{0.1} + 1.1 \beta^{0.2}] \epsilon^{0.5} f'_{sp} b D \quad - - - - - (3.10)$$

Where, $\alpha = a/D$

$a =$ Shear span.

$\epsilon =$ Ratio of the yield value of reinforcement used in the beam to the yield value of mild steel (2500 kg/cm²).

$f'_{sp} =$ Cylinder split tensile strength of concrete.

3.4.7 Mau and Hsu⁽²⁰⁾ Approach

This is one of the latest formula for the determination of shear strength capacity of simply supported deep beams. It is an explicit formula and is derived by using the three equilibrium equations from the truss model theory. The formula is dimensionless and contains four variables that express the horizontal and vertical reinforcement ratios, the concrete strength, and the shear span ratio. The formula is as follows -

$$\frac{V}{f'_c} = 0.5 [K(w_h + 0.03) + \sqrt{K^2(w_h + 0.03)^2 + 4(w_h + 0.03)(w_v + 0.03)}] \leq 0.3 \quad - - - - - (3.11)$$

with the limitations -

$$w_h = (p_h f_y) / f'_c \leq 0.26$$

$$w_v = (p_v f_y) / f'_c \leq 0.12$$

where, $p_h =$ total horizontal reinforcement ratio

$$= \frac{A_h}{b d}$$

$p_v =$ vertical web reinforcement ratio

$$= \frac{A_v}{b s}, \quad \text{and}$$

the value of K depends on the shear span-to-depth ratio a/D as follows :

$$K = \frac{2 d_v}{D} \quad \text{for } 0 < a/D \leq 0.5$$

$$\text{or, } K = \frac{d_v}{D (D/a (4/3 - 2a/3D))} \quad \text{for } 0.5 < a/D \leq 2$$

$$= 0 \quad \text{for } a/D > 2$$

where, d_v = distance between the centers of flexural steel and the topmost horizontal steel.

This formula gives accurate predictions in the range where the horizontal shear steel ratio is less than 0.009, vertical shear steel ratio is less than 0.0245, and the span-depth ratio is less than 3.3 .

3.5 MECHANISM OF SHEAR RESISTANCE IN RC DEEP BEAMS

In the case of deep beams with relatively small percentage of reinforcement, the cracks develop vertically from the soffit and remains practically vertical in comparison with the diagonal tension cracks observed in conventional shallow beams as shown in fig. 3.16 .

It is clear from the figures that the diagonal tension which is characteristic of a shallow beam changes gradually into plain horizontal tension as the beam becomes a deep girder. Hence the conventional shear investigations are not strictly applicable to deep beams.

For deep beams, a significant part of the shear force is transferred directly from the loads to the supports by tied-arch action (fig. 3.17).

The effectiveness of this mechanism clearly depends upon the proportions of the member as well as on the placement of the loads and reactions. The tied-arch mechanism is effective only if the shear span/depth ratio is about 2 or, less. For a deep beam with load uniformly distributed along the compression face or top edge, this mechanism is effective⁽²²⁾ when

$$\frac{M_u}{V_u d} \leq 1.0$$

3.5.1 Role of Shear Reinforcements

Because of the orientation of the principal stresses in deep beams, when diagonal cracking occurs, it will be at a slope steeper than 45° in most cases. Consequently, while it is important to include vertical stirrups, they are apt to be less effective than the horizontal web steel. The horizontal bars are effective not only because they act more in the direction perpendicular to the diagonal crack. Better dowel action in turn, helps to improve shear transfer by aggregate interlock.

3.5.2 Role of Main Flexural Reinforcements

Main flexural reinforcements in deep beam provides the necessary tensile force for tied-arch mechanism to equilibrate the loads. Besides, the flexural reinforcements also contribute to shear transfer by dowel action. Flexural reinforcements must have sufficient embedment or anchorage over the supports so that the arch action can develop fully.

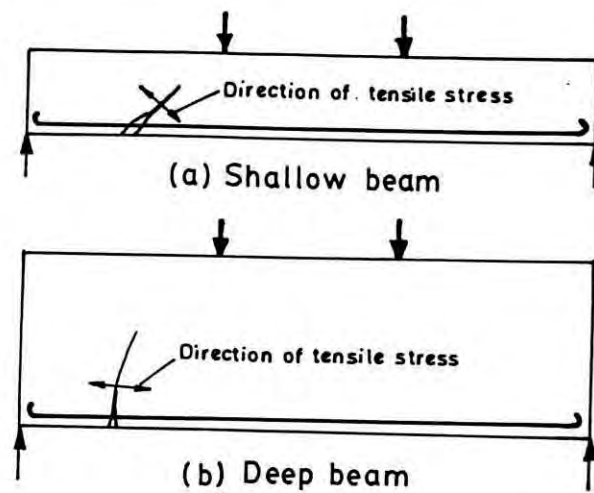


Fig. 3-16 Diagonal tension cracks in shallow and deep beams(22)

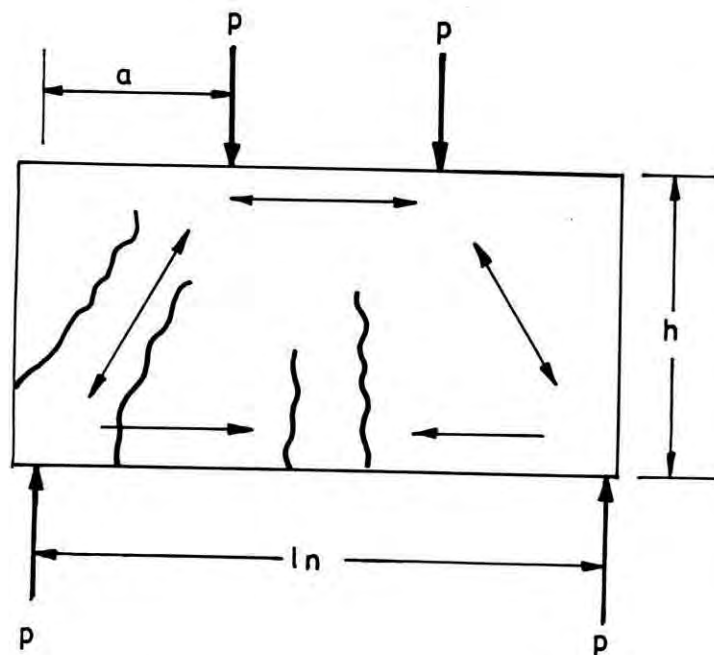


Fig. 3-17 Shear transfer by tied-arch mechanism(1)

3.6 MODE OF SHEAR FAILURE

When the shear capacity of a beam is less than the bending capacity, it fails in shear. Some of the characteristic features that are inherent to each type of shear failures are described below -

3.6.1 Beam Action Failure

The characteristic feature of beam action failure is the formation of diagonal cracks as an extension of flexural cracks and the tension zone is therefore divided into a comblike structure. The beam action failure may result in a total collapse shortly after the application of diagonal cracking load indicating that the subsequent arch mechanism is incapable of sustaining the cracking load. This type of failure is common in beams with a/D ratio between 3 and 7.

3.6.2 Shear Compression Failure

This type of failure occurs in rectangular reinforced concrete beams when $2 \leq a/D \leq 3$. When a/D ratio is relatively low, considerably higher load can be sustained by arch action after the failure of the beam action mechanism. The diagonal cracks penetrating slowly into the compression zone at higher loads may reduce the area under arch compression excessively. At one stage, the available area of concrete in the vicinity of the load point becomes too small to resist the compression force and the arch fails by crushing of concrete at the crown. This type of failure is usually accompanied by the formation of diagonal cracks and the inclined cracks in the shear span and the slow progress of the later. Crushing of concrete below or near the loading point (for concentrated loading) is the distinctive feature.

3.6.3 Diagonal Tension or Diagonal Compression Failure

Failure by crushing or splitting of concrete in the shear span of a reinforced concrete beam are frequent with a/D ratio below 2.5. This is obviously the failure of the arch action. But this time the failure is in the inclined rib of the arch. When the line of thrust is quite steep, considerable reserve strength may be available owing to more effective arch action. Ultimately the failure may be accompanied by either diagonal compression crushing or diagonal tension splitting.

CHAPTER 4

EXPERIMENTAL INVESTIGATIONS

4.1 GENERAL

The experimental phase of this Study is distinctly divided into a sequence of works. The sequences are stated below:

- (a) Determination of the properties of the constituents of reinforced concrete.
- (b) Design of concrete mix.
- (c) Preparation of test beams and control cylinders.
- (d) Curing of test beams and control cylinders.
- (e) Preparing of two sets of load transfer (a concentrated load from the Universal Testing Machine is transformed into a uniformly distributed load upon the test beam) device sets with steel I-joist, steel plates, and bars.
- (f) Testing operation.

4.2 PROPERTIES OF THE CONSTITUENTS OF REINFORCED CONCRETE

The different constituents of reinforced concrete used in the test beams are Cement, Sand as fine aggregate, Brick khoa as coarse aggregate, and the Mild steel as reinforcement. The necessary properties of these materials were determined in the laboratory and are given below :

4.2.1 Cement

Portland cement was used as a binding material. Cement available in BUET Store was "Assam Bengal (ASTM Type-I) Brand". Properties of the cement as determined are :

Unit weight	= 91.0 lbs.
Normal consistency	= 23 %
Initial setting time	= 2 hrs. and 25 minutes.
Final setting time	= 7 hrs. and 40 minutes.
28 days compressive strength	= 3150 psi
28 days tensile strength	= 365 psi

4.2.2 Fine aggregate

Ordinary Sylhet sand passing No.4 sieve was used as fine aggregate in the experimental concrete mix. The absorption capacity, specific gravity, unit weight, and fineness modulus of the fine aggregate were determined as per ASTM recommendations (ASTM C136-84a) and are listed below :

Unit wt. of sand (dry loose)	= 86.5 lb/cft.
Bulk sp. gravity (ovendry basis)	= 2.46
Bulk sp. gravity (S.S.D. basis)	= 2.52
Absorption capacity (% of dry wt.)	= 1.75 %
Moisture content	= 0.55 %

Table 4.1 shows the grading of sand used.

4.2.3 Coarse Aggregate

For the preparation of concrete, manually crushed first class brick khoa were used as coarse aggregate. The brickchips were initially sieved through 3/4" to No.4 size sieve and the aggregate passing 3/4" size and retained on No.4 were stored

Table 4.1 Grading of Fine Aggregate

Sieve No.	% Retained	Cumulative % Retained
# 4	0.0	0.0
# 8	3.0	3.0
#16	16.0	19.0
#30	45.0	64.0
#50	24.0	88.0
#100	10.0	98.0
Pan	1.93	-
Total	---	272.0

(Fineness Modulus of sand = $272/100 = 2.72$)

separately for use. The unit weight, moisture content, absorption capacity, fineness modulus were determined as per ASTM recommendations⁽²⁵⁾ and their values are listed below :

Unit wt. of khoa (dry loose)	= 74.20 lb/cft.
Unit wt. of khoa (S.S.D. compacted)	= 92.30 lb/cft.
Bulk sp. gravity (oven dry basis)	= 1.88
Bulk sp. gravity (S.S.D. basis)	= 2.04
Absorption capacity (% of dry wt.)	= 10.80 %
Moisture content	= 3.50 %

Table 4.2 shows the grading of coarse aggregate.

4.2.4 Reinforcements

Mild steel plain bars of 5/8", 3/4", 7/8" and 1" nominal diameters were used as the main flexural reinforcements in

Table 4.2 Grading of Coarse Aggregate

Sieve size	% Retained	Cumulative % Retained
3/4"	0.0	0.0
3/8"	62.0	62.0
#4	38.0	100.0
#8	0.0	100.0
#16	0.0	100.0
#30	0.0	100.0
#50	0.0	100.0
#100	0.0	100.0
Total	100.0	662.0

(Fineness modulus of coarse aggregate = $662.0/100 = 6.62$)

different test beams. 1/4" nominal diameter plain bars were used as web reinforcements. The two bars used in the compression zone as the stirrup-holder were also 1/4" diameter plain bars. The reinforcement bars, mentioned above were procured from the local market and were slightly undersized and the actual cross-sectional area of these bars were used for computations. Three specimens from each size of bars were tested as per ASTM A370-77. The test results are shown in table 4.3.

In figure 4.1, the stress-strain diagram of structural test specimen prepared from a 7/8" diameter bar is shown.

4.3 DESIGN OF CONCRETE MIX

There is no standard method for brick aggregate concrete mix design. However, in Bangladesh, available standard methods for designing crushed stone or gravel aggregate concrete mix are used for designing brick aggregate concrete mix. Here ACI method

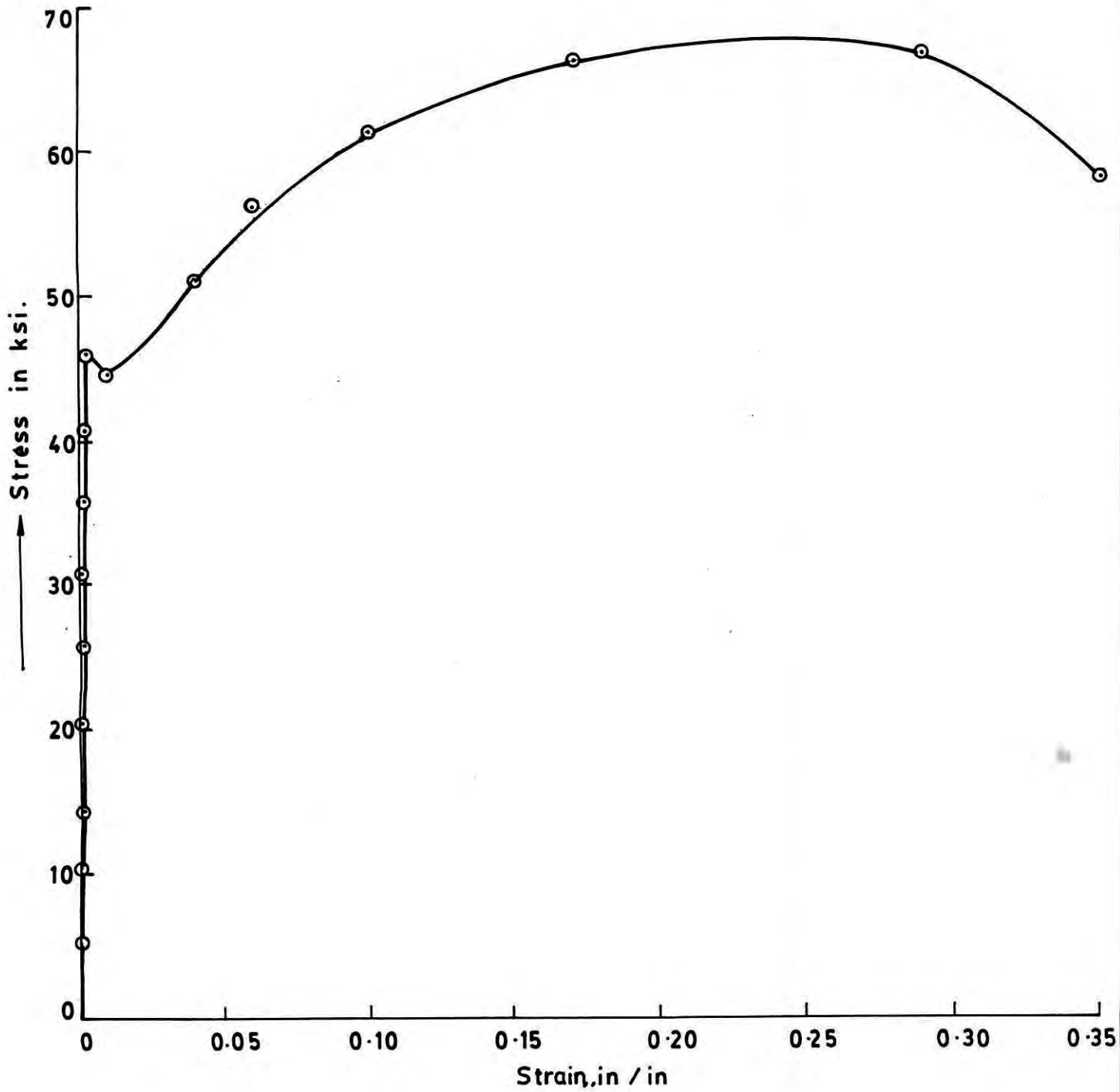


Fig. 4.1 Stress—Strain diagram of 7/8" dia steel bar

Table 4.3 Physical Properties of Reinforcements used in Test Beams

Bar size	Nominal diameter (inch.)	Average diameter (inch.)	Average area (sq.in.)	Average yield strength (psi)	Average ultimate strength (psi)	Average % elongation in 8" gauge length.
#8	1.0	0.9485	0.707	38700	60000	18 %
#7	0.875	0.8441	0.560	43400	63000	29 %
#6	0.75	0.70	0.385	42500	58000	17 %
#5	0.625	0.6117	0.294	51000	78000	19 %
#2	0.25	0.2613	0.0536	33000	53000	18 %

of proportioning was used. Maximum size of coarse aggregate used was 3/4" and the concrete mixes were designed for a mean target strength of 3000 psi strength. The mix proportion was :

Cement:Sand:Khoa = 1:2.2:2.7 (by weight) and the water/cement ratio was = 0.50.

Slump of the fresh concrete varied from 1.5" to 2.25".

The mix contents of each batch for the two series of beams (including cylinder specimens) are given in table 4.4.

Table 4.4 Contents of Concrete-mix Batch

Beam Series	Quantity (by wt.) of				Water-Cement ratio, w/c
	Cement lbs.	Sand lbs.	Brick aggregate lbs.	water lbs.	
DB - P	76.0	167.2	205.2	38.0	0.50
DB - Q	45.0	99.0	121.5	22.5	0.50

4.4 PREPARATION OF TEST BEAMS

4.4.1 Preparation of Moulds

Two moulds for casting of concrete deep beams were made by appropriate bolting of the steel plates. The size of the moulds were such that the concrete beams of sizes 6"x12"x33" and 6"x21"x33" can be prepared. Care was taken to keep the moulds approximately water-tight during casting of the test beams.

4.4.2 Prelude to the Test Beams

A total of fourteen rectangular deep beams divided into two series DB-P and DB-Q were designed to fail in shear. Each series consisted of seven beams. Nominal cross section of DB-P series of beams were 6"x21" while that of DB-Q series were 6"x12". The span to overall depth ratio of the former series was 1.0 and that of the latter was 2.0. The total length of beams of either series was kept invariable at 33". In all the beams, the vertical and the longitudinal web reinforcements were provided using 1/4 inch diameter mild steel bars. The spacings of horizontal web reinforcements used in different beams of each series were varied to know its effect on the strength of the beams. The area of flexural reinforcements used in different beams were varied to study their effect upon the strength of deep beams. The amount of vertical web reinforcement in each series of beams was kept constant.

Two 1/2" thick and 3"x6" mild steel plates were welded to either end of the flexural bars to prevent any premature bond failure (fig. 4.2). The centroid of the flexural reinforcements were maintained at 1.5" from the bottom face of the test beams.

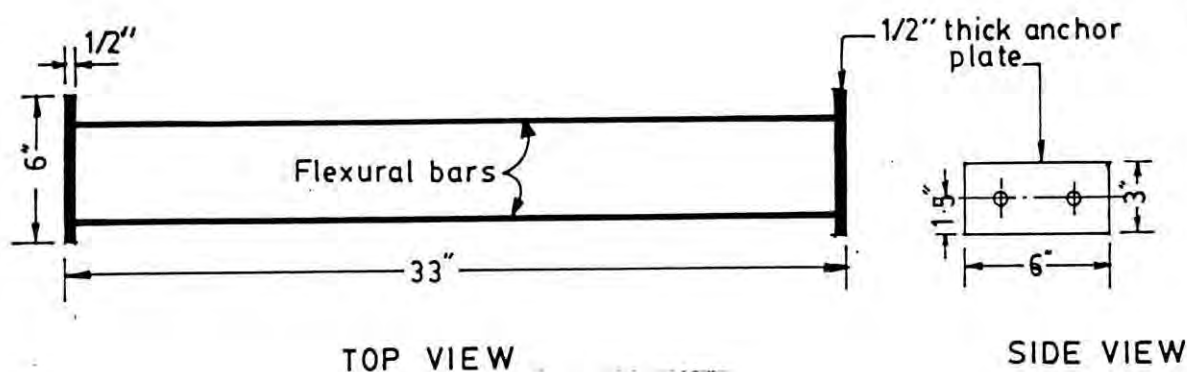


Fig. 4.2 Tension (flexural) steel assembly with anchor plates.

The beams were designed with the intention to achieve either diagonal tension or shear compression failure. To accomplish this the following procedures were adopted :

- (i) Flexural steel ratio was kept below the balanced steel ratio to check against the failure by crushing of concrete.
- (ii) Adequate flexural reinforcement was provided to safeguard against flexural tension failure prior to shear failure.
- (iii) Anchor plates were provided to prevent any premature bond failure of the tension (flexural) steel.

Thus in order to achieve shear failure the following relation was satisfied for all test beams -

$$M_{us} < M_{uf}$$

where,

M_{us} = the ultimate moment corresponding to available shear capacity.

M_{uf} = the ultimate moment capacity of the beam in flexure.

Design calculations were based on the ACI 318-89⁽¹⁾ Code provisions. In appendix-A, example of design of test beam DB-P1 is shown. Besides, in order to prevent the bearing failure, extra vertical and/or horizontal web reinforcements were provided near the supports of the beams according to ACI requirements.

4.4.3 Fabrication of the Test Beams

The arrangements of reinforcements for the test beams are shown in fig.4.3 through fig.4.16. Photographs of reinforcement assembly of DB-P1, and DB-Q1 are shown in fig.4.17 and fig.4.18 respectively.

On completion of the reinforcement assembly, certain selective locations on the reinforcements were prepared for the installation of electrical resistance strain gauges. The surfaces of the reinforcements at those locations were rubbed with sand-paper to remove rusts completely and then cleaned with cleaning solution and finally the selective surfaces were washed with clean water. Drying of the wet surfaces were done immediately after degreasing and cleaning operations.

Five millimeter 120 ohms "SHOWA" brand electrical resistance strain gauges were then installed on those prepared locations with the help of proper adhesive (F-3 type cementing fluid) and were left for 24 hrs. under certain pressure created by clips. After releasing the pressure, lead wires were soldered to the strain gauge leads.

The following measures were employed to protect the gauges from water present in concrete. Initially the gauges and open leads along with the portion of steel rod were wrapped around by scotch tapes. Care was taken so that no short-circuit is formed. Then the strain gauges were covered with covering putty AK22. Finally the covering putty AK22 was covered by plastic

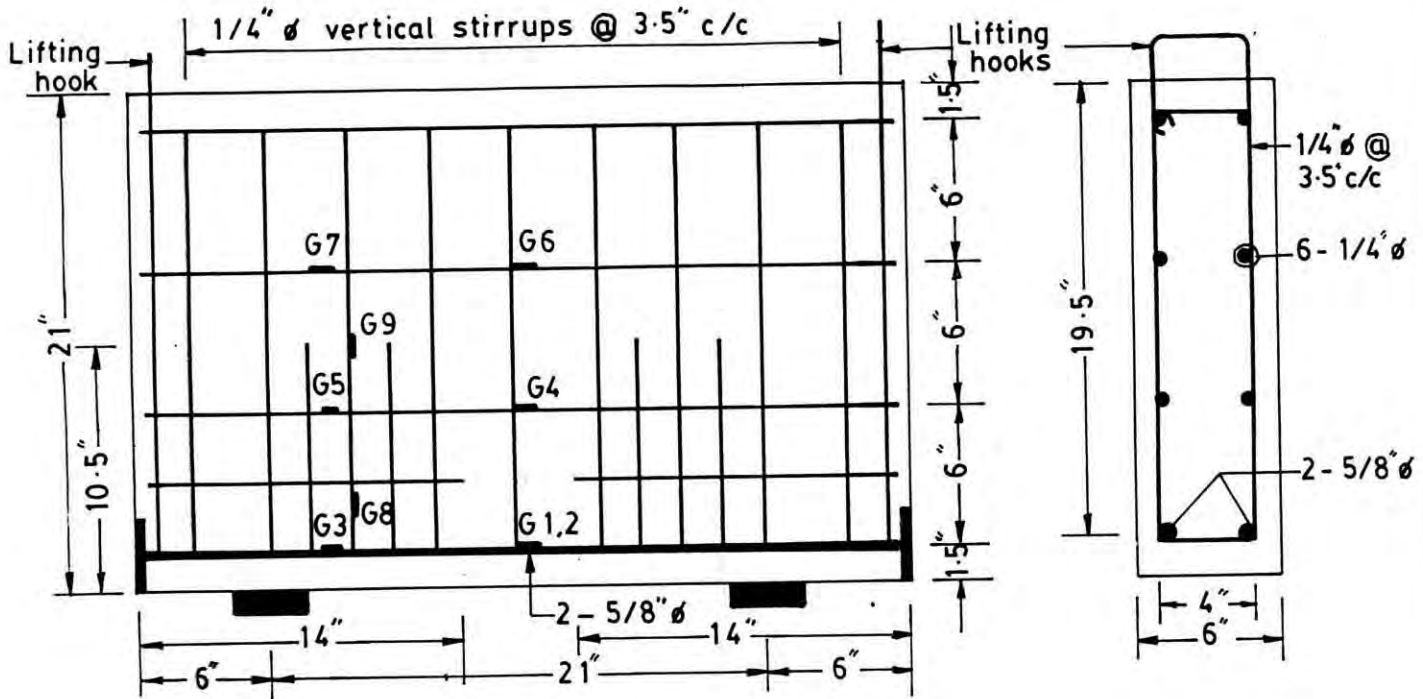


Fig. 4-3 Reinforcement arrangement of beam DB-P1

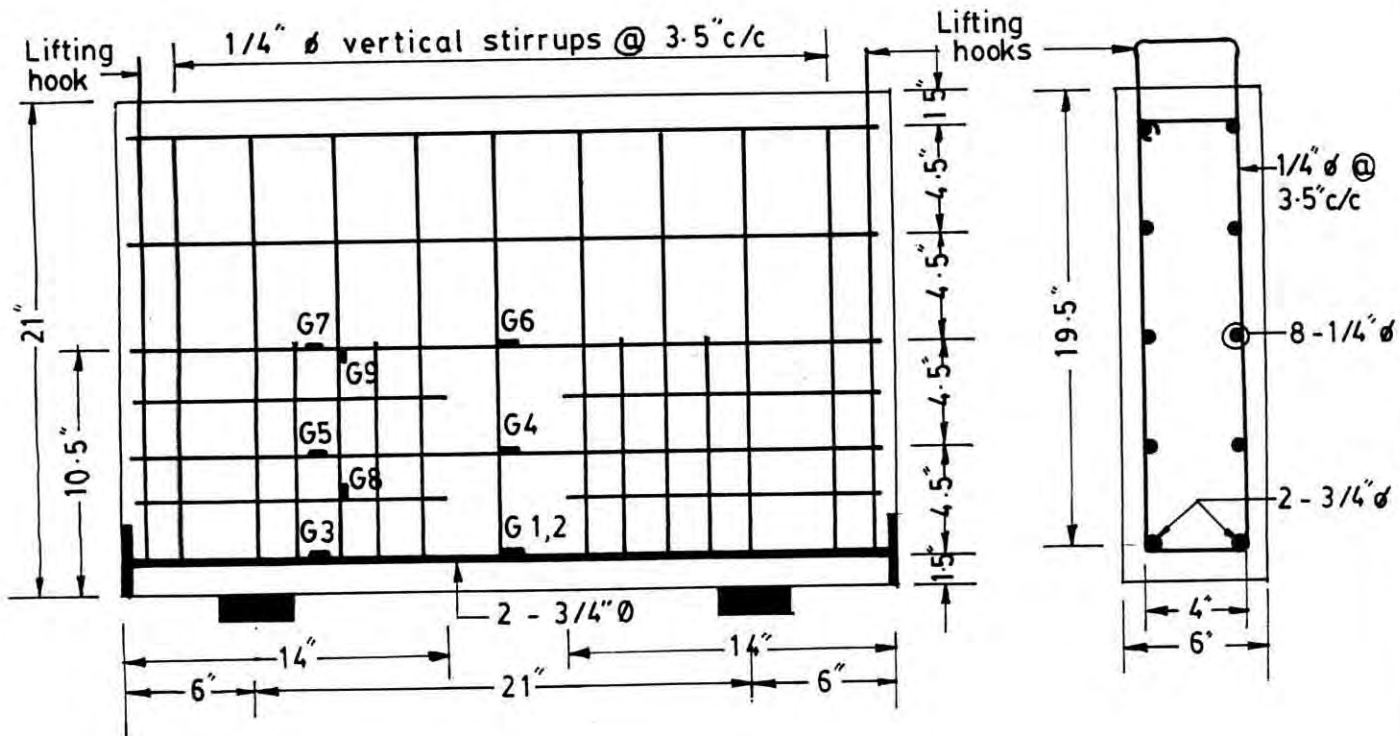


Fig. 4-4 Reinforcement arrangement of beam DB-P2

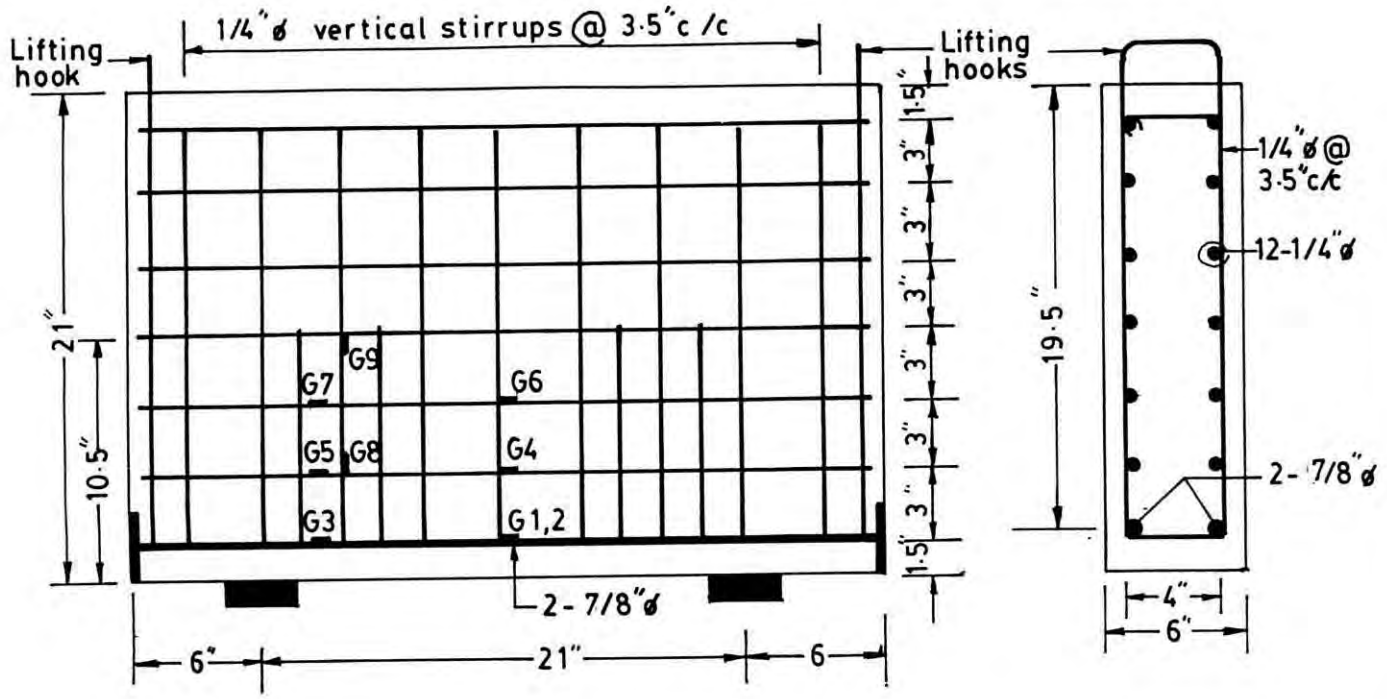


Fig. 4.5 Reinforcement arrangement of Beam DB-P3

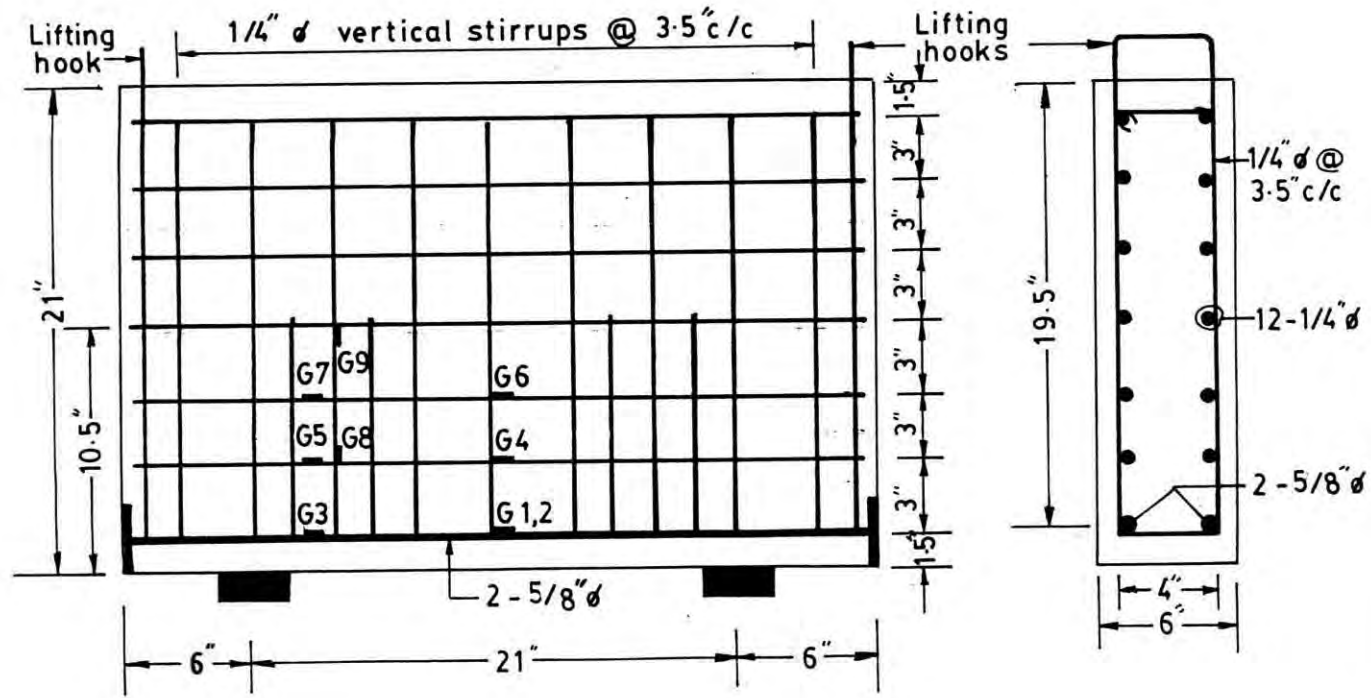


Fig. 4.6 Reinforcement arrangement of Beam DB-P4

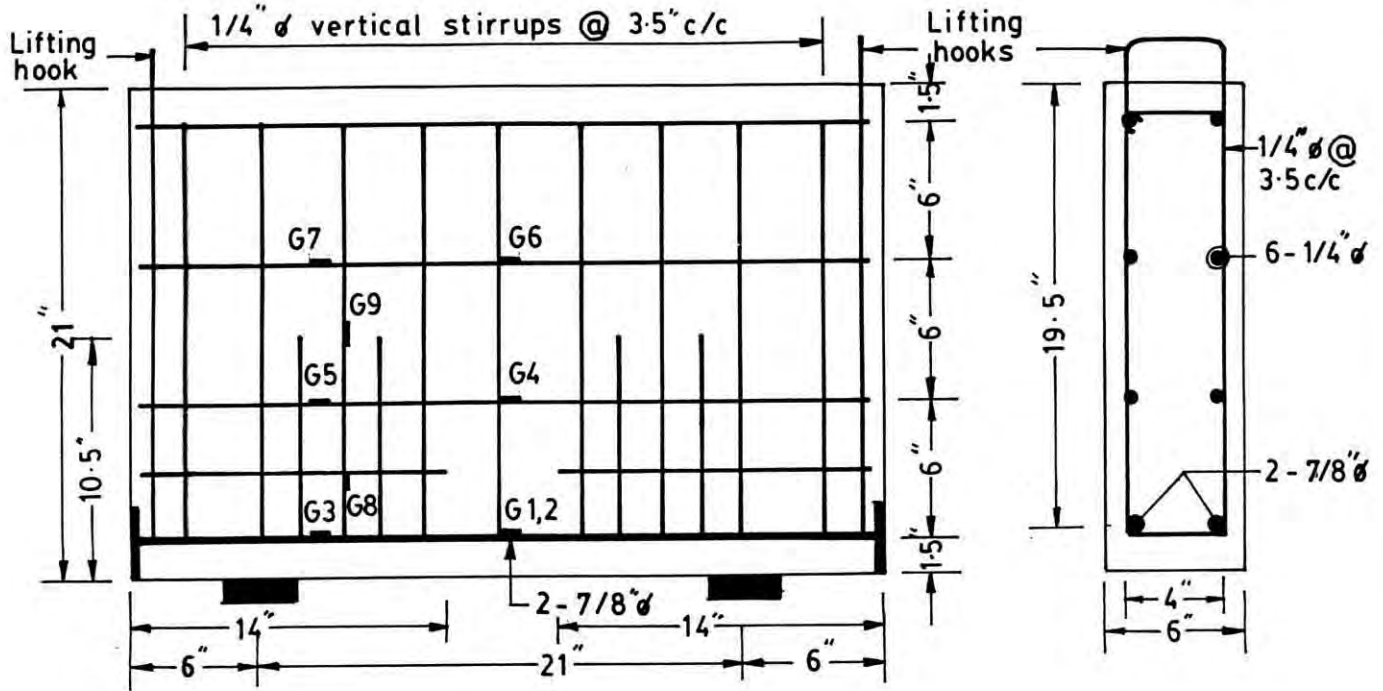


Fig. 4.7 Reinforcement arrangement of beam DB-P5

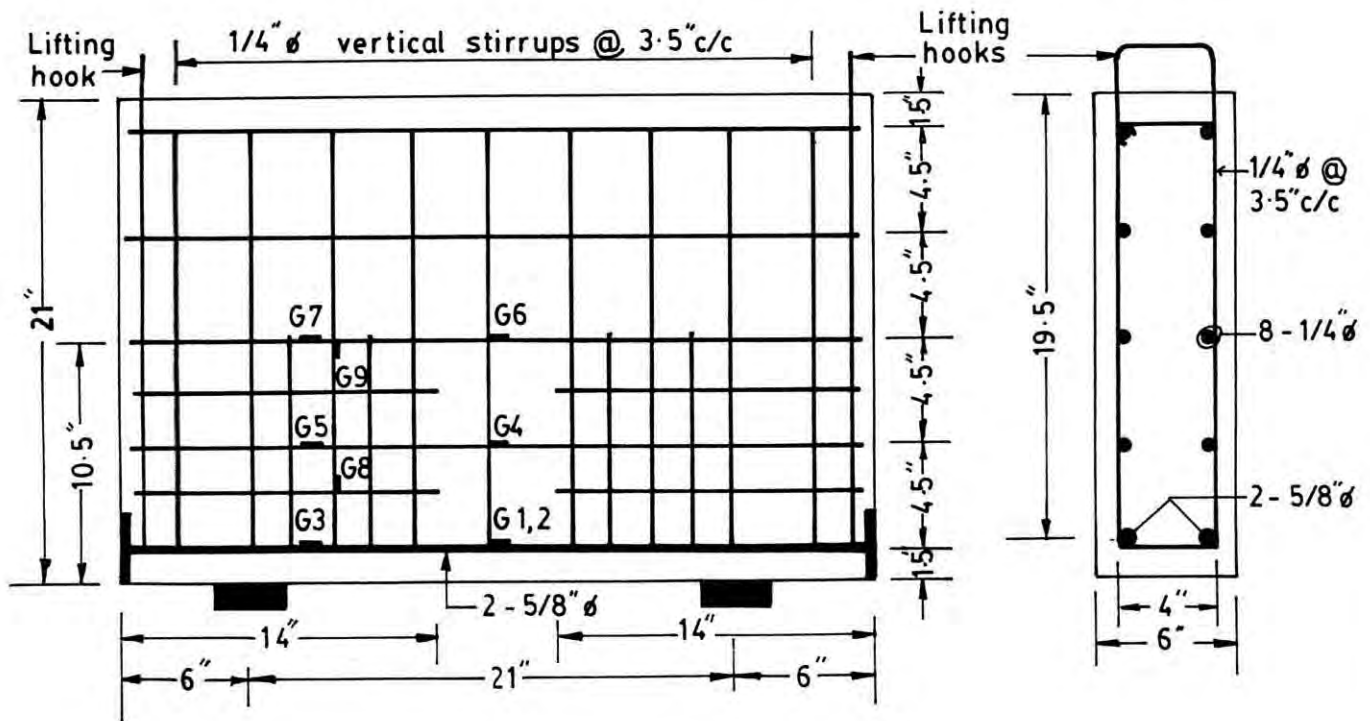


Fig. 4.8 Reinforcement arrangement of beam DB-P6

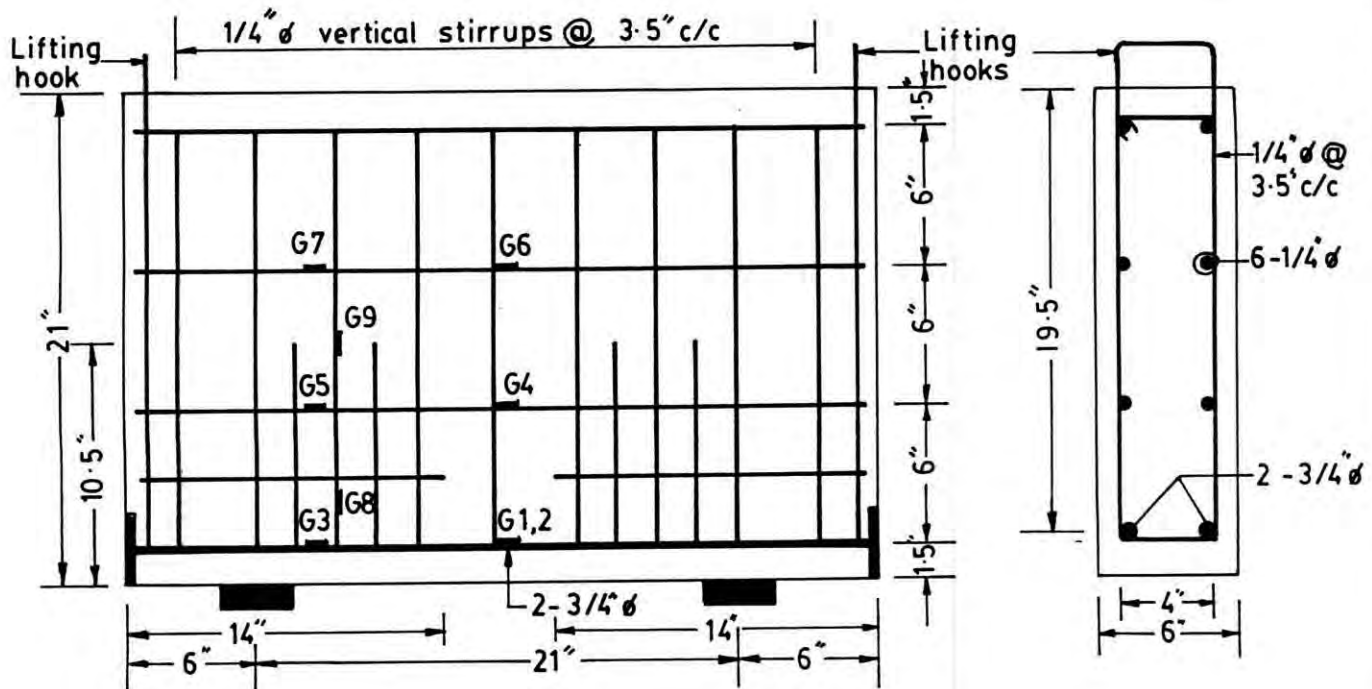


Fig. 4.9 Reinforcement arrangement of beam DB-P7

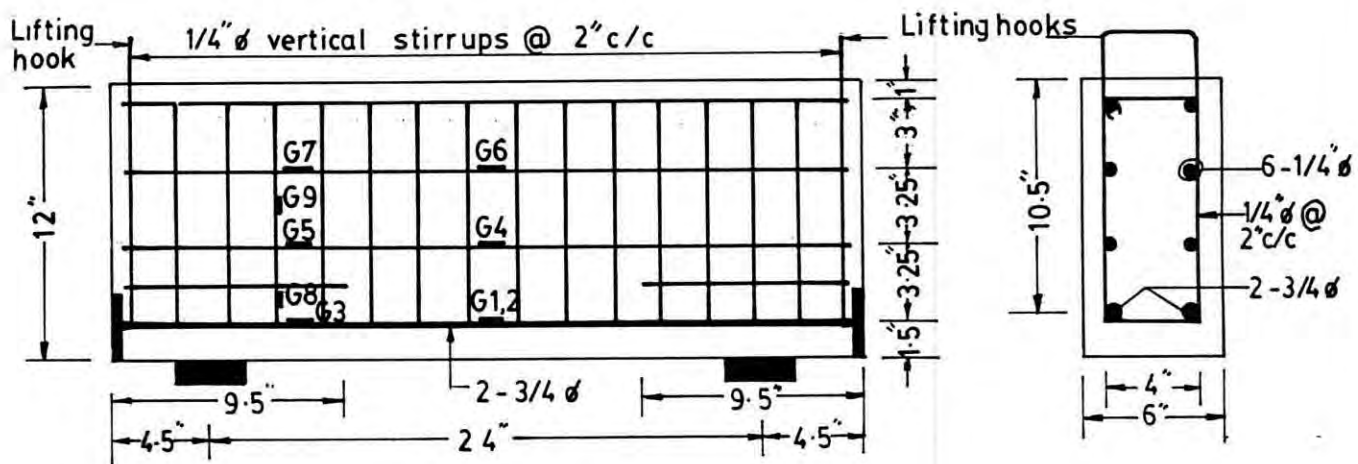


Fig. 4.10 Reinforcement arrangement of beam DB-Q1

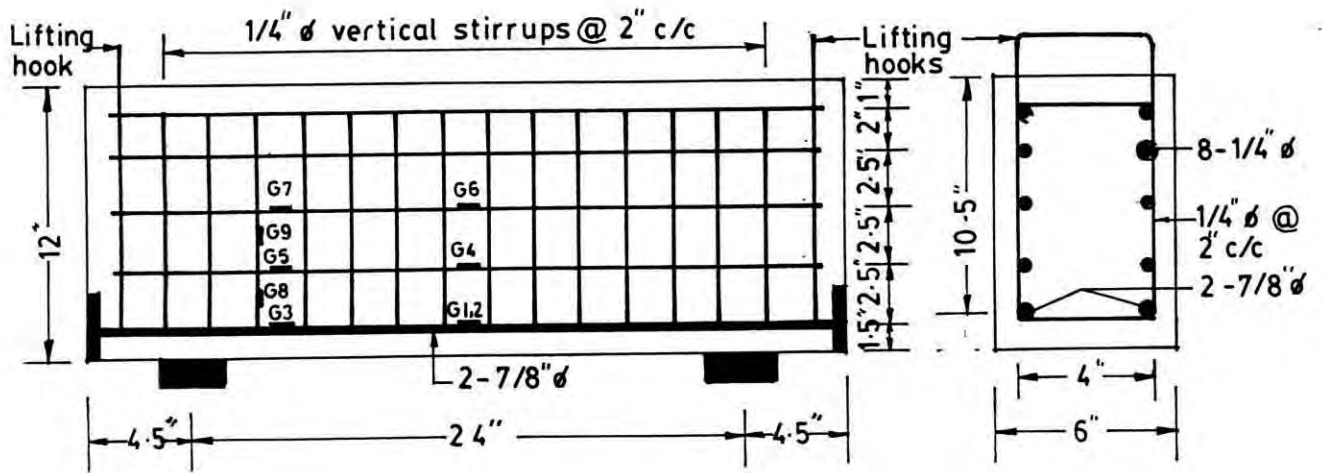


Fig. 4-11 Reinforcement arrangement of beam DB - Q2

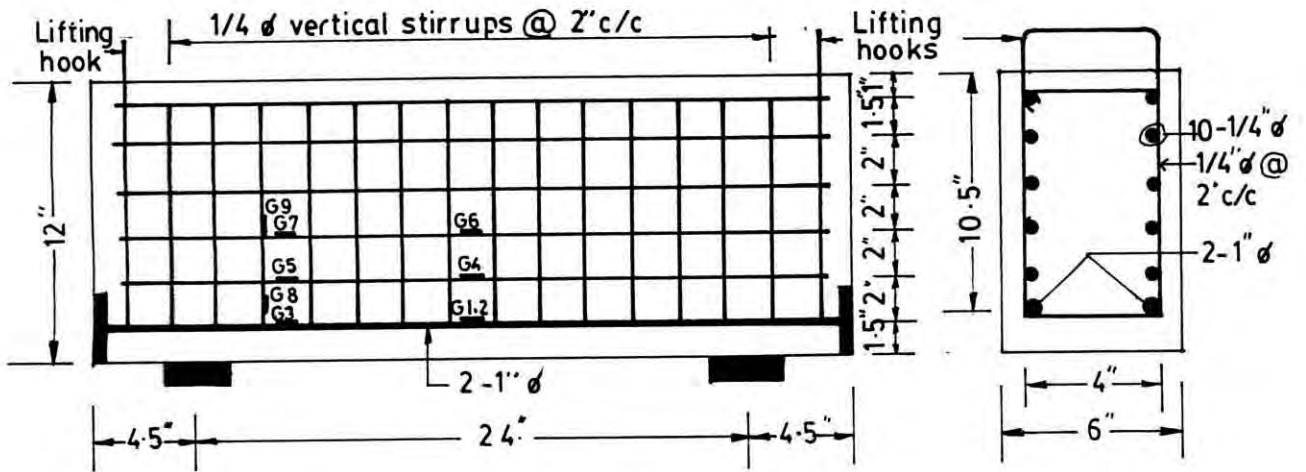


Fig. 4-12 Reinforcement arrangement of beam DB - Q3

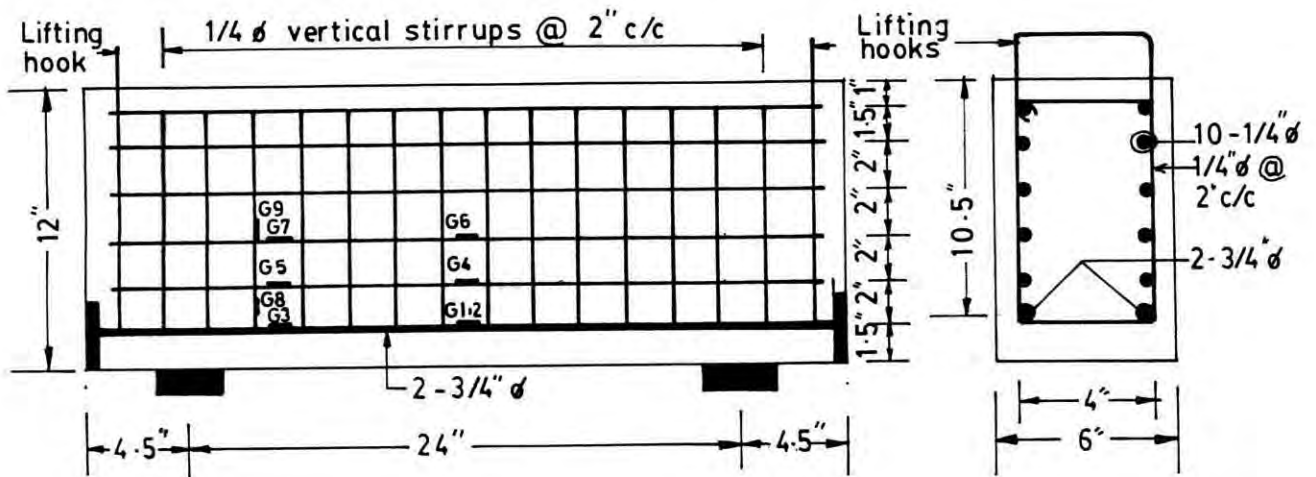


Fig. 4-13 Reinforcement arrangement of beam DB - Q4

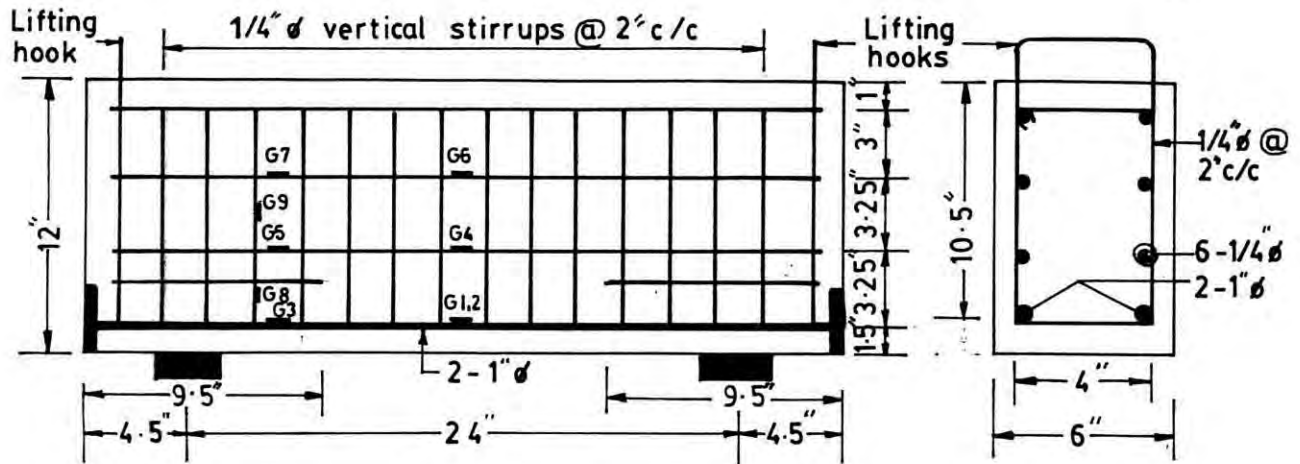


Fig. 4-14 Reinforcement arrangement of beam DB-Q5

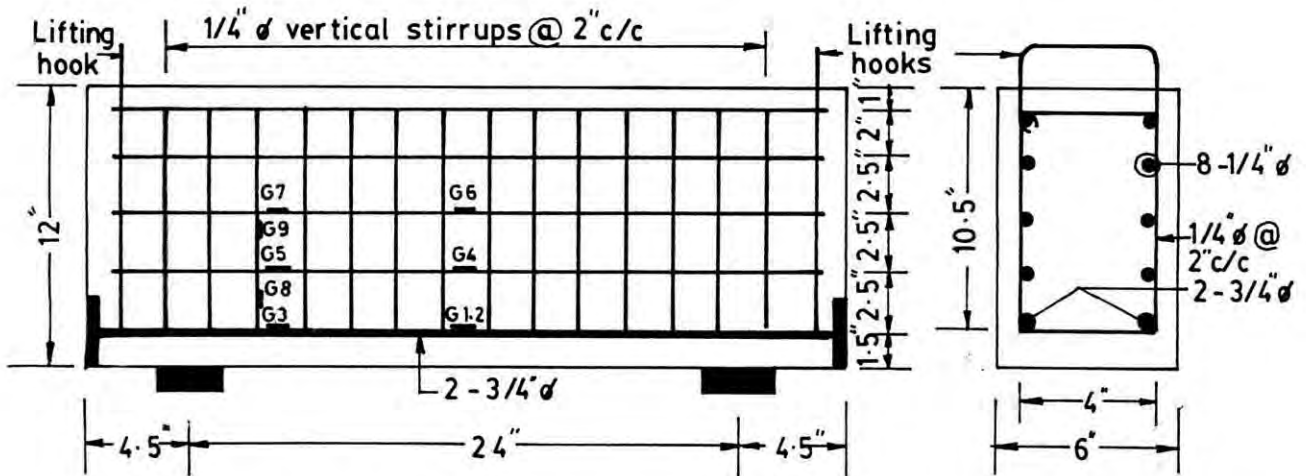


Fig. 4-15 Reinforcement arrangement of beam DB-Q6

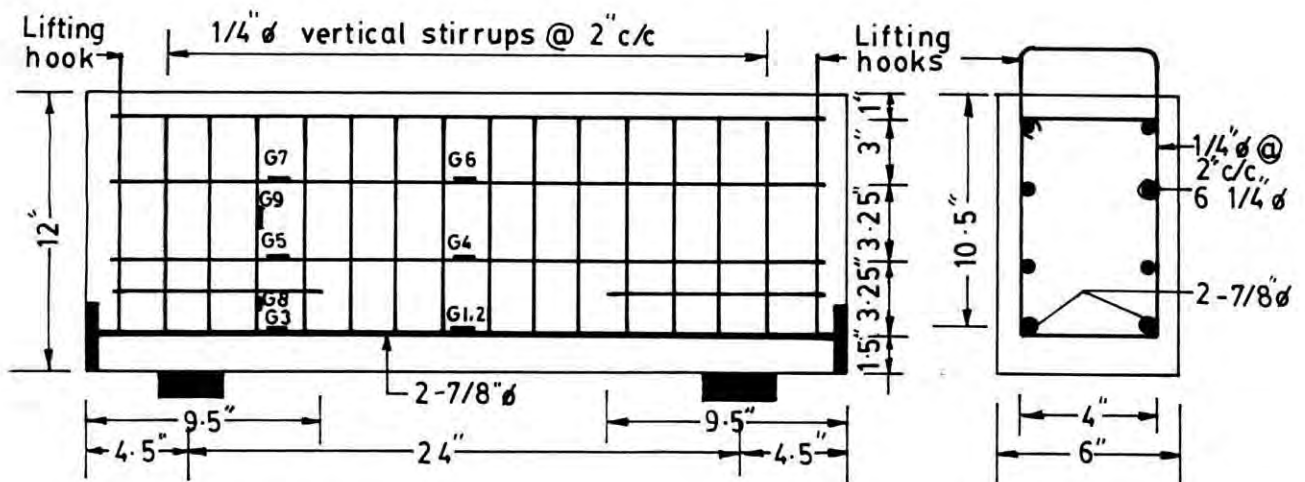


Fig. 4-16 Reinforcement arrangement beam DB-Q7



Fig. 4.17 Reinforcement Assembly for Beam DB-P1

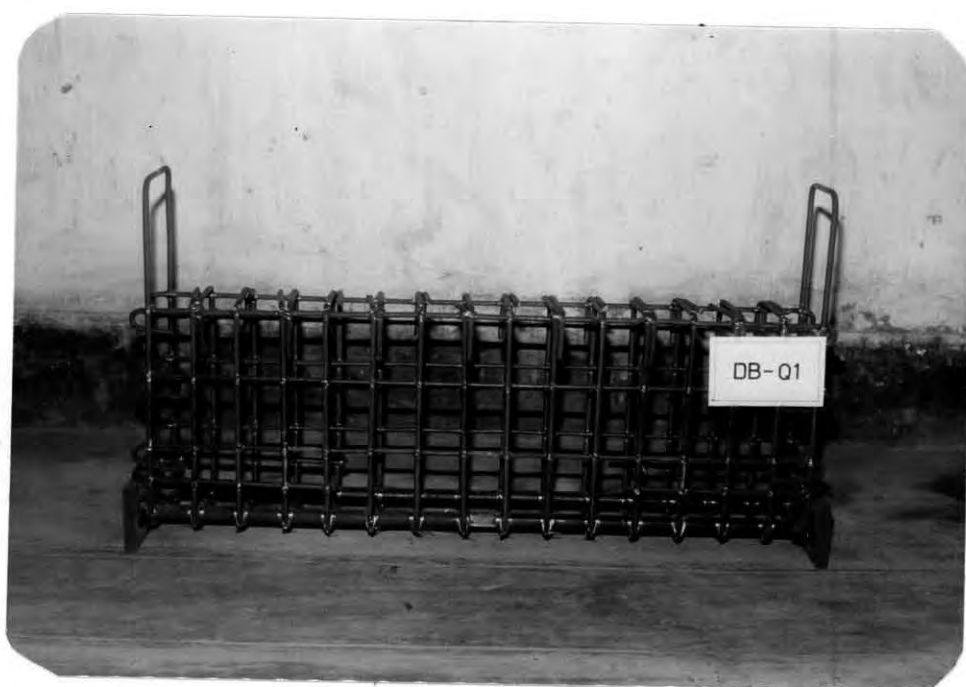


Fig. 4.18 Reinforcement Assembly for Beam DB-Q1

tape to protect the gauges and their coverings from any external disturbances. A tag with identification of the gauge location was tied to the free end of the lead wire.

Concrete mixes were prepared in the laboratory with mixer machine. In one day, two beams of two series were cast and 6(six) control cylinders were prepared. Compaction of concrete was achieved by vibrating the mould filled with fresh concrete on a table vibrator.

The beams were stripped off the moulds after about 48 hours of casting. Two extended stirrups were provided near the ends of each beam and these were used as lifting hooks. Curing of test beams were performed for 28 days by wrapping these with moist gunny bags. These gunny bags were moistened thrice daily. The control cylinders were kept under water for curing till the date of test.

4.5 TESTING OPERATIONS

4.5.1 Testing of Beams

The beams were subjected to uniformly distributed load applied at the top surface of the beams in a 400 Kip capacity Universal Testing Machine (hydraulic type) of the Structures Laboratory in the department of Civil Engineering, BUET, Dhaka. Two series of steel I-joists with rollers, steel plates, and rubber pads were employed as load transfer devices for the two series of beams. This system transferred the concentrated load from the machine into a uniformly distributed load system upon the top surface of the test beam. One of the reaction plates was rested on a steel block that itself was placed on the anvil of the testing machine. The other reaction plate was placed upon a steel block supported by 5/8" diameter steel rollers. These steel rollers were placed on a steel block which was supported on

the anvil of the Universal Testing Machine. Details of the arrangement stated above are shown in fig.4.19, and fig. 4.20. Photographs of the test set-up are shown in fig. 4.21 and fig. 4.22 .

Four deflectometers having smallest division of 0.01 mm were employed to measure the central deflection of the test beams. Two of the deflectometers were placed at the bottom surface of the beam at mid-span. The other two were placed under two plates each extended from one support to account for the support settlements. Deflectometer readings were recorded at each load increment and the mid-span deflection would be the difference of readings of the average of the mid-span deflectometers and the average of the end deflectometer readings. Strains in the flexural reinforcements and in the shear reinforcements were measured for all beams with 'SHOWA' brand electrical resistance strain gauges of 5 mm gauge length.

Each beam was initially loaded upto 5 Kips and then released. This operation was done before the deflectometer dials were set to zero to achieve an uniform and better setting of the beam specimen with the loading system.

The lead wires and cables coming from the strain gauges (set upon reinforcement bars into the test beam) and deflectometers were connected to the Scanner-Case (of type "San-ei 7901") which was then connected to the Datalogger of type "San-ei 7V08". The beam was then loaded and the readings of deflectometers and the strain gauges were recorded in a diskette (placed into the Datalogger) at each regular interval of load increment and this operation was continued until the failure of the test beam. Side by side we got the printout also as the Datalogger had the simultaneous recording and printing facilities.

Beams' surfaces were white washed on all surfaces to

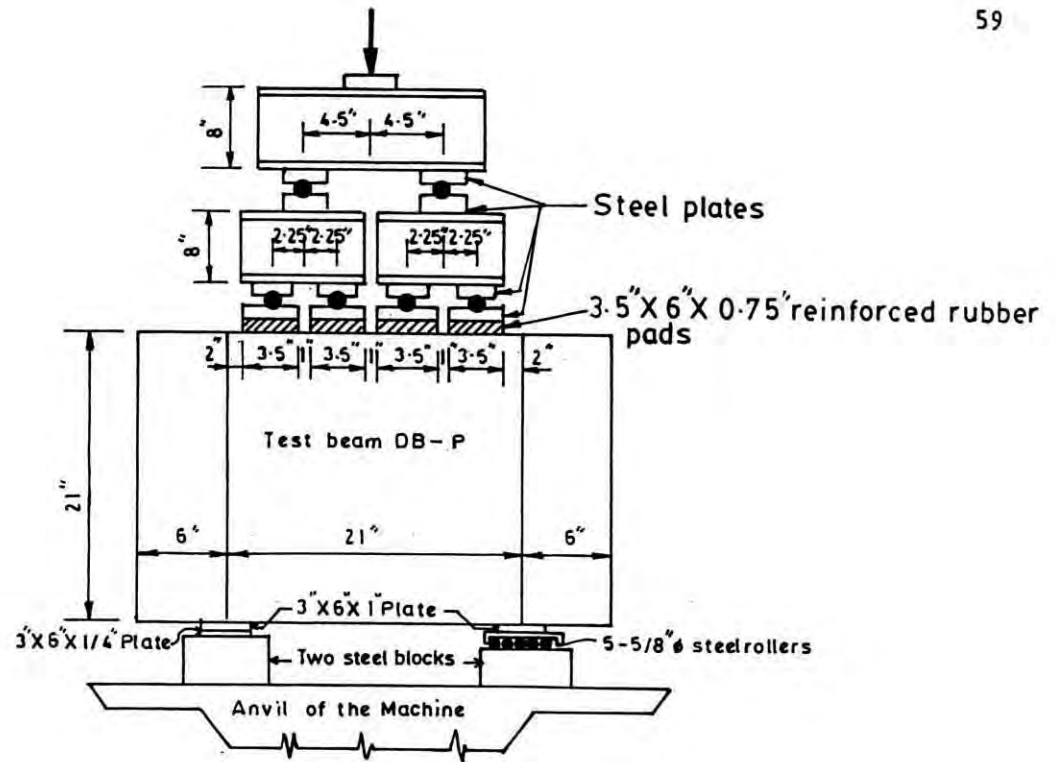


Fig. 4.19 Test set-up for loading of beam DB-P

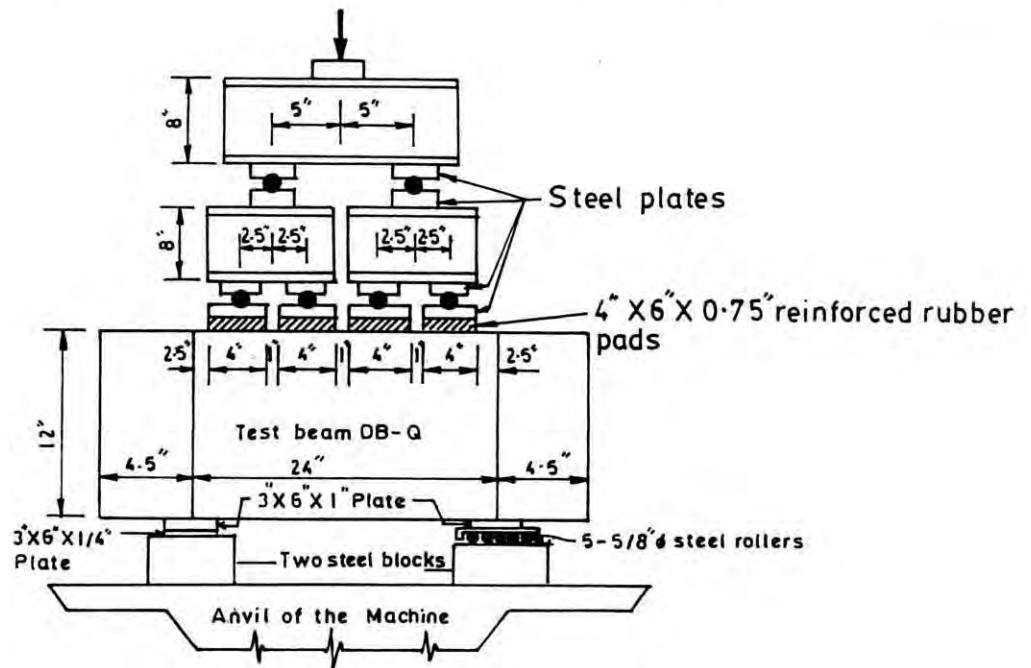


Fig. 4.20 Test set-up for loading of beam DB-Q

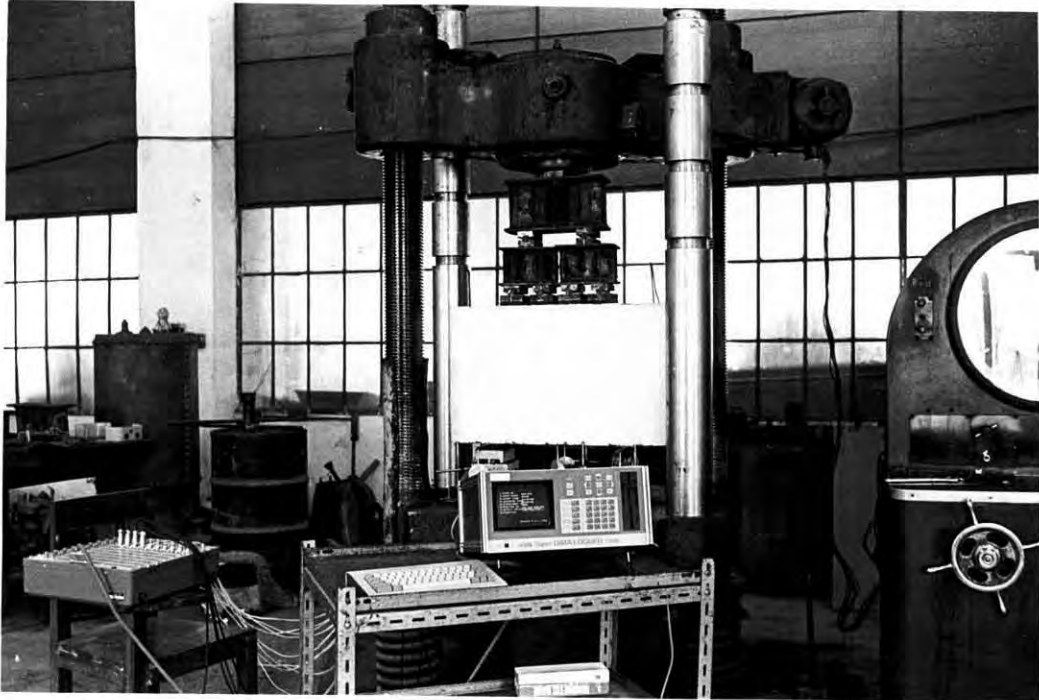


Fig. 4.21 Photograph of Test Set-up for Loading.

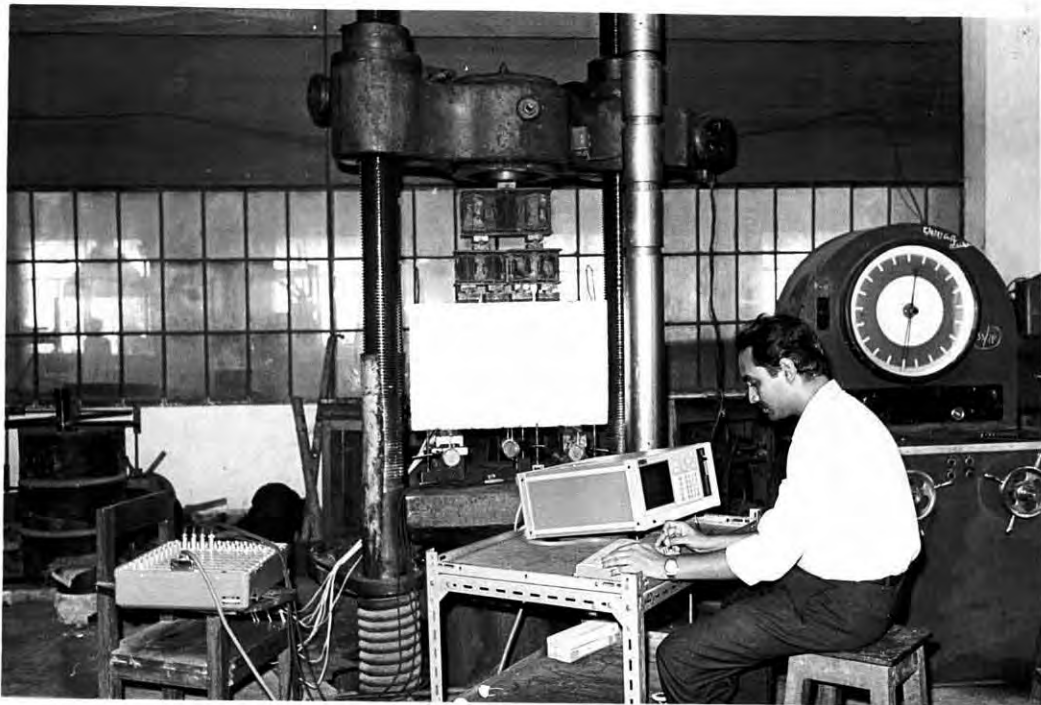


Fig. 4.22 Photograph of Beam Testing

facilitate visual observation of the propagation of cracks on the beam surfaces. A 3"-square grid mesh were drawn on the white washed face, between the supports only to establish the relative location of cracks with ease. A magnifying glass was used to help searching of cracks. Cracks were deeply marked with a soft pencil upon their formation on the beam surface and the load intensity at which it was formed was noted beside the crack.

4.5.2 Testing of control cylinders

Testing of the corresponding control cylinders were done on the same day as that of the test beams. For compressive strength determination, cylinders were capped before testing. Three of the cylinders cast along with each of the test beam were tested under axial compression to determine the average ultimate compressive strength (f'_c) of concrete. The remaining three cylinders were tested under diametral compression to find the split cylinder tensile strength (f'_{sp}) of concrete.

CHAPTER 5

TEST RESULTS

5.1 GENERAL

A total of 14 (fourteen) deep reinforced concrete beams were tested under uniformly distributed load applied at the top surfaces of the beams. The beams were divided into two series, each consisting of seven beams. The length to overall depth ratio of the two series of beams and the web reinforcement arrangements have been described in the preceding chapter. The test programme was undertaken to study the effects of variation of the flexural and the horizontal web reinforcements on the following characteristic parameters. These are :

- (i) The cracking load.
- (ii) The ultimate load.
- (iii) The cracking pattern.
- (iv) The mid-span deflections.
- (v) Stresses in reinforcements.

The specific observations of interest during the tests had been recorded and is being presented in this chapter.

5.2 SUMMARY OF THE TEST RESULTS

The critical load at diagonal tension cracking, the load at flexural cracking, the ultimate load, the deflections, and strains at the selective locations under different load intensities had all been recorded in a systematic manner during the test. For an easy grasp of the overall performance of the beams the test results are presented here in a tabular form. A general description of the contents of the different tables containing various test data seems necessary and is furnished below :

In table 5.1, properties of beams in DB-P series and DB-Q series are presented. It may be mentioned here that both vertical and horizontal web reinforcements were selected according to the minimum requirements of ACI 318-89 Code⁽¹⁾. According to this code, the flexural reinforcements for beams DB-P1 and DB-Q1 were provided to ensure shear failure. It is specified that the minimum vertical web steel ratio is 0.15% and minimum horizontal web steel ratio is 0.25%. However, the Code Specification states that the spacings of vertical web steel shall not exceed $d/5$ and those of horizontal web steel shall not exceed $d/3$. For the dimensions of the beams under study and 1/4" diameter bar as web reinforcement, the limits $d/5$ and $d/3$ govern the spacings for both of DB-P1 and DB-Q1. On the other hand, 6 other beams in each of the series DB-P and DB-Q, the amount of horizontal web steels were increased in relation to those of DB-P1 and DB-Q1 respectively. The variation in the amount of the flexural and the horizontal web reinforcements as percentages of ACI requirements is especially indicated in table 5.1.

The critical load (P_f) at flexural cracking, the load (P_{cr}) at the initiation of diagonal crack, the ultimate load (P_u) are all listed in table 5.2.

5.3 LOAD-DEFLECTION RECORDS

Mid-span deflections of test beams were recorded at a regular interval of increasing load with deflectometers (graduated in 0.01 mm division) placed at the bottom surfaces of the beams. Compensation was made for the support settlements by placing other similar deflectometers under two extended plates located at the bottom of the two supporting blocks. The net mid-span deflection was the average of the readings of two mid-span deflectometers minus the average of the readings of two deflectometers near supports. The observed loads and the

Table 5.1 Properties of Test Beams.

Beam mark	Span length L, in.	Measured overall depth D, in.	Measured beam width b, in.	Actual L/D	Nominal L/D	Flexural reinf. ratio, ρ_F	% Change of flexural reinf. over 1st. beam (ACI beam)	Web steel ratio		%change of vert. web reinf. over 1st. beam	%change of hor. web reinf. over 1st. beam	f'_c psi	f'_{sp} psi
								vertical ρ_v	horizontal ρ_h				
Series DB-P : L/D=1.0													
DB-P1	21	21.0	6.00	1.0	1.0	0.00503	---	0.00514	0.003	---	---	2510	240
DB-P2	21	21.0	6.063	1.0	1.0	0.00651	+29.4%	0.00509	0.00396	*-0.97%	+32.0%	2870	310
DB-P3	21	21.0	6.063	1.0	1.0	0.00947	+88.3%	0.00509	0.00594	*-0.97%	+98.0%	2930	325
DB-P4	21	21.0	6.188	1.0	1.0	0.00487	*-3.2%	0.0050	0.00582	*-2.72%	+94.0%	2920	395
DB-P5	21	21.0	6.125	1.0	1.0	0.00938	+86.5%	0.00504	0.00294	*-1.95%	*-2.0%	2930	338
DB-P6	21	21.0	6.125	1.0	1.0	0.00492	*-2.2%	0.00504	0.00392	*-1.95%	+30.67%	2890	350
DB-P7	21	21.0	6.125	1.0	1.0	0.00645	+28.2%	0.00504	0.00294	*-1.95%	*-2.0%	2730	320
Series DB-Q : L/D=2.0													
DB-Q1	24	12.18	6.125	1.97	2.0	0.01197	---	0.00882	0.00543	---	---	2510	240
DB-Q2	24	12.18	6.063	1.97	2.0	0.01759	+46.95%	0.00891	0.00713	*+1.02%	+31.31%	2870	310
DB-Q3	24	12.06	6.063	1.99	2.0	0.02221	+85.55%	0.00891	0.00891	*+1.02%	+64.09%	2930	325
DB-Q4	24	12.30	6.125	1.95	2.0	0.01197	0.0	0.00882	0.00882	0.0	+62.43%	2920	395
DB-Q5	24	12.30	6.063	1.95	2.0	0.02221	+85.55%	0.00891	0.00548	*+1.02%	*+0.92%	2930	338
DB-Q6	24	12.24	6.188	1.96	2.0	0.1185	*-1.0%	0.00873	0.00698	*-1.02%	+28.55%	2890	350
DB-Q7	24	12.37	6.00	1.94	2.0	0.01778	+48.54%	0.009	0.00554	*+2.04%	*+2.03%	2730	320

f'_c = Compressive strength of concrete ; and f'_{sp} = Splitting tensile strength of concrete.

*The change was considered as zero but this small amount of change appears due to the unintentional change in beam size during casting.

Table 5.2 Observed Cracking and Ultimate Loads of Test Beams.

Beam mark	Concrete crushing strength f'_c , psi	Flexural cracking load P_f , kip	Diagonal cracking load P_{cr} , kip	Ultimate load P_u , kip
Series DB-P : L/D=1.0				
DB-P1	2510	90	80	166
DB-P2	2870	120	90	210
DB-P3	2930	120	110	222
DB-P4	2920	100	90	183
DB-P5	2930	100	90	187
DB-P6	2890	80	90	200
DB-P7	2730	110	80	175
Series DB-Q : L/D=2.0				
DB-Q1	2510	40	55	118
DB-Q2	2870	50	50	150
DB-Q3	2930	50	50	170
DB-Q4	2920	40	50	136
DB-Q5	2930	50	80	135
DB-Q6	2890	30	30	133
DB-Q7	2730	40	30	130

corresponding mid-span deflections of test beams are given in table 5.3.

The observed and the theoretical deflections (considering cracked section and using the deflection formula for shallow beams) and load records of the test beams are presented graphically in figures 5.1 through 5.4 .

5.4 STRESSES IN REINFORCEMENTS

Observed strains at different gauge locations inside the test beams (gauges were placed upon reinforcement bars only) were recorded at each interval of increasing load with the " San-ei SCANNER CASE 7901" Scanner and the "San-ei Super DATA LOGGER 7V08" . From these readings the corresponding stresses in the flexural as well as in the web reinforcements are calculated.

5.5 GENERAL CRACK PATTERN

The surfaces of test beams were white-washed so that every hairline crack would be visible. During the testing of beams the propagation of cracks on the beam surfaces were marked with a soft pencil (2B type). The amount of the applied load (at the end of each increment of additional load) causing the crack was written at the end of that crack on the beam surface. The crack patterns as observed on different test beams' surfaces have been reproduced in drawings and are presented in figures 5.5 through 5.18 and the photographs follow in figures 5.19 through 5.32 .

Table 5.3 Observed maximum deflections (at mid-span) of Test Beams.

Beam mark	Maximum deflection (mm) of the beam at the applied load level of																			
	0 ^k	10 ^k	20 ^k	30 ^k	40 ^k	50 ^k	60 ^k	70 ^k	80 ^k	90 ^k	100 ^k	110 ^k	120 ^k	130 ^k	140 ^k	150 ^k	160 ^k	170 ^k	180 ^k	190 ^k
Series DB-P : L/D=1.0																				
DB-P1	0.0	0.06	0.09	0.13	0.17	0.21	0.26	0.30	0.36	0.46	0.54	0.65	0.74	0.85	0.97	1.16	1.47	2.0	--	--
DB-P2	0.0	0.11	0.09	0.08	0.08	0.10	0.12	0.14	0.15	0.19	0.23	0.28	0.33	0.37	0.43	0.48	0.56	0.64	0.72	0.83
DB-P3	0.0	0.25	0.27	0.32	0.34	0.40	0.42	0.44	0.49	0.50	0.56	0.59	0.66	0.69	0.76	0.80	0.84	0.93	1.02	1.09
DB-P4	0.0	0.26	0.43	0.53	0.62	0.68	0.74	0.79	0.85	0.93	1.01	1.06	1.14	1.22	1.28	1.44	1.57	1.78	2.29	2.73
DB-P5	0.0	0.21	0.33	0.40	0.47	0.53	0.59	0.64	0.70	0.78	0.87	0.95	1.01	1.10	1.23	1.30	1.48	1.66	2.01	2.64
DB-P6	0.0	0.25	0.27	0.30	0.31	0.34	0.37	0.40	0.43	0.47	0.51	0.59	0.67	0.75	0.83	0.91	1.03	1.15	1.27	1.34
DB-P7	0.0	0.29	0.43	0.52	0.60	0.64	0.69	0.73	0.78	0.83	0.90	0.98	1.07	1.16	1.26	1.42	1.73	2.23	2.65	--
Series DB-Q : L/D=2.0																				
DB-Q1	0.0	0.17	0.27	0.38	0.50	0.58	0.69	0.84	0.96	1.14	1.31	1.67	2.22	--	--	--	--	--	--	--
DB-Q2	0.0	0.07	0.12	0.13	0.15	0.18	0.20	0.25	0.28	0.35	0.42	0.51	0.64	0.78	1.05	2.11	--	--	--	--
DB-Q3	0.0	-0.05	0.06	0.15	0.23	0.30	0.41	0.49	0.58	0.67	0.78	0.87	0.98	1.08	1.22	1.41	1.66	2.52	--	--
DB-Q4	0.0	-0.14	-0.09	-0.05	0.04	0.10	0.19	0.29	0.40	0.51	0.65	0.84	1.09	1.56	1.96	--	--	--	--	--
DB-Q5	0.0	0.16	0.33	0.46	0.57	0.68	0.82	0.96	1.12	1.27	1.44	1.66	1.88	2.32	2.85	--	--	--	--	--
DB-Q6	0.0	0.14	0.27	0.41	0.61	0.78	0.94	1.10	1.26	1.42	1.60	1.80	2.07	2.71	3.41	--	--	--	--	--
DB-Q7	0.0	-0.10	0.14	0.36	0.54	0.68	0.82	0.93	1.06	1.18	1.34	1.54	1.84	2.25	--	--	--	--	--	--

LEGEND

- Observed deflection
- △ Computed deflection

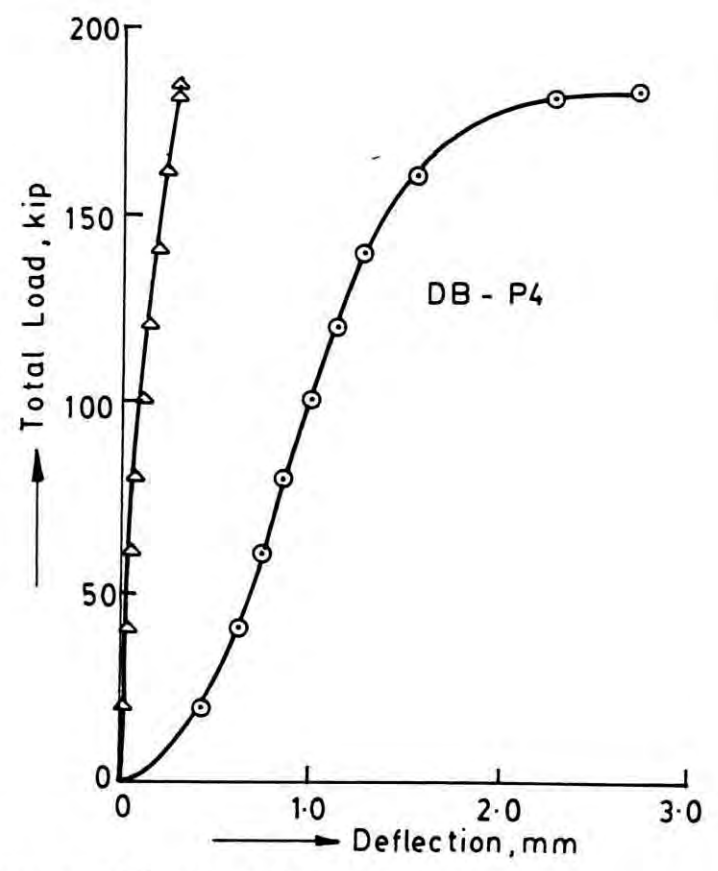
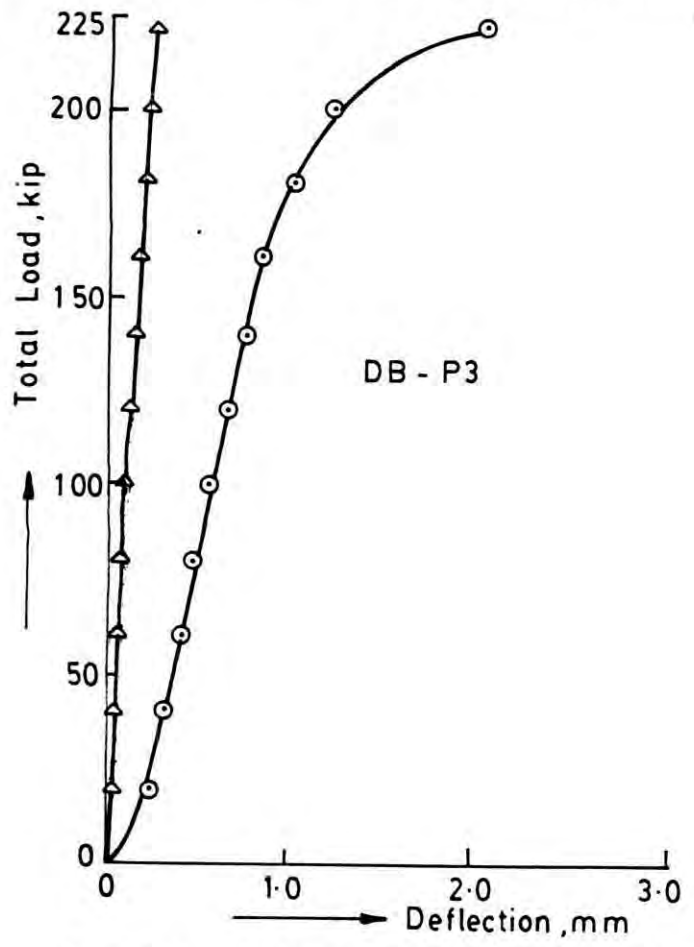
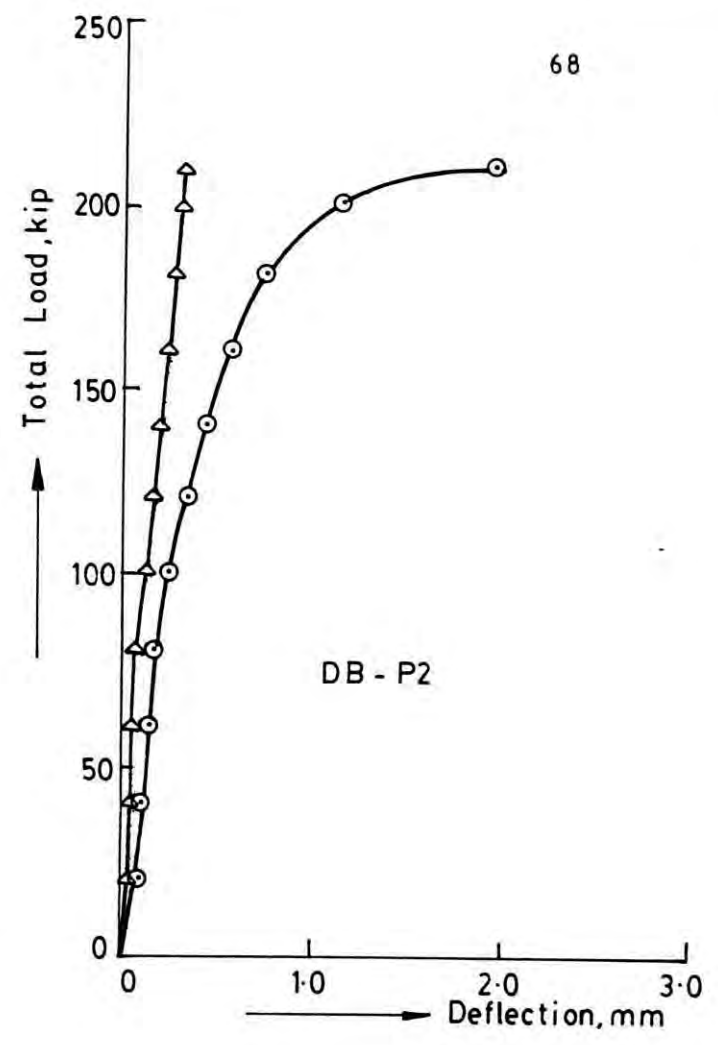
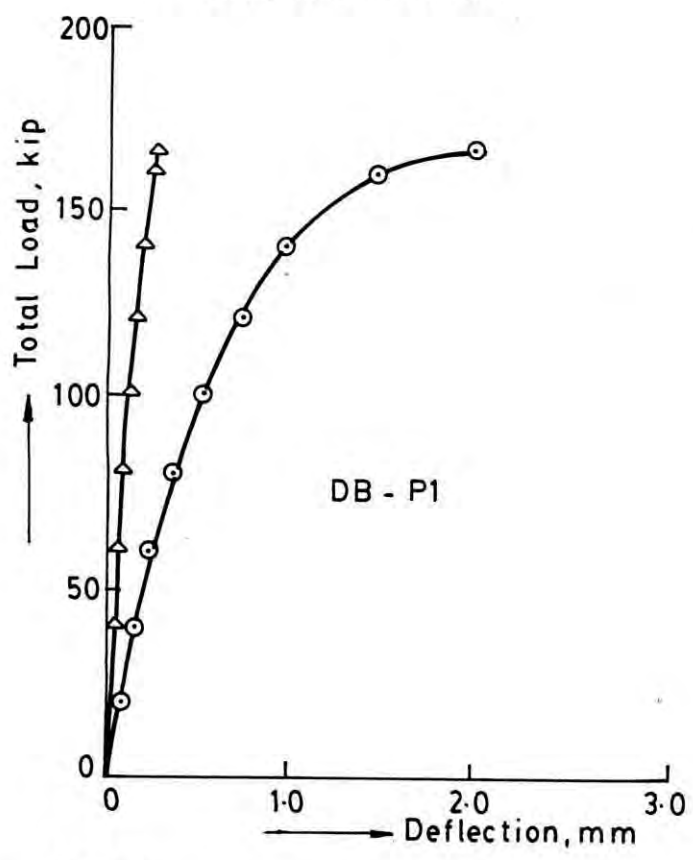


Fig. 5.1 Load Deflection Curves for Beams DB-P1, P2, P3, P4

LEGEND

- Observed deflection
 △ Computed deflection

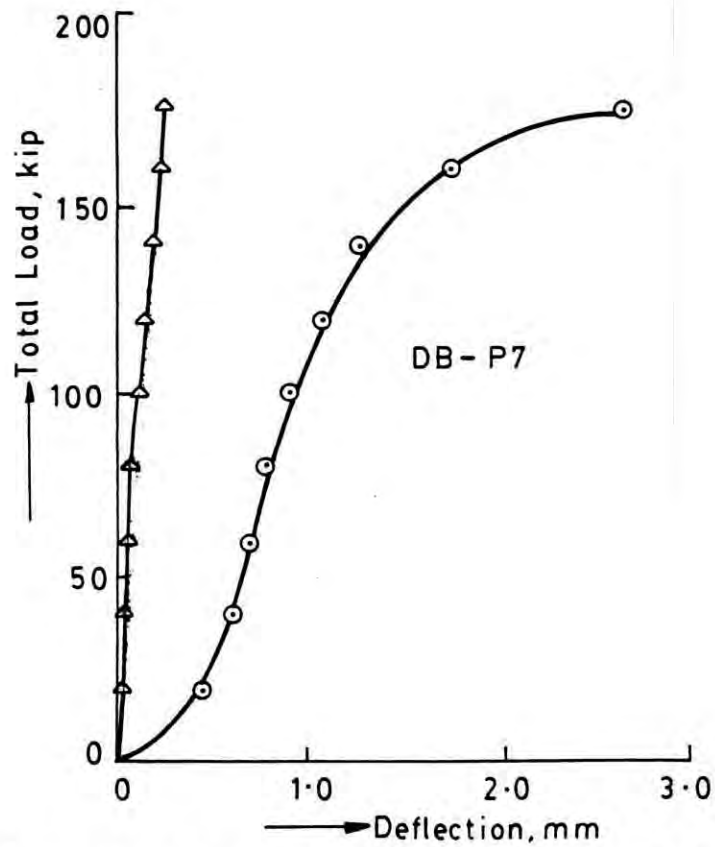
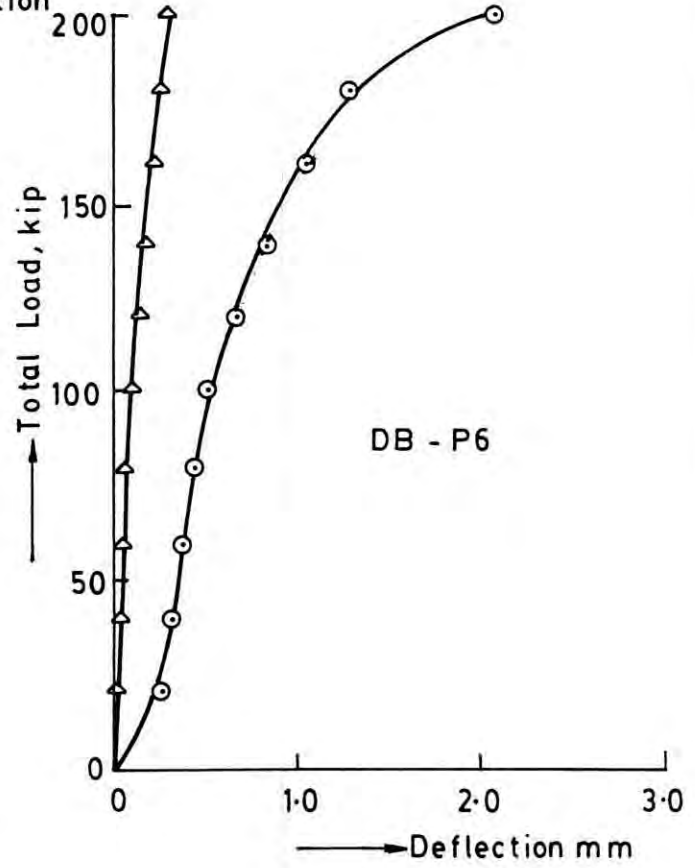
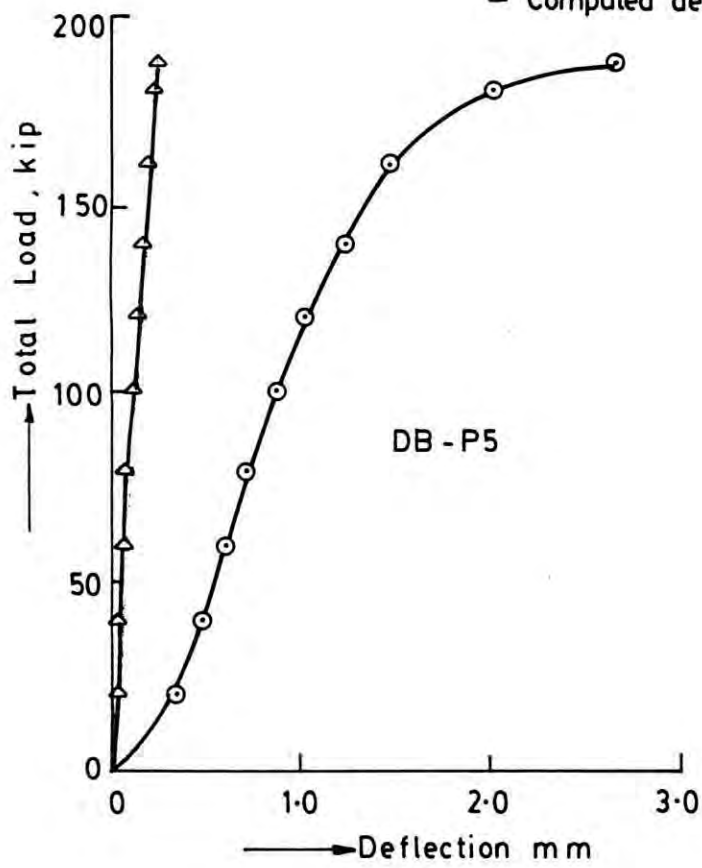


Fig. 5.2 Load Deflection Curves for Beams DB-P5, P6, P7

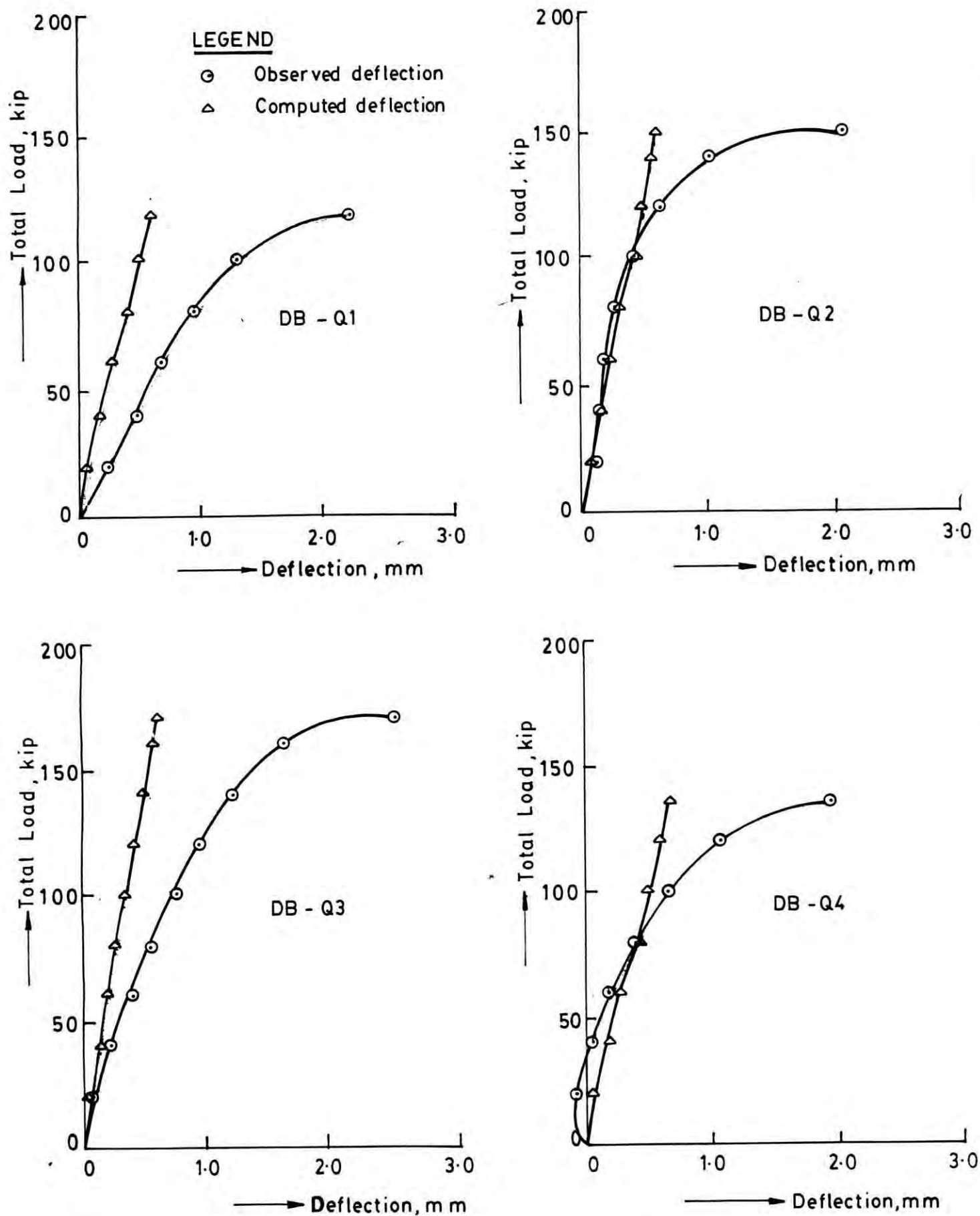


Fig. 5-3 Load Deflection Curves for Beams DB-Q1, Q2, Q3, Q4

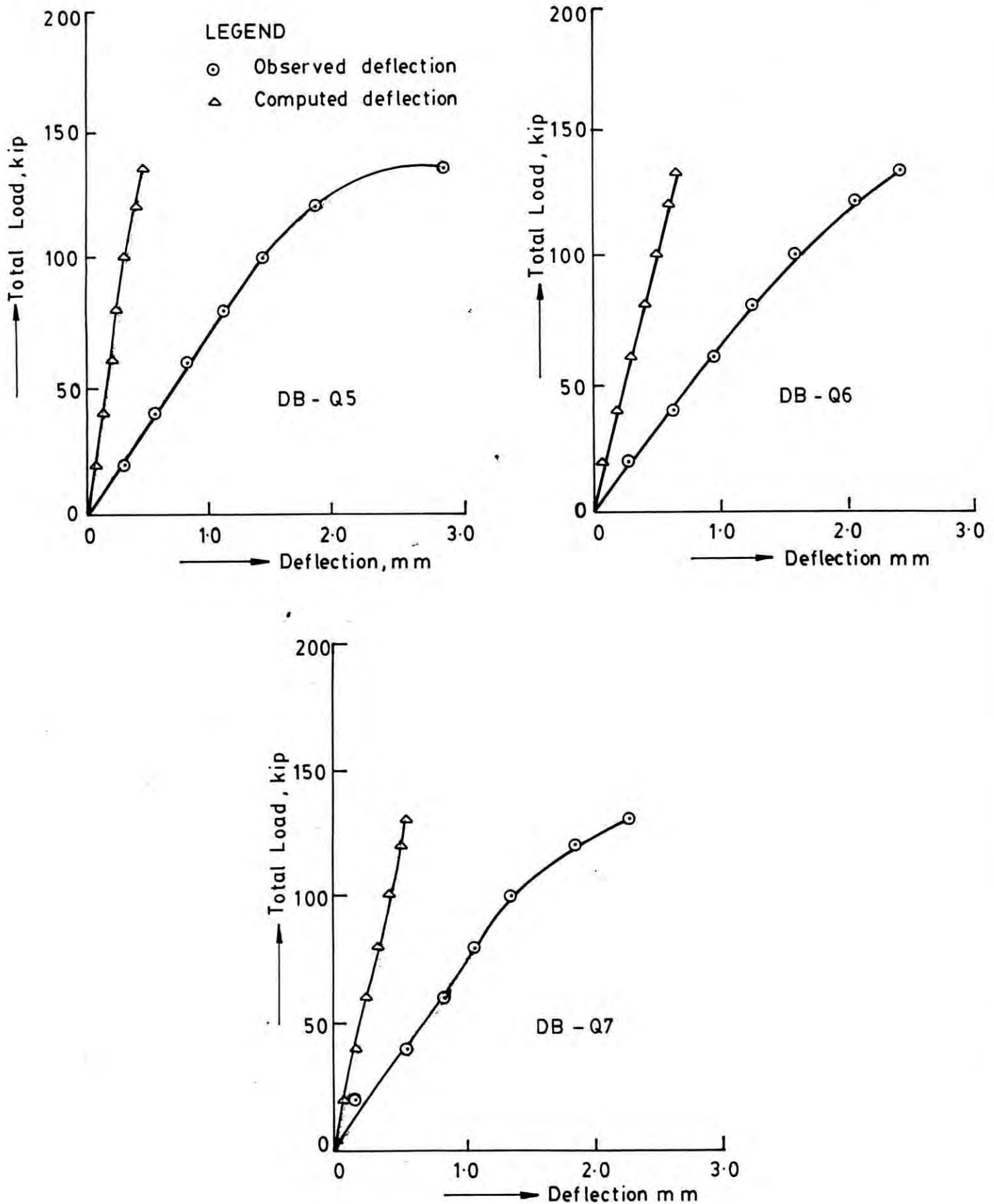


Fig. 5.4 Load Deflection Curves for Beams DB-Q5, Q6, Q7

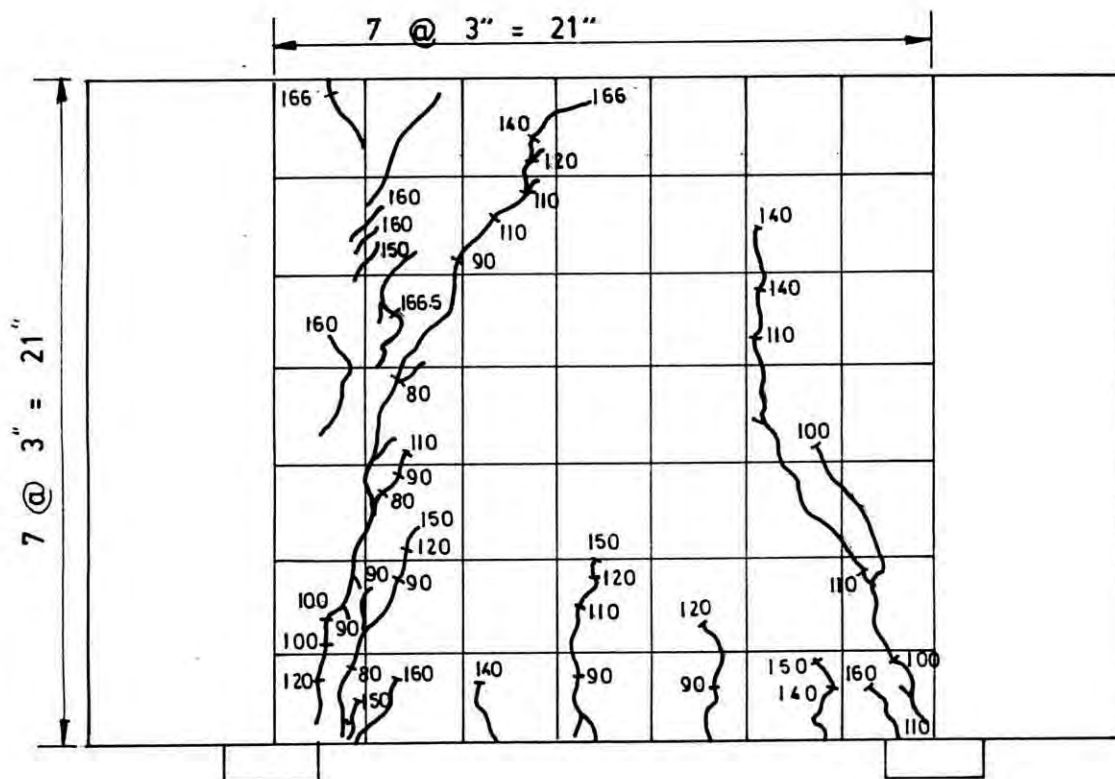


Fig. 5.5 Crack pattern of beam DB-P1

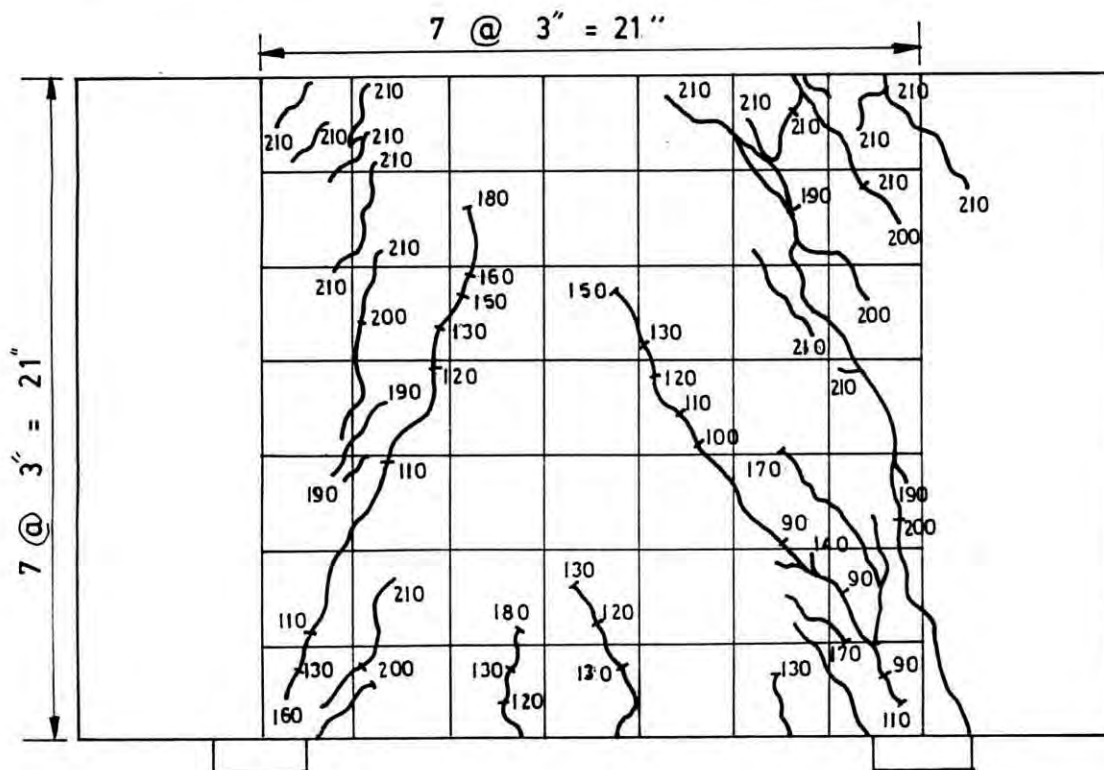


Fig. 5.6 Crack pattern of beam DB-P2

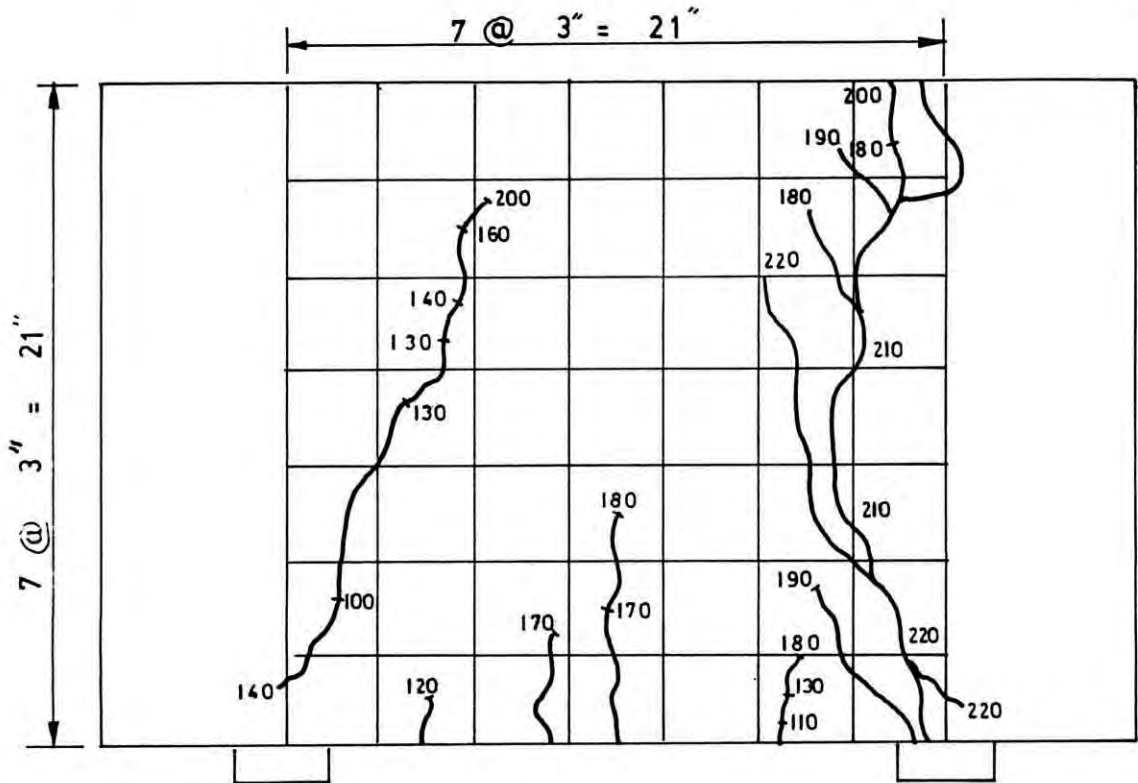


Fig. 5.7 Crack pattern of beam DB-P3

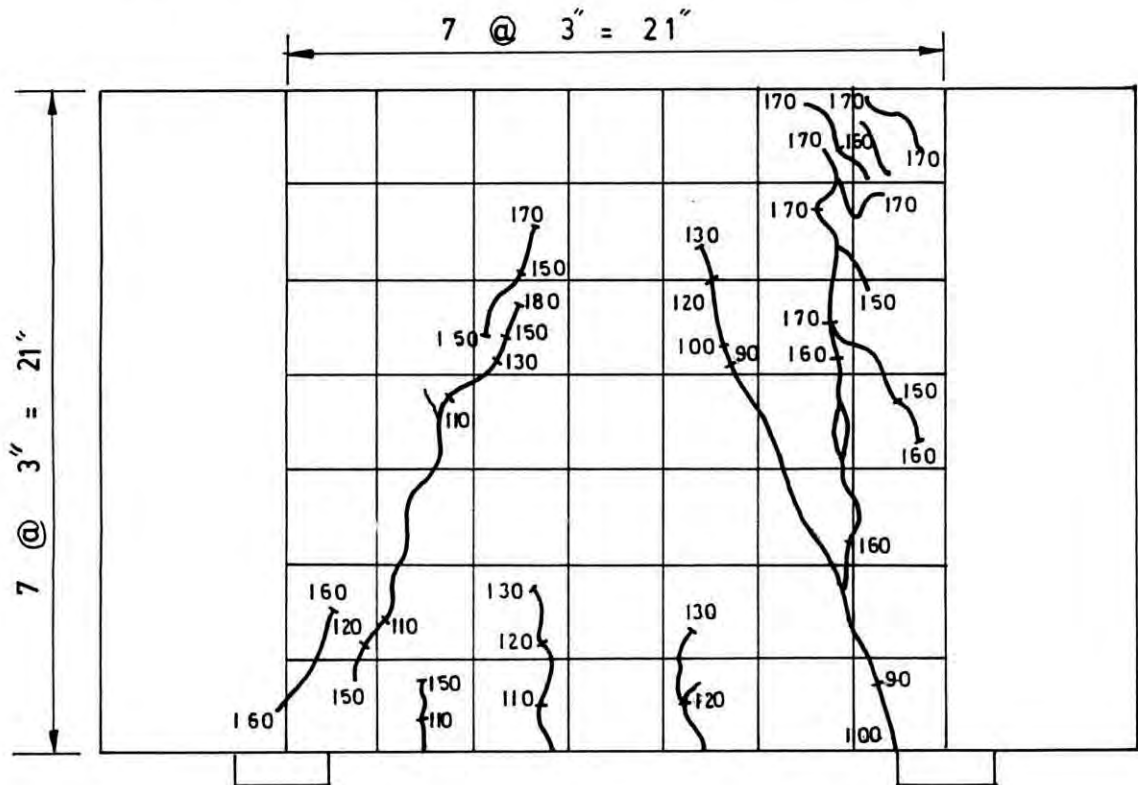


Fig. 5.8 Crack pattern of beam DB-P4

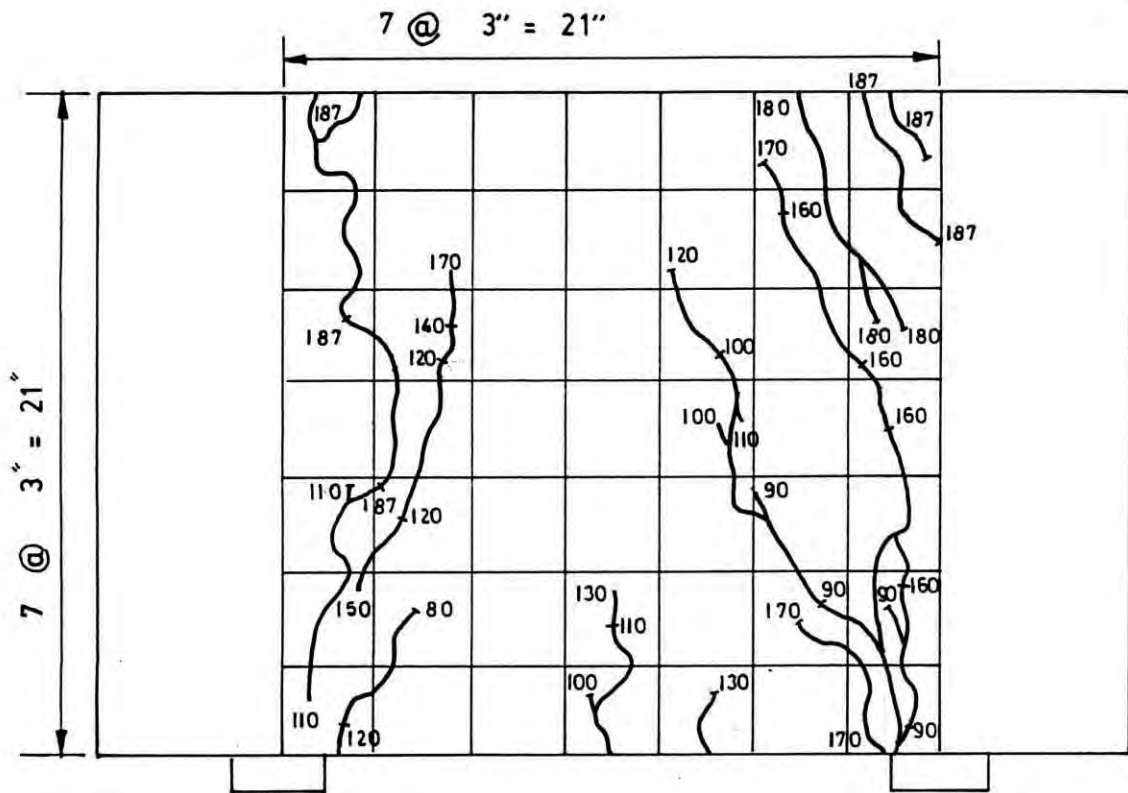


Fig. 5.9 Crack pattern of beam DB - P5

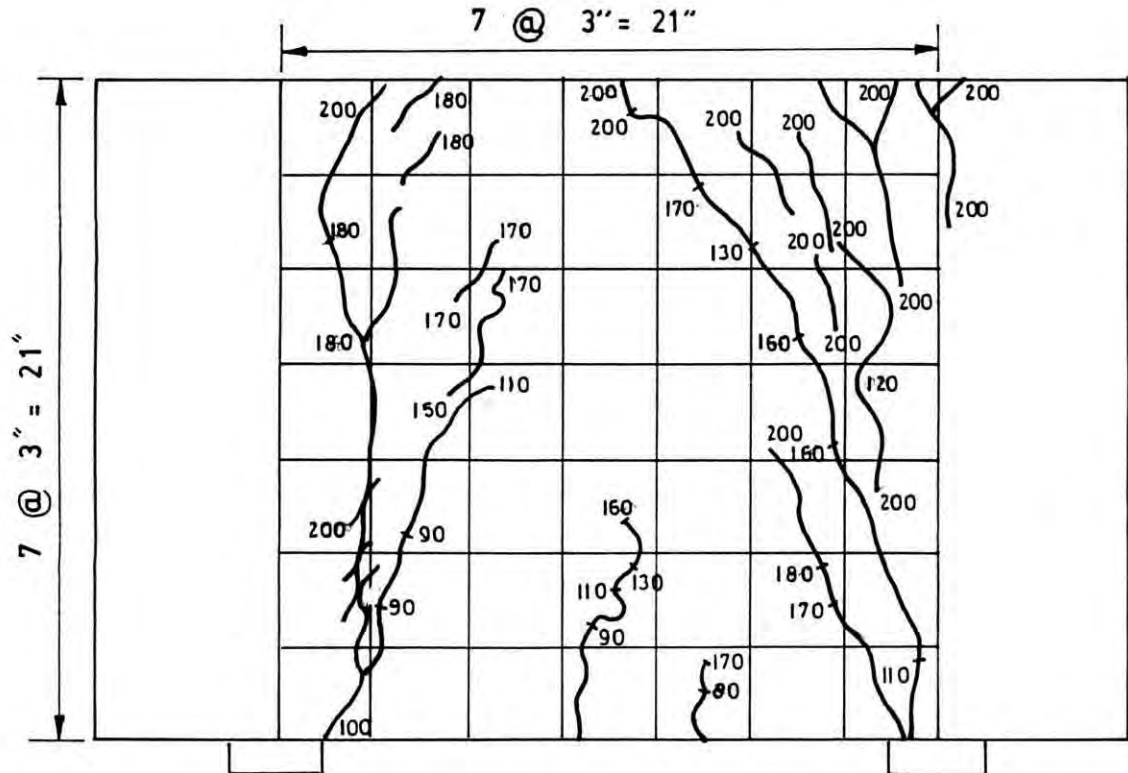


Fig. 5.10 Crack pattern of beam DB - P6

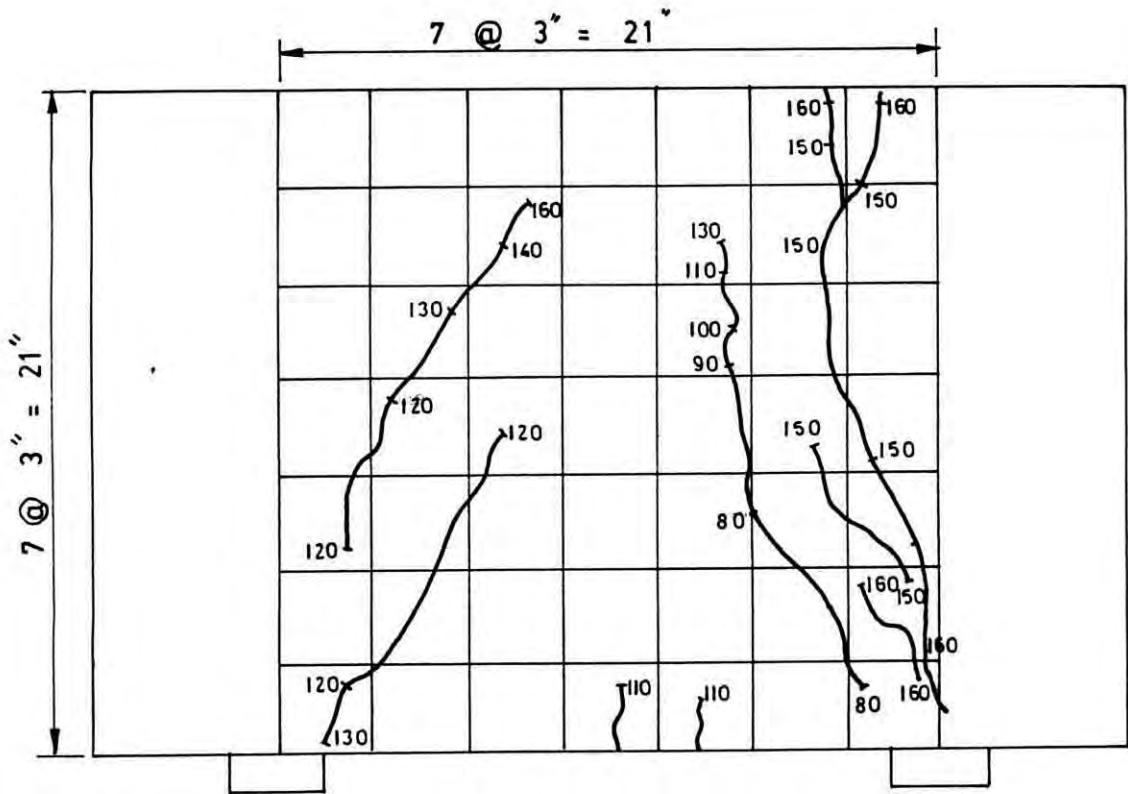


Fig. 5-11 Crack pattern of beam DB-P7

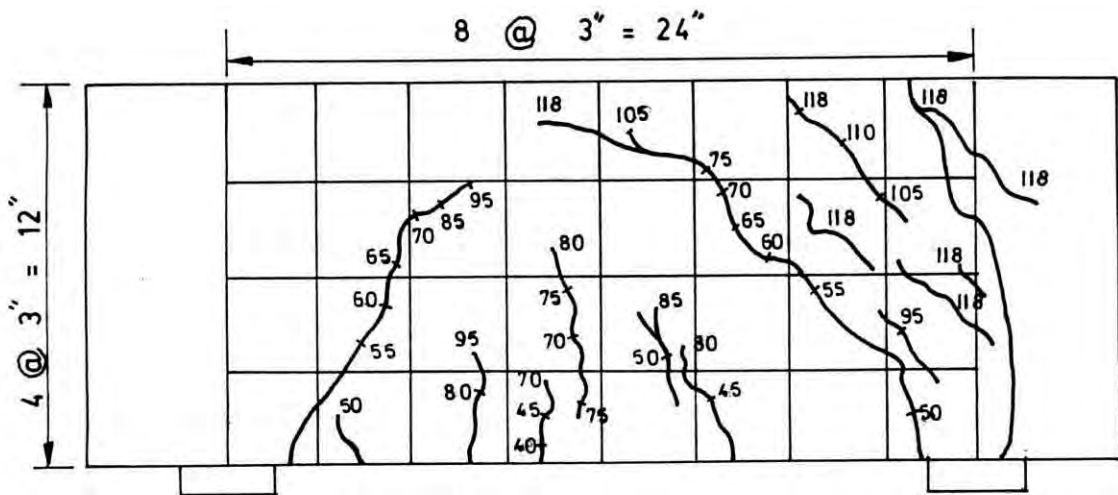


Fig. 5-12 Crack pattern of beam DB-Q1

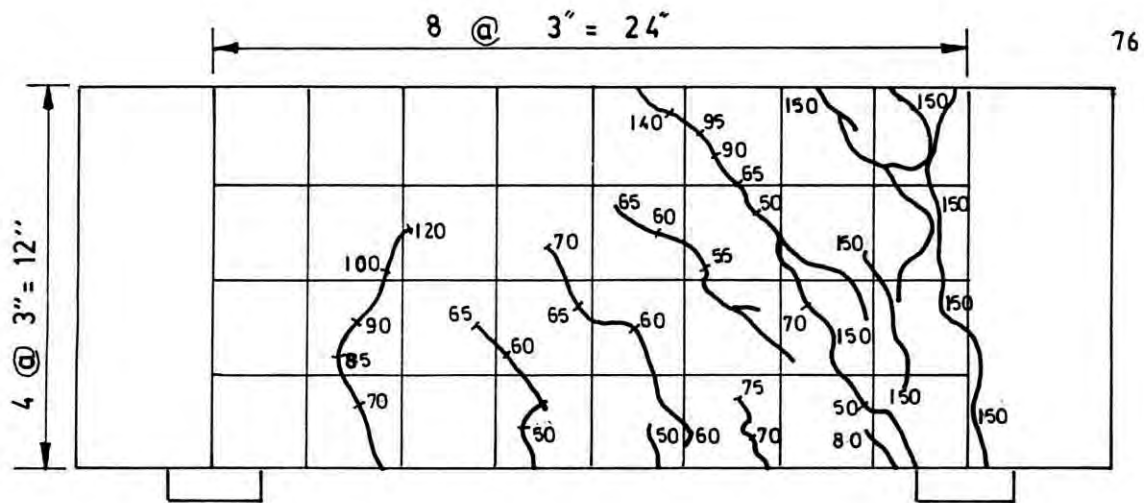


Fig. 5-13 Crack pattern of beam DB - Q2

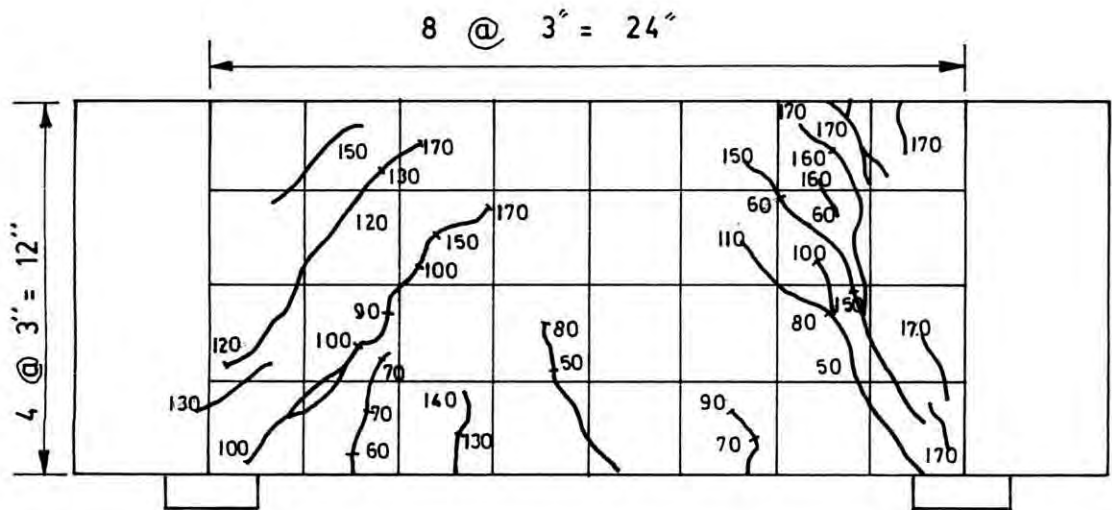


Fig. 5-14 Crack pattern of beam DB - Q3

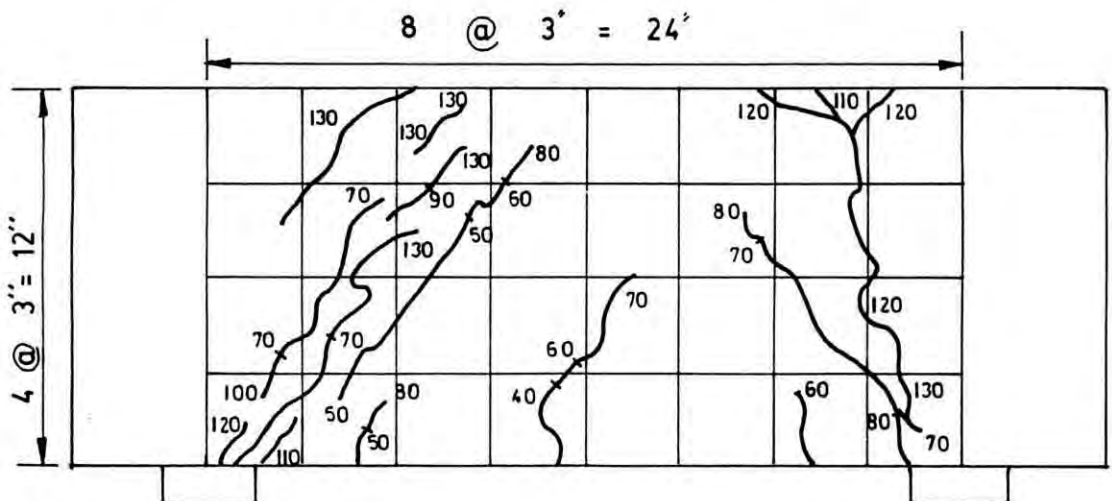


Fig. 5-15 Crack pattern of beam DB - Q4

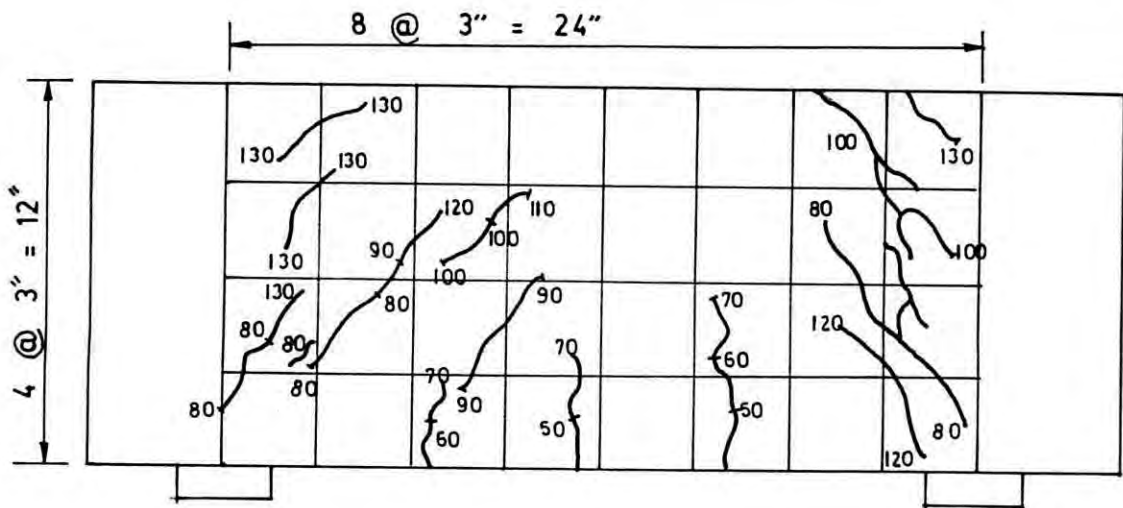


Fig. 5.16 Crack pattern of beam DB - Q5

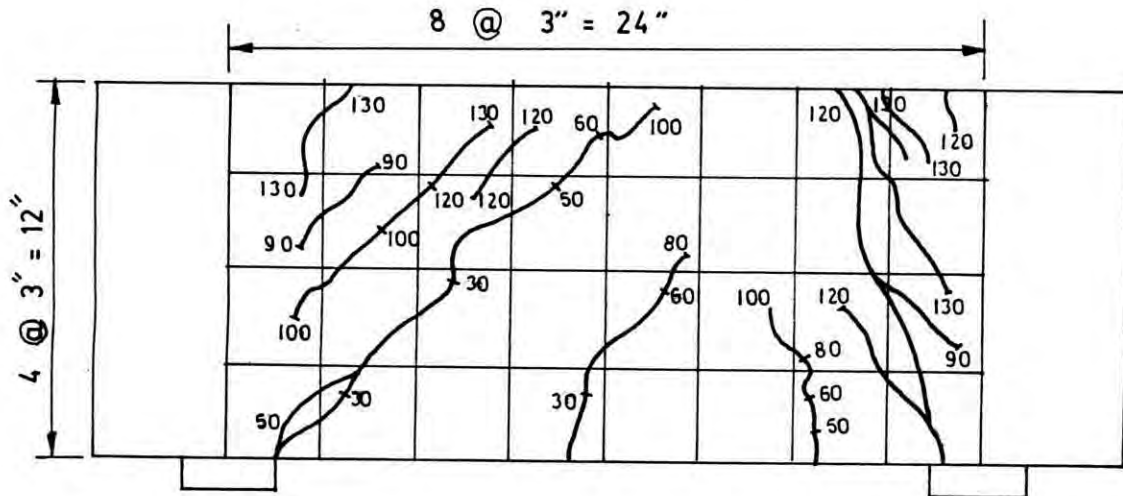


Fig. 5.17 Crack pattern of beam DB Q6

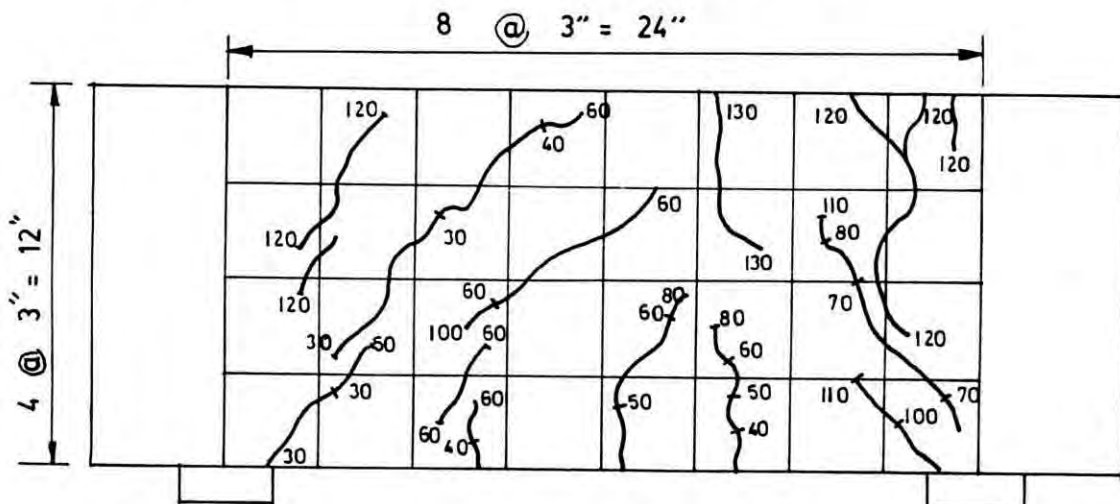


Fig. 5.18 Crack pattern of beam DB Q7



Fig. 5.19 Mode of Failure and Crack Pattern of Beam DB-P1



Fig. 5.20 Mode of Failure and Crack Pattern of Beam DB-P2

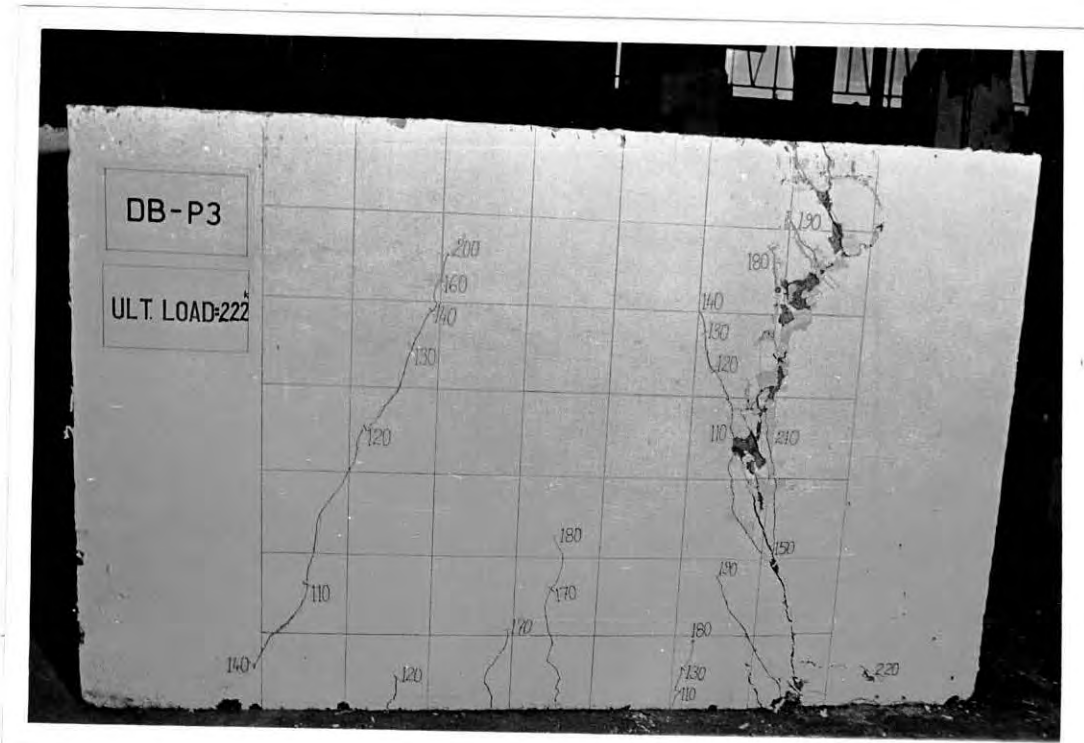


Fig. 5.21 Mode of Failure and Crack Pattern of Beam DB-P3



Fig. 5.22 Mode of Failure and Crack Pattern of Beam DB-P4



Fig. 5.23 Mode of Failure and Crack Pattern of Beam DB-P5

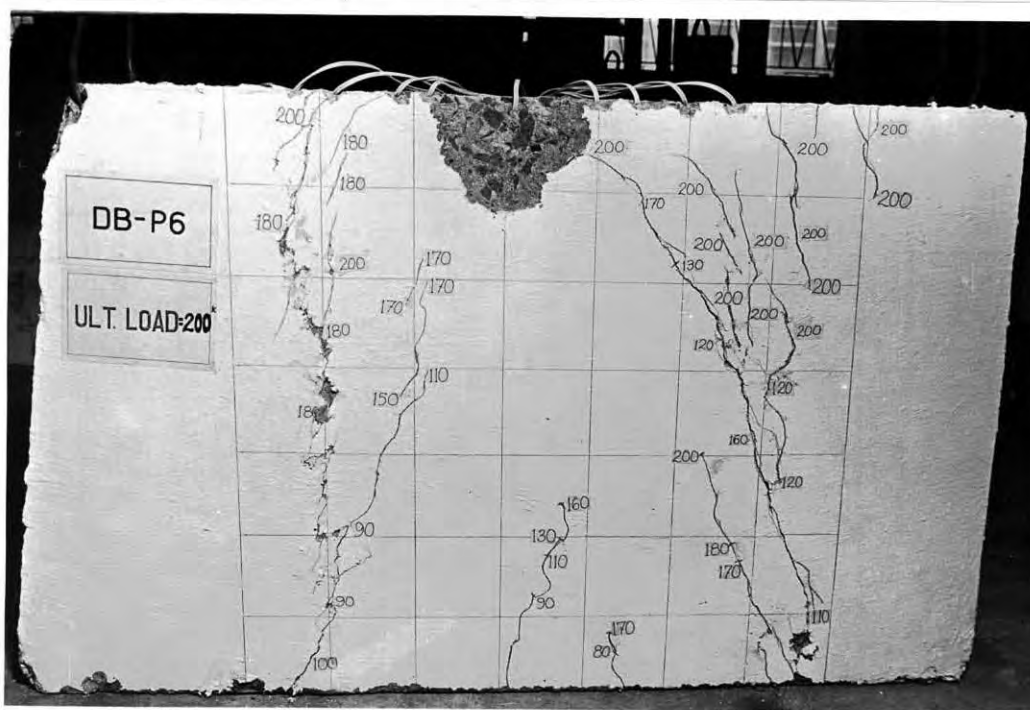


Fig. 5.24 Mode of Failure and Crack Pattern of Beam DB-P6

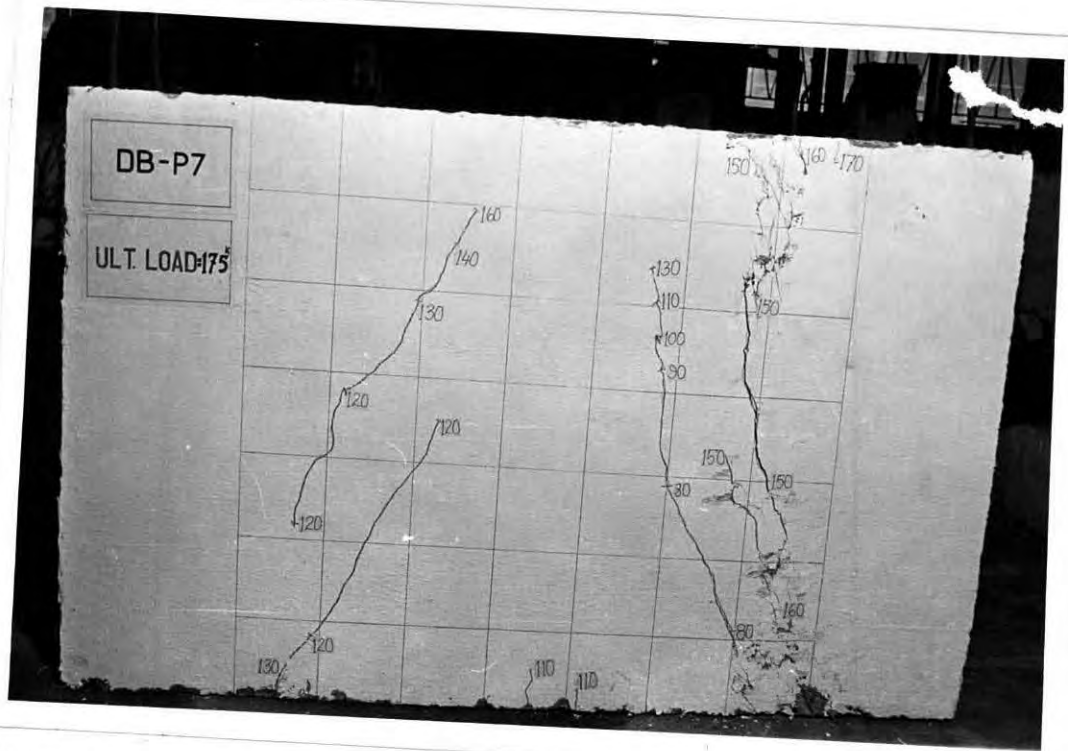


Fig. 5.25 Mode of Failure and Crack Pattern of Beam DB-P7

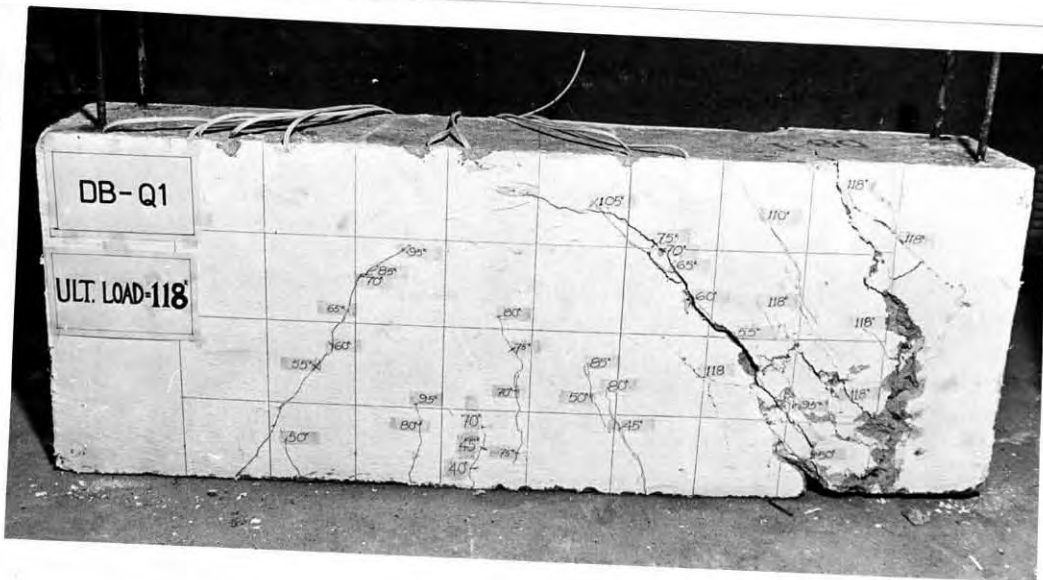


Fig. 5.26 Mode of Failure and Crack Pattern of Beam DB-Q1



Fig. 5.27 Mode of Failure and Crack Pattern of Beam DB-Q2

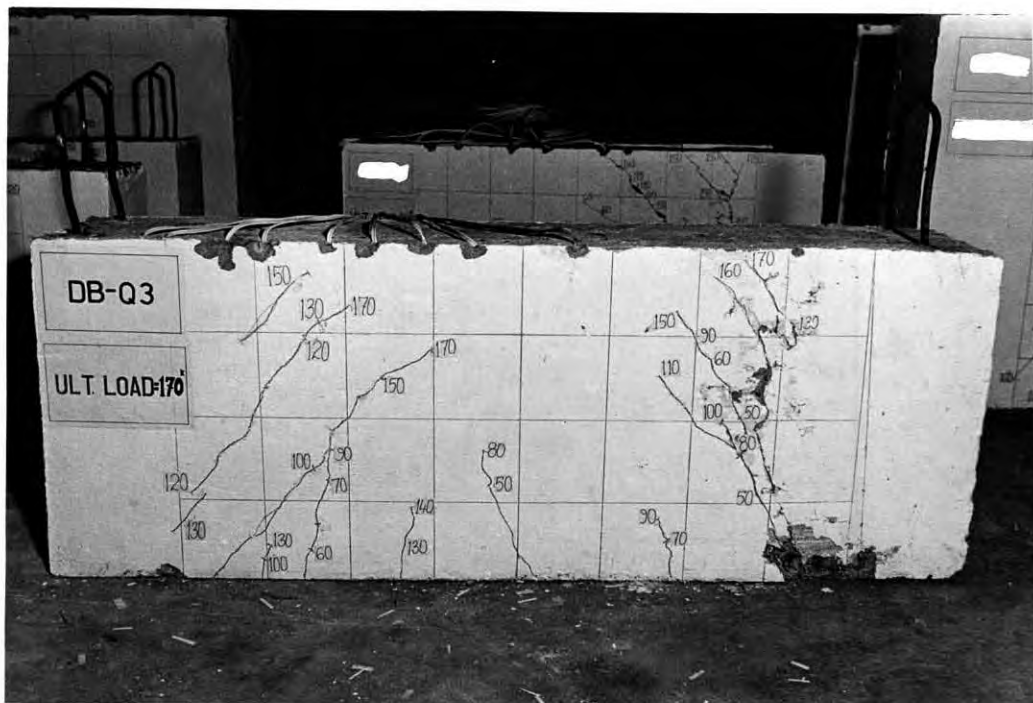


Fig. 5.28 Mode of Failure and Crack Pattern of Beam DB-Q3

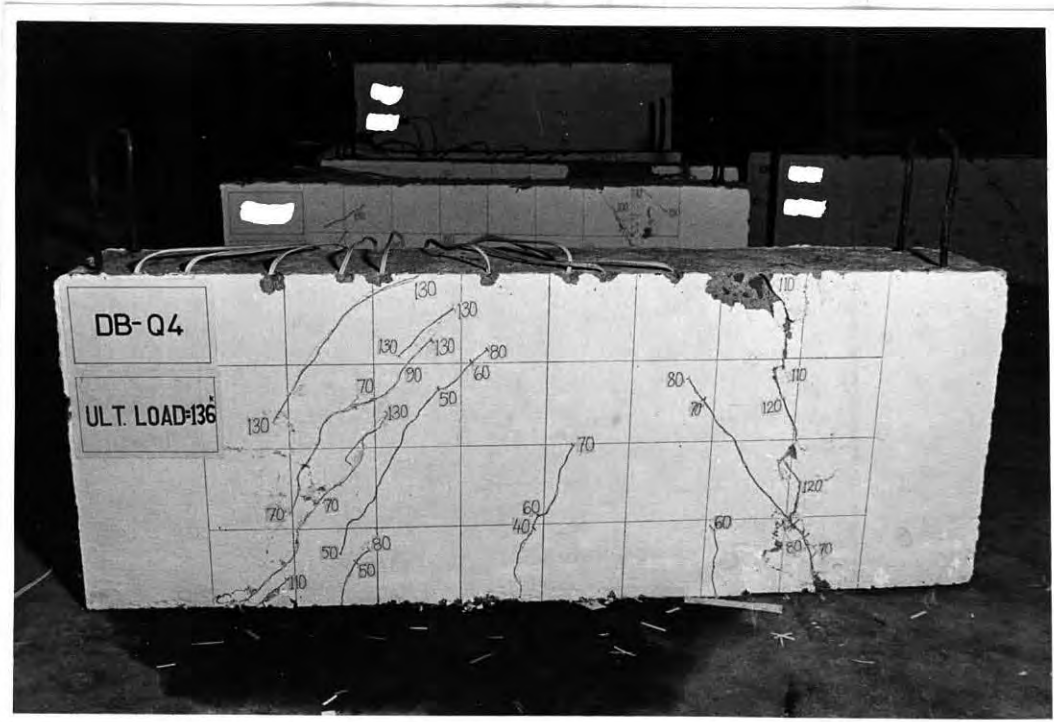


Fig. 5.29 Mode of Failure and Crack Pattern of Beam DB-Q4

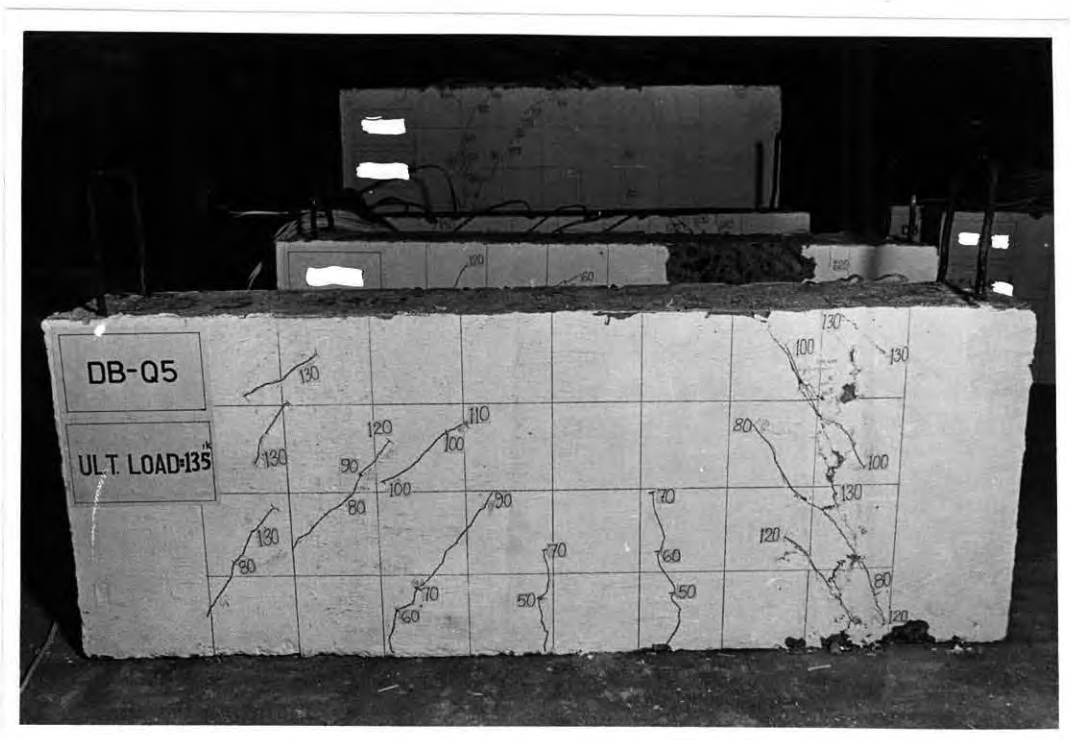


Fig. 5.30 Mode of Failure and Crack Pattern of Beam DB-Q5

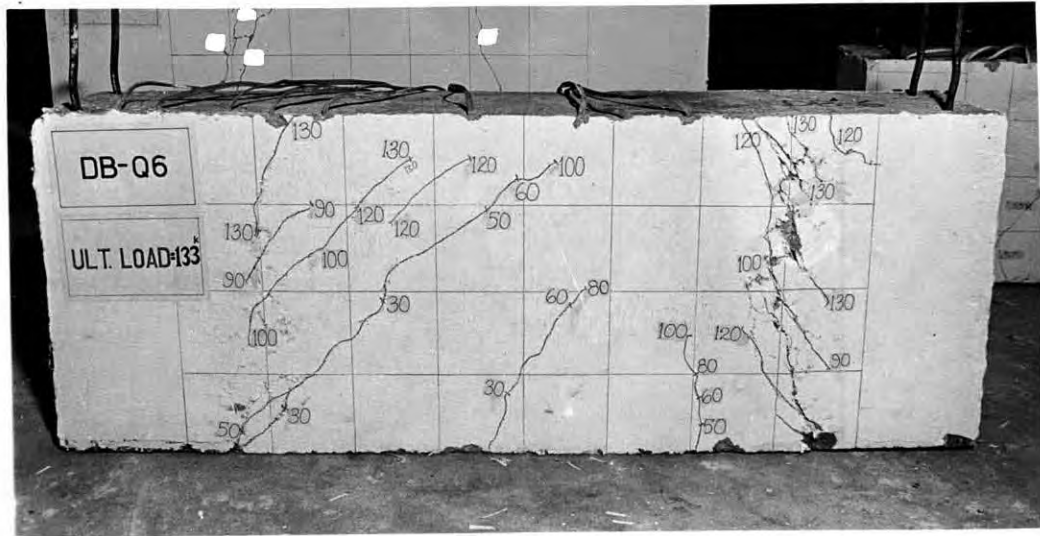


Fig. 5.31 Mode of Failure and Crack Pattern of Beam DB-Q6

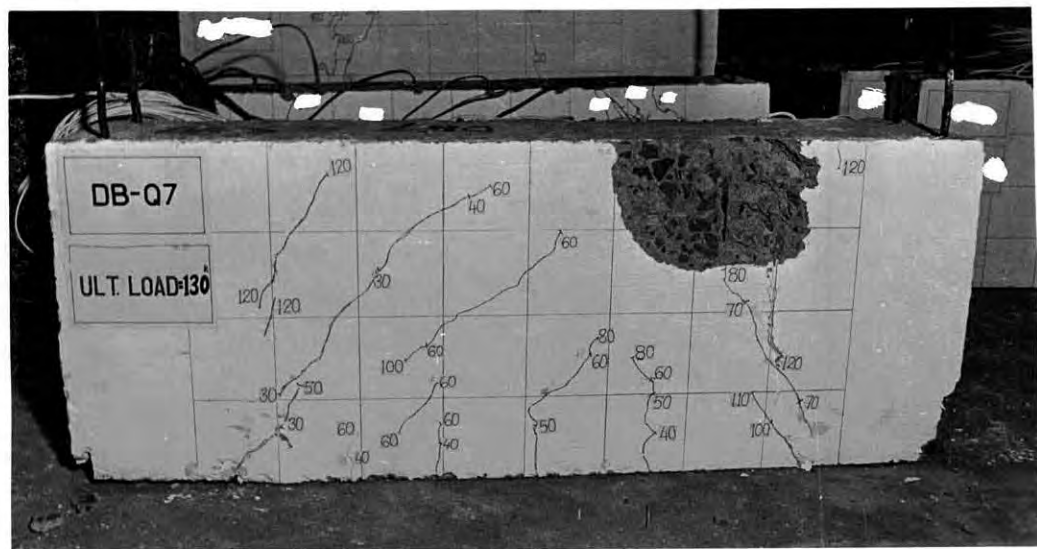


Fig. 5.32 Mode of Failure and Crack Pattern of Beam DB-Q7

CHAPTER 6

ANALYSIS AND DISCUSSION OF TEST RESULTS

6.1 GENERAL

The test programme was performed in a systematic way and the necessary test data are presented in the preceding chapter. These data were recorded during the testing operations as accurately as possible. These test data are analyzed and discussed in the following articles.

6.2 STRAINS IN REINFORCEMENTS

The electrical resistance strain gauge readings on certain selective locations on the flexural and the shear reinforcements of the test beams were recorded. The direct readings were found in the unit of micro-strain and are presented in Appendix-D. Among these strain gauges a few were out of order during the testing of beams. However, the rest of data indicate some overall performance of the test beams at different critical load condition.

The axial strains developed at different sections of flexural reinforcement were different before the arch-action was formed in the respective beam. And the strain values should be nearly same after the initiation of arch-action. But it is seen (Ref. table D.1 through table D.14) that after the formation of arch-action the strain values in flexural reinforcement near the support (Gauge no. 3) are larger than that of the mid-section (Gauge no. 1 or, 2). On the other hand the horizontal and the vertical web reinforcements were stressed in tension and/or compression when subjected to different load levels. The above are true for both the DB-P and the DB-Q series of beams. In case of DB-P series of beams the strains in flexural reinforcement

corresponding to the respective yield stress were reached in DB-P1 only. And yield strains (or nearly so) were attained in all the beams of DB-Q series. Hence smaller amount of flexural reinforcement can be provided for deeper beam utilizing the strengths of steel and concrete.

In table 6.1, the load P_a , at which arch-action initiated, the ultimate load P_u and their ratios are shown. From this table it is found that arch-action initiated at about 50% of the ultimate load for beams of $L/D=1.0$ (i.e. DB-P series of beams) and that was at about 70% of the ultimate load for beams of $L/D=2.0$ (i.e. DB-Q series of beams).

Also It is seen from the strain records that arch action developed in all the beams of DB-P series ($L/D=1$). On the other hand, arch action developed in those beams of DB-Q series ($L/D=2$) which contained smaller amounts of horizontal reinforcements (both flexural and shear).

It is interesting to note that in case of DB-P series of beams ($L/D=1$) P_a is always less than or equal to either the diagonal cracking load or the flexural cracking load (except DB-P7). But P_a is always greater than these cracking loads in case of DB-Q series of beams ($L/D=2$).

From table 6.1 it is seen that the ratio of arch-action initiation load to ultimate load of the test beams has a mean value of 0.483 and 0.703 for DB-P and DB-Q series of beams respectively. Hence it may be concluded that in deeper beam arch action mechanism develops quite early in the loading process compared to it's ultimate load.

6.3 SHEAR CHARACTERISTICS OF TEST BEAMS

During the testing operation the cracking loads (flexural

Table 6.1 Checking for the "Arch-action" Mechanism in Test Beams.

Beam Mark	Diagonal Cracking Load P_{cr} (Kip)	Flexural Cracking Load P_f (Kip)	Load at which Arch Action formed P_a (Kip)	Ultimate Load P_u (Kip)	Ratio P_a/P_u	Mean Ratio
1	2	3	4	5	6	7
Series DB-P : L/D=1.0						
DB-P1	80	90	80	166	0.482	0.483
DB-P2	90	120	200	210	0.952	
DB-P3	110	120	100	222	0.450	
DB-P4	90	100	*	183	--	
DB-P5	90	100	80	187	0.428	
DB-P6	90	80	*	200	--	
DB-P7	80	110	100	175	0.571	
Series DB-Q : L/D=2.0						
DB-Q1	55	40	90	118	0.763	0.703
DB-Q2	50	50	**	150	--	
DB-Q3	50	50	**	170	--	
DB-Q4	50	40	110	136	0.809	
DB-Q5	80	50	**	135	--	
DB-Q6	30	30	**	133	--	
DB-Q7	30	40	70	130	0.538	

* Strain gauge is out of order.

** No arch-action is formed.

and diagonal) and the ultimate loads of different test beams were recorded properly. Obviously these loads were different for different test beams because the flexural and the horizontal shear reinforcements were varied in the beams even in each series. The percentage changes of the flexural and the horizontal shear reinforcements along with above mentioned different loads of all the test beams are shown in table 6.2. The effects of the variations of horizontal reinforcements upon the different shear stress capacities of the test beams are discussed in the following articles.

6.3.1 The Cracking Load and the Shear Capacity of Test Beams

Two types of cracking loads namely Diagonal Cracking load and Flexural Cracking load were studied during the test programme. Observed cracking loads and ultimate loads are shown in table 6.2. All of the test beams failed in diagonal tension mode. In DB-P series of beams the diagonal cracks developed before the flexural cracks (except DB-P6 only). On the other hand flexural cracks developed first in case of DB-Q series (except DB-Q7). Hence it can be concluded that in deeper beam ($L/D=1.0$) the diagonal cracks appear prior to flexural cracks.

From table 6.2 it is seen that the mean ratio of diagonal cracking load to ultimate load are 0.469 for beams of DB-P series and 0.359 for beams of DB-Q series. These observations are similar to those of Ali⁽⁶⁾ for deep beams with uniformly distributed loads.

In table 6.3 shear stresses at observed load causing diagonal cracking are compared with the corresponding theoretical values using both ACI⁽¹⁾ method and Diaz de Cosio⁽⁷⁾ method. ACI method estimates the stress causing diagonal cracking by the formula

Table 6.2 Observed cracking and ultimate load for different percentage of flexural and horizontal shear reinforcements.

Beam Mark	Concrete crushing strength f'_c (ksi)	Flexural steel ratio $p=A_s/bd$	% change of flexural reinforcement over first beam(ACI beam)	Horizontal web steel ratio $p_h=A_h/s_2b$	% change of horizontal web reinforcement over first beam(ACI beam)	Flexural cracking load, P_f Kip	Diagonal cracking load, P_{cr} Kip	Ultimate load, P_u Kip	Ratio $\frac{P_f}{P_u}$	Ratio $\frac{P_{cr}}{P_u}$
Series DB-P : L/D=1.0										
DB-P1	2.51	0.00503	----	0.003	----	90	80	166	0.542	0.482
DB-P2	2.87	0.00651	+30.95 %	0.00396	+33.33 %	120	90	210	0.571	0.429
DB-P3	2.93	0.00947	+90.48 %	0.00594	+100.00 %	120	110	222	0.541	0.495
DB-P4	2.92	0.00487	0.00	0.00582	+100.00 %	100	90	183	0.546	0.492
DB-P5	2.93	0.00938	+90.48 %	0.00294	0.00	100	90	187	0.535	0.481
DB-P6	2.89	0.00492	0.00	0.00392	+33.33 %	80	90	200	0.40	0.450
DB-P7	2.73	0.00645	+30.95 %	0.00294	0.00	110	80	175	0.629	0.457
								Mean	0.538	0.469
Series DB-Q : L/D=2.0										
								C	11.86%	4.85%
DB-Q1	2.51	0.01197	----	0.00543	----	40	55	118	0.339	0.466
DB-Q2	2.87	0.01759	+45.45 %	0.00713	+30.00 %	50	50	150	0.333	0.333
DB-Q3	2.93	0.02221	+83.64 %	0.00891	+62.50 %	50	50	170	0.294	0.294
DB-Q4	2.92	0.01197	0.00	0.00882	+62.50 %	40	50	136	0.294	0.368
DB-Q5	2.93	0.02221	+83.64 %	0.00548	0.00	50	80	135	0.370	0.593
DB-Q6	2.89	0.01185	0.00	0.00698	+30.00 %	30	30	133	0.226	0.226
DB-Q7	2.73	0.01778	+45.45 %	0.00554	0.00	40	30	130	0.308	0.231
								Mean	0.309	0.359
								C	13.70%	34.16%

C = Coefficient of variation.

Table 6.3 Diagonal Cracking Shear Stress Properties of Test beams.

Beam mark	Concrete crushing strength f'_c (psi)	Deviation of Flexural and horizontal web reinforcements from ACI minimum requirements.	Shear stress causing diagonal cracking				Ratio of stresses			Ratio v_{cr} / f'_c	
			Observed stress, v_{cr} (psi)	Stress after ACI (psi)	Stress after de Cosio (psi)	Stress after Kabir (psi)	Observed ACI	Observed de Cosio	Observed Kabir		
Series DB-P : L/D=1.0											
DB-P1	2510	----	205.13	138.98	187.78	162.57	1.476	1.092	1.262	4.10	
DB-P2	2870	F+31 & W+33.3	228.37	158.46	218.92	231.97	1.441	1.043	0.984	4.26	
DB-P3	2930	F+90.5 & W+100	279.12	185.29	267.53	393.79	1.506	1.043	0.709	5.16	
DB-P4	2920	F+0.0 & W+100	223.76	145.07	193.65	141.85	1.542	1.155	1.577	4.14	
DB-P5	2930	F+90.5 & W+0.0	226.06	184.50	266.08	385.40	1.225	0.850	0.587	4.18	
DB-P6	2890	F+0.00 & W+33.3	226.06	144.97	193.85	149.45	1.559	1.166	1.513	4.21	
DB-P7	2730	F+31 & W+0.00	200.94	155.42	215.13	234.34	1.293	0.934	0.857	3.85	
Series DB-Q : L/D=2.0							Mean	1.436	1.04	1.07	4.27
Series DB-Q : L/D=2.0							C	8.23%	10.23%	33.63%	8.95%
DB-Q1	2510	----	257.49	147.40	203.29	216.93	1.747	1.267	1.187	5.14	
DB-Q2	2870	F+45.5 & W+30	236.48	178.52	255.83	356.52	1.325	0.924	0.663	4.41	
DB-Q3	2930	F+83.70 & W+62.5	239.16	189.45	292.10	477.69	1.262	0.819	0.501	4.42	
DB-Q4	2920	F+0.0 & W+62.5	231.48	155.47	212.80	208.85	1.489	1.088	1.108	4.28	
DB-Q5	2930	F+83.70 & W+0.0	374.16	189.45	296.10	486.08	1.975	1.264	0.770	6.91	
DB-Q6	2890	F+0.0 & W+30	138.24	154.12	210.69	207.78	0.897	0.656	0.665	2.57	
DB-Q7	2730	F+45.50 & W+0.0	140.87	178.21	257.06	372.01	0.790	0.548	0.379	2.70	
Series DB-Q : L/D=2.0							Mean	1.355	0.938	0.753	4.35
Series DB-Q : L/D=2.0							C	29.18%	28.00%	36.68%	31.45%

C = Coefficient of variation.

F+31 = Increase of flexural reinforcement by 31% from ACI Code minimum requirement.

W+33.3 = Increase of horizontal web reinforcement by 33.3% from ACI Code minimum requirement, etc.

$$v_{cr} = \frac{V_{cr}}{bd} = (1.9\sqrt{f'_c} + 2500 \frac{p V_{cr} d}{M_{cr}}) \leq 3.5\sqrt{f'_c} \quad \text{--- (6.1)}$$

Where,

V_{cr} = external shear force at critical section,

M_{cr} = external bending moment at critical section.

On the other hand, Diaz de Cosio⁽⁷⁾ estimates the shear stress causing diagonal cracking by the formula

$$v_{cr} = \frac{V_{cr}}{bd} = (2.14\sqrt{f'_c} + 4600 \frac{p V_{cr} d}{M_{cr}}) \quad \text{--- (6.2)}$$

Cosio did not, however, prescribe any upper limit of this shear stress value.

From columns 6 and 8 of the table 6.3, it is evident that ACI method underestimates the shear stress causing diagonal cracking. Observed stress values on average are 1.44 times higher than those calculated by ACI method for beams of DB-P series and 1.36 times higher for beams of DB-Q series. The upper limit of $3.5\sqrt{f'_c}$ in this critical stress formula also seems to be conservative (Ref. Col.10 of table 6.3). And this upper limit of diagonal cracking stress can be raised to a value of $4\sqrt{f'_c}$.

Ali⁽⁶⁾ concluded that Diaz de Cosio⁽⁷⁾ equation overestimates the cracking shear capacity for beams of smaller span to depth ratio ($L/D=1.0$) and it underestimates the cracking shear capacity for beams of greater span to depth ratio ($L/D=2.0$). However, the test results (Ref. Col.4 and 7 of table 6.3) in this study shows that these are not true for deep beams under study subjected to uniformly distributed loads.

Shear stresses at diagonal cracking load calculated by Diaz de Cosio (Ref. Col.7 of table 6.3) agree fairly well with the

observed stresses in some beams of DB-P series, but other values are higher. As an example, observed shear stress and shear stress after de Cosio at the formation of initial diagonal cracking are 226 psi and 266 psi respectively for DB-P5 and 200 psi and 215 psi respectively for DB-P7. But in cases of DB-P4 and DB-P6 this formula underestimates the diagonal cracking shear stress. Similar occurrences are observed for the beams of DB-Q series.

It appears, however, that the variation of horizontal web steel alone does not influence the diagonal cracking shear stress value significantly (Ref. Col.3 and 4 of table 6.3). As an example the cracking shear for ACI beam DB-P1 is 205 psi whereas that for the beams DB-P4 and DB-P6 are 224 psi and 226 psi respectively though they have additional (as compared to DB-P1) horizontal web reinforcements of 100% and 34% respectively. Similarly the increase of flexural reinforcement alone does not significantly influence the diagonal cracking shear capacity of deep beams subjected to uniform loading. For example, the increase in flexural steel only, for beams DP-P7 and DB-P5 over the ACI beam (DB-P1) are 31% and 90.5% respectively but the increase in cracking shear capacities are (201-205) or, -4 psi and (226-205) or, 21 psi respectively. Similar results are observed in cases of beams of DB-Q series. Hence it can be concluded that the increase of flexural reinforcement or, horizontal web reinforcement alone has no significant influence upon the diagonal cracking shear stress of deep beams subjected to uniformly distributed load.

The diagonal cracking shear stress formula suggested by Kabir⁽⁵⁾ is

$$v_{cr} = \frac{V_{cr}}{bd} = (-2.18\sqrt{f'_c} + 15500 \frac{p V_{cr} d}{M_{cr}}) \quad \text{--- (6.3)}$$

Column 8 of table 6.3 shows the diagonal cracking shear stress after Kabir. But these estimated stresses differ greatly

from their observed corresponding values (Ref. Col.11 of table 6.3). Hence it is not an accurate formula for the estimation of the shear stress of deep beam at the initiation of diagonal cracking under uniformly distributed load.

Attempts were made to develop an expression for the test beams of this investigation correlating the diagonal shear stress v_{cr} with the major variables like the flexural reinforcement ratio (p), and the concrete crushing strength (f'_c) which are considered to influence the shear strength of beams. Although the numbers of test data were not large enough to bring about a definite conclusion yet an apparent trend for linear relationship appeared to exist between the terms $V_{cr}/(bd/f'_c)$ and $(1000 p V_{cr} d)/(M_{cr}/f'_c)$.

Where, V_{cr} and M_{cr} are the shear force and bending moment respectively at the critical section of the beam at the initiation of diagonal cracking.

The numerical values of these two terms for the test beams are presented in table 6.4. Using these data and with the Least Square Method it reveals that the critical shear stress may tentatively be expressed as a linear relationship. This may be stated as -

$$v_{cr} = \frac{V_{cr}}{bd} = \left(2.90/f'_c + 2800 \frac{p V_{cr} d}{M_{cr}} \right) \leq 4/f'_c \quad \text{--- (6.4)}$$

The maximum limit of the stress is set up as $4/f'_c$ since the mean values of the ratio of nominal diagonal cracking shear stress to square root of concrete crushing strength are 4.27 and 4.35 for beams of DB-P and DB-Q series respectively (Ref. Col.4 of Table 6.4).

Table 6.4 Observed diagonal cracking stress variation.

Beam mark	Concrete crushing strength f'_c (psi)	Observed diagonal cracking stress $v_{cr} (=V_{cr}/bd)$ psi	Ratio $\frac{v_{cr}}{f'_c}$	Ratio $\frac{1000 p V_{cr} d}{M_{cr} f'_c}$
1	2	3	4	5
Series DB-P : L/D=1.0				
DB-P1	2510	205.13	4.10	0.35
DB-P2	2870	228.37	4.26	0.42
DB-P3	2930	279.12	5.16	0.61
DB-P4	2920	223.76	4.14	0.31
DB-P5	2930	226.06	4.18	0.60
DB-P6	2890	226.06	4.21	0.32
DB-P7	2730	200.94	3.85	0.43
		Mean	4.27	
		C	8.97%	
Series DB-Q : L/D=2.0				
DB-Q1	2510	257.49	5.14	0.42
DB-Q2	2870	236.48	4.41	0.57
DB-Q3	2930	239.16	4.42	0.71
DB-Q4	2920	231.48	4.28	0.39
DB-Q5	2930	374.16	6.91	0.72
DB-Q6	2890	138.24	2.57	0.39
DB-Q7	2730	140.87	2.70	0.61
		Mean	4.35	
		C	31.43%	

C = Coefficient of variation.

The observed diagonal cracking shear stress and the stress estimated by the suggested formula (eqn. 6.4) are compared in table 6.5 .

6.3.2 Nominal Shear Stress at Failure

Table 6.6 shows the nominal shear stresses at failure loads. These stresses are found to vary between 425.6 psi and 563.3 psi with an average value of 484.0 psi for the test beams of DB-P series. On the other hand this value ranges between 552.4 psi and 813.2 psi with a mean value of 651.3 psi for the beams of DB-Q series. It is apparent from the table that the beams of DB-Q series attained relatively a higher value of nominal shearing stress at failure compared to other set of beams. This is quite in agreement with the fact that higher percentage of longitudinal reinforcement can have a positive influence in increasing the shear capacity of reinforced concrete beam.

In column 6 of table 6.6, the ratios of nominal ultimate shear stress to square root of concrete crushing cylinder strength are shown. These ratios vary between 8.41 and 10.41 with an average value of 9.10 for beams of DB-P series. On the other hand this value ranges between 11.03 and 15.02 with a mean value of 12.24 for the beams of DB-Q series. Thus it appears that the beams of DB-Q series ($L/D=2.0$) attained relatively a higher value of nominal shear stress at failure compared with the beams of DB-P series ($L/D=1.0$). Therefore it can be said that higher percentage of longitudinal steel can have a positive influence in increasing the shear capacity of reinforced concrete deep beams.

It may be noted that Kabir⁽⁵⁾ suggested that ACI method for the computation of ultimate shear stress of deep beams might be effectively used for brick aggregate concrete deep beams by considering the maximum limit of ultimate shear stress as $10/f'_c$ instead of $8/f'_c$ suggested by ACI code for stone aggregate deep

Table 6.5 Comparison of Measured and Suggested Estimate of diagonal cracking stress.

Beam mark	Concrete crushing strength f'_c (psi)	% of flexural reinforcement P	Observed diagonal cracking stress v_{oc} (psi)	Suggested estimate of the cracking stress v_{cr} (psi)	Ratio $\frac{v_{cr}}{v_{oc}}$
1	2	3	4	5	6
Series DB-P : L/D=1.0					
DB-P1	2510	0.503	205.13	194.39	0.948
DB-P2	2870	0.651	228.37	214.29	0.938
DB-P3	2930	0.947	279.12	216.52	0.776
DB-P4	2920	0.487	223.76	203.61	0.910
DB-P5	2930	0.938	226.06	216.52	0.958
DB-P6	2890	0.492	226.06	204.07	0.903
DB-P7	2730	0.645	200.94	209.00	1.04
				Mean	0.925
				C	7.96%
Series DB-Q : L/D=2.0					
DB-Q1	2510	1.197	257.49	200.40	0.778
DB-Q2	2870	1.759	236.48	214.29	0.906
DB-Q3	2930	2.221	239.16	216.52	0.905
DB-Q4	2920	1.197	231.48	215.72	0.932
DB-Q5	2930	2.221	374.16	216.52	0.579
DB-Q6	2890	1.185	138.24	214.60	1.552
DB-Q7	2730	1.778	140.87	209.00	1.484
				Mean	1.019
				C	32.87%

C = Coefficient of variation.

Table 6.6 Nominal Ultimate Shear Stress Properties of Test Beams

Beam mark	Concrete crushing strength f'_c (psi)	$\sqrt{f'_c}$	% of Total horizontal reinf. P_t	Measured ultimate shearing stress at critical section v_u (psi)	Ratio $\frac{v_u}{\sqrt{f'_c}}$
1	2	3	4	5	6
Series DB-P : L/D=1.0					
DB-P1	2510	50.10	0.803	425.64	8.50
DB-P2	2870	53.57	1.047	532.87	9.95
DB-P3	2930	54.13	1.541	563.32	10.41
DB-P4	2920	54.04	1.069	454.97	8.42
DB-P5	2930	54.13	1.232	469.70	8.68
DB-P6	2890	53.76	0.884	502.35	9.34
DB-P7	2730	52.25	0.939	439.56	8.41
				Mean	9.10
				C	8.28%
Series DB-Q : L/D=2.0					
DB-Q1	2510	50.10	1.740	552.43	11.03
DB-Q2	2870	53.57	2.472	709.43	13.24
DB-Q3	2930	54.13	3.112	813.16	15.02
DB-Q4	2920	54.04	2.079	629.63	11.65
DB-Q5	2930	54.13	2.769	631.39	11.66
DB-Q6	2890	53.76	1.883	612.88	11.40
DB-Q7	2730	52.25	2.332	610.43	11.68
				Mean	12.24
				C	10.65%

C = Coefficient of variation.

beams with $L/D \leq 2$. Ali⁽⁶⁾ proposed the maximum limit of the same stress value as $9/f'_c$ for brick aggregate RC deep beams having adequate reinforcements and subjected to uniform loading. From table 6.6 it is clear that both the suggestions seem to be slightly inadequate for predicting the ultimate shear stress in deep beams with smaller span to depth ratio ($L/D=1.0$) and both of the methods underestimate the upper limit of the ultimate shear stress in beams with larger span to depth ratio ($L/D=2.0$). Hence for brick aggregate deep beams with adequate reinforcements and subjected to uniformly distributed load the maximum limit of the nominal ultimate shear stress can be expressed as follows :

$$\text{For } L/D=1.0 \quad : \quad v_u = 8.5/f'_c \quad - - - - - (6.5a)$$

$$\text{For } L/D=2.0 \quad : \quad v_u = 11.0/f'_c \quad - - - - - (6.5b)$$

It is interesting to note that the increase in the ultimate shear stress depends on the increase in both the flexural and the horizontal web reinforcements (Ref. Col.5 of Table 6.6). The increase in either the flexural or the horizontal web steel does not increase the ultimate shear stress in significant amount.

The variation of nominal ultimate shearing stress with the total amount of horizontal (flexural +web) reinforcements are studied carefully and an attempt is made to make a relation between the nominal ultimate shear stress (v_u), concrete crushing strength (f'_c), and the percentage of total horizontal reinforcements (p_t). Using the test data and with the Least Square Method we had the following relation -

$$v_{us} = (6.0 + 2.15 p_t)/f'_c \quad - - - - - (6.6)$$

In table 6.7, a comparison is made between the measured (v_u) and the suggested (v_{us}) values of ultimate shear stresses of test beams. Column 6 of this table shows the ratios of v_{us}/v_u with mean values of 0.916 and 0.904 for test beams of DB-P and DB-Q

Table 6.7 comparison of Measured and Suggested Estimate of the Ultimate Shear Stress.

Beam mark	% Of Total horizontal reinf. p_t	Concrete crushing strength f'_c (psi)	Observed nominal ult. shear stress v_u (psi)	Suggested estimate of ult. shear v_{us} (psi)	Ratio $\frac{v_{us}}{v_u}$
1	2	3	4	5	6
Series DB-P : L/D=1.0					
DB-P1	0.803	2510	425.64	387.10	0.909
DB-P2	1.047	2870	532.87	442.01	0.829
DB-P3	1.541	2930	563.32	504.12	0.895
DB-P4	1.069	2920	454.97	448.44	0.986
DB-P5	1.232	2930	469.70	468.16	0.997
DB-P6	0.884	2890	502.35	424.74	0.845
DB-P7	0.939	2730	439.56	418.98	0.953
				Mean	0.916
				C	6.64%
Series DB-Q : L/D=2.0					
DB-Q1	1.740	2510	552.43	488.02	0.883
DB-Q2	2.472	2870	709.43	606.13	0.854
DB-Q3	3.112	2930	813.16	686.95	0.845
DB-Q4	2.079	2920	629.63	565.79	0.899
DB-Q5	2.769	2930	631.39	647.03	1.025
DB-Q6	1.883	2890	612.88	540.20	0.881
DB-Q7	2.332	2730	610.43	575.47	0.943
				Mean	0.904
				C	6.36%

C = Coefficient of variation.

series respectively. It is seen that a fair agreement appears to exist between the measured and the suggested ultimate shear stress of test beams.

6.4 ULTIMATE LOAD CAPACITY OF TEST BEAMS

The measured ultimate load capacity of different test beams are shown in table 5.2. It is seen that the load carrying capacity of the test beams vary from 166 kips to 222 kips for the beams of DB-P series and from 118 kips to 170 kips for that of DB-Q series. It is evident that these variations of the ultimate load capacity of test beams are due to the variations of their concrete strengths and amounts of horizontal reinforcements in a particular series of beams. The computed ultimate loads by the various methods are compared with the measured ultimate loads of test beams and the variations of the ultimate load capacity with the amount of horizontal reinforcements are discussed below.

6.4.1 Variation of Ultimate Load Capacity with the Horizontal Reinforcement.

In table 6.8, the measured ultimate load along with the ratios of horizontal reinforcements of each test beam are shown. The first beam of each series are provided with the ACI Code⁽¹⁾ minimum requirements of horizontal reinforcements (both flexural and web reinf.). The horizontal reinforcements in the rest of the beams are increased above that minimum requirements. From this table it is seen that the ultimate load capacity of test beams increase with the increase of total horizontal reinforcements only.

It may be mentioned here that ultimate crushing strength of concrete (f'_c) are not same in all the test beams. To find out the exclusive effect of horizontal reinforcements on the ultimate load, the observed load values were modified to eliminate the

Table 6.8 Variation of Ultimate Load Capacity with the
Variation of horizontal Reinforcements.

Beam mark	Concrete crushing strength f'_c (ksi)	Flexural reinf. ratio $p_f = A_s/bd$	Horizontal web reinf. ratio $p_h = A_{vh}/bs_2$	Total hor. reinf. ratio $p_t = p_f + p_h$	Observed ultimate load P_u (kip)	Ultimate load corresponding to $f'_c = 2.51$ ksi, P_u' k.
1	2	3	4	5	6	7
Series DB : L/D=1.0						
DB-P1	2.51	0.00503	0.003	0.00803	166	166.00
DB-P2	2.87	0.00651	0.00396	0.01047	210	196.39
DB-P3	2.93	0.00947	0.00594	0.01541	222	205.47
DB-P4	2.92	0.00487	0.00582	0.01069	183	169.67
DB-P5	2.93	0.00938	0.00294	0.01232	187	173.08
DB-P6	2.89	0.00492	0.00392	0.00884	200	186.39
DB-P7	2.73	0.00645	0.00294	0.00939	175	167.80
Series DB-Q : L/D=2.0						
DB-Q1	2.51	0.01197	0.00543	0.01740	118	118.00
DB-Q2	2.87	0.01759	0.00713	0.02472	150	140.28
DB-Q3	2.93	0.02221	0.00891	0.03112	170	157.34
DB-Q4	2.92	0.01197	0.00882	0.02079	136	126.09
DB-Q5	2.93	0.02221	0.00548	0.02769	135	124.95
DB-Q6	2.89	0.01185	0.00698	0.01883	133	123.95
DB-Q7	2.73	0.01778	0.00554	0.02332	130	124.65

effect of variation of f'_c . The modifications were made by multiplying the observed load values for beams with $\sqrt{f'_c}$ of the ACI beam (DB-P1 or, DB-Q1) and dividing the results by $\sqrt{f'_c}$ of the beam under consideration.

The flexural reinforcements of 7th and 5th beams were increased over that of the 1st beam of each series while the horizontal shear reinforcements were kept constant. But it is seen that the ultimate load capacities of DB-P1, DB-P7 and DB-P5 are 166^k , 167.80^k , and 173.08^k respectively and that of the beams DB-Q1, DB-Q7, DB-Q5 are 118^k , 124.65^k , 124.95^k respectively. Hence the increase in ultimate load due to the increase in flexural reinforcement alone is negligible. On the other hand the horizontal web reinforcements of 6th and 4th beams were increased over that of the 1st beam of each series keeping the flexural reinforcements constant. But the differences in their ultimate load capacity (Ref. Col.4 and 7 of Table 5.8) are also negligible. It may, therefore, be concluded that the increase in either the flexural or, the horizontal web reinforcement alone can not increase in a considerable amount of the ultimate load of deep beams subjected to uniformly distributed load.

The 2nd and 3rd beams of each series faced the increase in both the flexural and the horizontal web reinforcements over that of the ACI beam (1st beam). The ultimate load capacity of beams DB-P1, DB-P2, DB-P3 are 166^k , 196.39^k , 205.47^k respectively and that of the beams DB-Q1, DB-Q2, DB-Q3 are 118^k , 140.28^k , 157.34^k respectively. Here in each series of beams the increase in ultimate load capacity is of considerable amount. Hence it may be concluded that the increase in both the flexural and the horizontal web reinforcements brings about a positive effect upon the ultimate strength of deep beams subjected to uniformly distributed loads.

6.4.2 Estimate of Ultimate Load Capacity using Different Methods

Five of the several available formulas were used to determine the ultimate load capacity of our test beams. The ACI 318-89 Code⁽¹⁾ recommendations were used as the basis of design of the beams to ensure failure by shear. After casting of beams and testing of control cylinder specimens, the actual values of the materials and dimensions of the cast beams were used to compute the ultimate load of the beams following ACI 318-89 Code provisions, Singh, Ray and Reddy's⁽⁹⁾ method, Ramakrishnan and Ananthanarayana's⁽¹⁰⁾ method, Selvam and Kuruvilla's⁽¹⁹⁾ method, and Mau and Hsu's⁽²⁰⁾ method (See Appendix - B). Computation of ultimate load by these methods with its component share of concrete, flexural steel, horizontal web steel, and vertical web steel respectively are shown in Table 6.9a, and Table 6.9b for the two series of beams tested. Ramakrishnan and Ananthanarayana, & Selvam and Kuruvilla consider the contribution of concrete only. On the other hand Mau and Hsu consider (Ref. Table 6.10) the combined action of concrete and reinforcements (both flexural and web) and the contribution of each component can not be separated.

The measured ultimate loads are compared with the theoretical ultimate loads computed by above mentioned five methods and are given in Table 6.11. The comparison reveals that:

- (i) The mean ratio of the computed ultimate load by ACI method to the measured ultimate load is 0.953 for beams of DB-P series and is equal to 0.703 for beams of DB-Q series.
- (ii) The above mentioned ratios are 1.65 and 1.366 for the beams of DB-P and DB-Q series respectively in case of Singh, Ray and Reddy's method.

Table 6.9a Ultimate Load Capacity of Test Beams Computed by Various methods

Beam mark	Components of ultimate load carried by				Computed total ultimate load (kip)
	Concrete (kip)	Flexural reinf(kip)	Horizontal web reinf. (kip)	Vertical web reinf. (kip)	
ACI Method (ACI 318-89)					
DB-P1	99.94	26.30	34.39	12.35	*172.98 168.32
DB-P2	108.02	28.45	45.84	12.35	*194.66 181.89
DB-P3	109.13	28.72	68.78	12.35	*218.98 183.80
DB-P4	111.17	29.26	68.78	12.35	*221.56 187.25
DB-P5	110.24	28.99	34.39	12.35	*185.97 185.66
DB-P6	109.48	28.81	45.84	12.35	*196.48 184.41
DB-P7	106.40	28.00	34.39	12.35	*181.14 179.20
S.P. Ray C.S. Reddy method					
DB-P1	133.20	108.92	19.44	1.84	263.40
DB-P2	166.84	110.72	24.12	1.76	303.44
DB-P3	173.16	161.84	35.60	1.72	372.32
DB-P4	200.24	87.88	31.36	1.56	321.04
DB-P5	179.60	157.92	17.36	1.68	356.56
DB-P6	182.72	94.52	22.48	1.64	301.36
DB-P7	168.84	105.28	17.20	1.68	293.00
Ramakrishnan and Ananthanarayana method					
DB-P1	67.74	---	---	---	67.74
DB-P2	88.41	---	---	---	88.41
DB-P3	92.69	---	---	---	92.69
DB-P4	114.98	---	---	---	114.98
DB-P5	97.39	---	---	---	97.39
DB-P6	100.84	---	---	---	100.84
DB-P7	92.20	---	---	---	92.20
Selvam and Kuruvilla method					
DB-P1	106.92	---	---	---	106.92
DB-P2	127.40	---	---	---	127.40
DB-P3	134.96	---	---	---	134.96
DB-P4	181.48	---	---	---	181.48
DB-P5	141.80	---	---	---	141.80
DB-P6	159.17	---	---	---	159.17
DB-P7	132.85	---	---	---	132.85

* Total summation of the contribution of each component but is dropped in the final consideration due to ACI Code limitation.

Table 6.9b Ultimate Load Capacity of Test Beams Computed by Various Methods

Beam mark	Components of ultimate load carried by				Computed total ultimate load (kip)	
	Concrete (kip)	Flexural reinf(kip)	Horizontal web reinf. (kip)	Vertical web reinf. (kip)		
ACI method (ACI 318-89)						
DB-Q1	39.79	18.82	29.70	17.91	*106.22	91.19
DB-Q2	42.12	27.34	38.64	17.91	*126.01	96.52
DB-Q3	42.09	30.28	47.62	17.84	*137.83	96.45
DB-Q4	43.41	19.03	48.97	17.98	*129.39	99.48
DB-Q5	43.03	30.92	30.12	17.98	*122.05	98.65
DB-Q6	43.37	18.92	38.89	17.95	*119.13	99.41
DB-Q7	41.35	27.86	30.36	18.02	*117.59	94.82
S.P. Ray and C.S. Reddy method						
DB-Q1	61.88	73.76	12.04	8.96	156.64	
DB-Q2	76.84	100.72	14.80	8.56	200.92	
DB-Q3	78.84	110.16	17.96	8.52	215.48	
DB-Q4	94.60	57.24	15.60	7.80	175.24	
DB-Q5	83.56	109.00	10.64	8.32	211.52	
DB-Q6	86.52	62.48	13.60	8.16	170.76	
DB-Q7	78.40	96.20	10.60	8.24	193.44	
Ramakrishnan and Ananthanarayana method						
DB-Q1	40.11	---	---	---	40.11	
DB-Q2	51.28	---	---	---	51.28	
DB-Q3	53.23	---	---	---	53.23	
DB-Q4	66.66	---	---	---	66.66	
DB-Q5	56.46	---	---	---	56.46	
DB-Q6	59.38	---	---	---	59.38	
DB-Q7	53.20	---	---	---	53.20	
Selvam and Kuruvilla method						
DB-Q1	57.79	---	---	---	57.79	
DB-Q2	74.69	---	---	---	74.69	
DB-Q3	73.20	---	---	---	73.20	
DB-Q4	96.05	---	---	---	96.05	
DB-Q5	77.63	---	---	---	77.63	
DB-Q6	85.56	---	---	---	85.56	
DB-Q7	77.46	---	---	---	77.46	

* Total summation of the contribution of each component but is dropped in the final consideration due to ACI Code limitations.

Table 6.10 Ultimate Load Capacity of Test Beams Computed by Mau and Hsu Method.

Beam mark	$K(=2d_v/D)$	w_v	w_h	$\frac{v}{f'_c}$	$V_n(=v.b.d_v)$ kip	Ultimate load capacity $P_n(=2V_n)$, kip
1	2	3	4	5	6	7
Series DB-P : L/D=1.0						
DB-P1	1.714	0.0671	0.1585	0.3727	81.324	162.648
DB-P2	1.714	0.0581	0.151	0.3551	93.964	187.928
DB-P3	1.714	0.0569	0.2222	0.4781	95.929	191.858
DB-P4	1.714	0.0559	0.1781	0.4012	97.572	195.144
DB-P5	1.714	0.0563	0.1792	0.4033	96.910	193.82
DB-P6	1.714	0.0571	0.150	0.3529	95.587	191.174
DB-P7	1.714	0.0604	0.1432	0.3433	90.295	180.59
Series DB-Q : L/D=2.0						
DB-Q1	1.589	0.1156	0.2673	0.5391	44.645	89.29
DB-Q2	1.589	0.1012	0.3421	0.5323	50.532	101.064
DB-Q3	1.585	0.0991	0.3877	0.5303	50.949	101.898
DB-Q4	1.593	0.0995	0.2658	0.5325	52.582	105.164
DB-Q5	1.593	0.0991	0.3487	0.5323	52.228	104.456
DB-Q6	1.592	0.0993	0.2480	0.5127	52.255	104.51
DB-Q7	1.596	0.1076	0.3422	0.5371	48.501	97.002

d_v = distance between the centers of flexural steel and the topmost horizontal steel.

Table 6.11 Comparison Of Observed Ultimate Loads and Computed Ultimate Loads by Various Methods.

Beam mark	Observed ultimate load, P_u (kip)	Computed ultimate load by the method					Ratios				
		ACI 318-89, P_{u1} (kip)	Singh, Ray and Reddy, P_{u2} (kip)	Ramakrishnan and Ananthanarayana, P_{u3} (kip)	Selvam and Kuruville, P_{u4} (kip)	Mau and Hsu, P_{u5} (kip)	$\frac{P_{u1}}{P_u}$	$\frac{P_{u2}}{P_u}$	$\frac{P_{u3}}{P_u}$	$\frac{P_{u4}}{P_u}$	$\frac{P_{u5}}{P_u}$
DB-P1	166.0	168.32	263.40	67.74	106.92	162.65	1.014	1.587	0.408	0.644	0.980
DB-P2	210.0	181.89	303.44	88.41	127.40	187.93	0.866	1.445	0.421	0.607	0.895
DB-P3	222.0	183.80	372.32	92.69	134.96	191.86	0.828	1.677	0.418	0.608	0.864
DB-P4	183.0	187.25	321.04	114.98	181.48	195.14	1.023	1.754	0.628	0.992	1.066
DB-P5	187.0	185.66	356.56	97.39	141.80	193.82	0.993	1.907	0.521	0.758	1.036
DB-P6	200.0	184.41	301.36	100.84	159.17	191.17	0.922	1.507	0.504	0.796	0.956
DB-P7	175.0	179.20	293.00	92.20	132.85	180.59	1.024	1.674	0.527	0.759	1.032
						Mean	0.953	1.650	0.490	0.738	0.976
						C	7.87%	8.71%	15.08%	17.11%	7.18%
DB-Q1	118.0	91.19	156.64	40.11	57.79	89.29	0.773	1.327	0.340	0.490	0.757
DB-Q2	150.0	96.52	200.92	51.28	74.67	101.06	0.643	1.339	0.342	0.498	0.674
DB-Q3	170.0	96.45	215.48	53.23	73.20	101.90	0.567	1.268	0.313	0.431	0.600
DB-Q4	126.0	99.48	175.24	66.66	96.05	105.16	0.731	1.289	0.490	0.706	0.773
DB-Q5	135.0	98.65	211.52	56.46	77.63	104.46	0.731	1.567	0.418	0.575	0.774
DB-Q6	133.0	99.41	170.76	59.38	85.56	104.51	0.747	1.284	0.446	0.643	0.786
DB-Q7	130.0	94.82	193.44	53.20	77.46	97.00	0.729	1.488	0.409	0.596	0.746
						Mean	0.703	1.366	0.394	0.563	0.730
						C	9.49%	7.82%	15.14%	15.75%	8.65%

C = Coefficient of variation.

- (iii) For Ramakrishnan and Ananthanarayana method the ratios are 0.490 and 0.394 for DB-P and DB-Q series of beams respectively.
- (iv) Selvam and Kuruvilla method determines the ratios as 0.738 and 0.563 for beams of DB-P and DB-Q series respectively, and
- (v) Mau and Hsu method shows the ratios 0.976 and 0.730 for the two series of beams respectively.

It is evident that the ratio of the computed (by all of the methods) and the measured ultimate load decreases with the increase in L/D ratio. If columns 2 and 6 of both the Tables 6.9a and 6.9b are compared, it becomes clear that a major bulk of the total ultimate load capacity is derived from concrete. Table 6.11 shows that ACI method is conservative in computation of ultimate loads of DB-Q beams (L/D=2.0) only while Singh, Ray and Reddy method overestimates the capacities for both the series of beams. On the other hand both Ramakrishnan and Ananthanarayana, & Selvam and Kuruvilla methods underestimate the ultimate load capacities of beams. Mau and Hsu method, which is one of the latest method, determines the ultimate load capacities of the beams of DB-P series with quite reasonable values but it also underestimates the ultimate load capacities of the beams of DB-Q series. Thus it seems that all these methods can be improved to predict the ultimate load capacity of deep beam with brick aggregate concrete.

6.4.3 Suggested Modifications of Different Methods for Determination of Ultimate Load Capacity.

ACI method⁽¹⁾ underestimates the ultimate loads of brick aggregate RC deep beams. The discrepancy is more prominent in beams having higher span to depth ratio. It may be noted that the ACI

method is based on beams using normal stone aggregate concrete for which the upper limit of nominal shear stress is $8/f'_c$. But for brick aggregate concrete the upper limit may be raised to $8.5/f'_c$ and $11/f'_c$ for beams of $L/D=1$ and $L/D=2$ respectively. Nominal shear strength depends on the tensile strength of concrete. It has been also observed by Akhtaruzzaman and Hasnat⁽²⁶⁾ that tensile strength of brick aggregate concrete is about 12% higher than that of stone aggregate concrete. Hence, it is suggested that the upper limit of nominal shear stress of $8/f'_c$ for stone aggregate concrete be raised for brick aggregate concrete deep beams.

The mean values of the ratios of computed ultimate load by Singh, Ray and Reddy⁽⁹⁾ method to observed ultimate load are 1.650 and 1.366 for DB-P and DB-Q beams respectively. This overestimation of ultimate load capacity is due to the variation of resisting shearing stress along the critical load path II but it was not considered by Ray and Reddy. They suggested the shear causing failure along critical load path II as :

$$Q_u = \frac{P_u}{4}$$

From which we get, $P_u = 4Q_u$ - - - - - (6.7)

But it is reasonable to consider the average value of the resisting shear and for the test beams It is found that the relation between the ultimate load capacity (P_u) and the average resisting shear force (Q_u) along the critical load path II (suggested by Singh, Ray and Reddy) are as follows :

(i) DB-P beams ($L/D = 1.0$)

From figure 6.1, the average value of resisting shear is

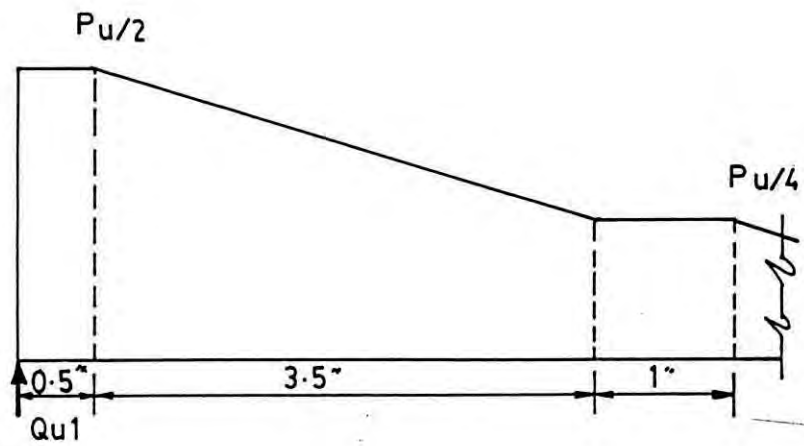


Fig. 6.1 Resisting shear force diagram near the left support (within the critical load path II).

$$Q_{u1} = \frac{1}{5} \left\{ \frac{1}{2} \times \frac{P_u}{2} + 3.5 \times \frac{1}{2} \left(\frac{P_u}{2} + \frac{P_u}{4} \right) + 1 \times \frac{P_u}{4} \right\}$$

$$\text{or, } Q_{u1} = \frac{29}{80} P_u$$

$$\text{or, } P_u = 2.7586 \times Q_{u1} \quad \text{----- (6.8)}$$

(ii) DB-Q beams ($L/D = 2.0$)

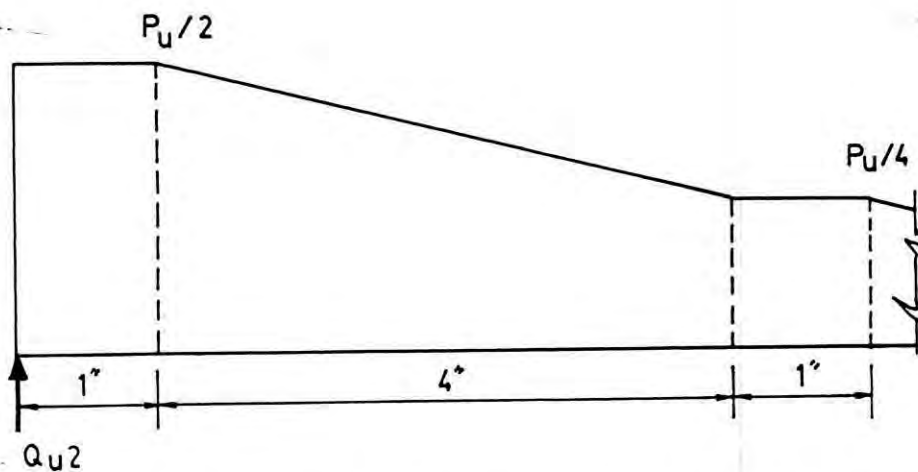


Fig. 6.2 Resisting shear force diagram near the left support (within the critical load path II).

Here the average value of resisting shear is

$$Q_{u2} = \frac{1}{6} \left(1 \times \frac{P_u}{2} + 4 \times \frac{1}{2} \left(\frac{P_u}{2} + \frac{P_u}{4} \right) + 1 \times \frac{P_u}{4} \right)$$

$$\text{or, } Q_{u2} = \frac{3}{8} P_u$$

$$\text{or, } P_u = 2.6667 \times Q_{u2} \quad \text{--- (6.9)}$$

Among the previously mentioned five methods the Ramakrishnan and Ananthanarayana⁽¹⁰⁾ one is the most conservative method (Ref. Table 6.11). The mean ratio of computed to observed ultimate loads are 0.490 and 0.394 for DB-P and DB-Q beams respectively. Here the contribution of concrete only is considered. Hence the resisting force taken by horizontal and vertical reinforcements should be included in the nominal ultimate load capacity of deep beams. Now, let us consider the two multiplying factors ϕ_h and ϕ_v for the contribution of total horizontal (flexural plus web reinf.) reinforcement and vertical web reinforcement respectively. Using the variation of ultimate load with the variation of reinforcements ratio and with the help of Least Square Method the two multiplying factors can be expressed as follows :

$$\phi_h = 1.60 + 20 \times p_h \quad \text{--- (6.10)}$$

$$\phi_v = 1.00 + 8 \times p_v \quad \text{--- (6.11)}$$

Where, p_h = total horizontal reinforcements ratio, and
 p_v = vertical web reinforcement ratio.

Therefore, the ultimate load capacity, by Ramakrishnan and

Ananthanarayana method, can be computed by the relation given below:

$$P_u = 2 \times K \times \phi_h \times \phi_v \times f'_{sp} \times b \times D \quad \text{--- (6.12)}$$

Where, $K = 1.12$ (suggested by Ramakrishnan and Ananthanarayana)
 f'_{sp} = cylinder splitting tensile strength of concrete,
 b = thickness of the beam,
 D = total depth of the beam.

Selvam and Kuruvilla⁽¹⁹⁾ method also underestimate the ultimate load capacity of deep beams (Ref. Table 6.11) subjected to uniformly distributed loads. This is also because of no consideration of resisting force taken by reinforcements provided in the beams. Two multiplying factors θ_h and θ_v can be considered for the contribution of horizontal and vertical reinforcements respectively. Using the test data and with the Least Square Method this two factors can be expressed as :

$$\theta_h = 1 + 22 \times p_h \quad \text{--- (6.13)}$$

$$\theta_v = 1 + 8 \times p_v \quad \text{--- (6.14)}$$

Where, p_h = total horizontal reinforcements ratio, and
 p_v = vertical web reinforcement ratio.

Thus the modified form of the method suggested by Selvam Kuruvilla can be expressed as follows :

$$P_u = (2.2 \times \alpha^{0.1} + 1.1 \times \beta^{0.2}) \times \epsilon^{0.5} \times \theta_h \times \theta_v \times f'_{sp} \times b \times D \quad \text{--- (6.15)}$$

Here the different letters except θ_h and θ_v indicate their usual meanings as suggested by Selvam and Kuruvilla.

Mau and Hsu⁽²⁰⁾ method is quite reasonable for deeper

beams ($L/D=1.0$) but it is conservative for beams with larger span to depth ratio (Ref. Col. 12 of Table 6.11). In our test programme the beams of DB-Q series ($L/D=2.0$) has larger horizontal reinforcement ratio (p_h) than the beams of DB-P series ($L/D=1.0$). Mau and Hsu set the limiting value of the ratio of resisting shearing stress (v) to concrete crushing strength (f'_c) as -

$$(v/f'_c) \leq 0.30 \quad - - - - - (6.16)$$

Including the span to depth ratio (L/D) and the total horizontal reinforcements ratio (p_h) in the above equation (eqn. 6.16) the modified expression can be written as

$$(v/f'_c) \leq \{0.30 + 12.5 (p_t - 0.015) (L/D - 1.0)\} \quad - - - - (6.17)$$

Ultimate load computed by various methods after suggested modifications (eqns. 6.5a and 6.5b and eqn. 6.8 through eqn. 6.15 and eqn. 6.17) are presented in Table 6.12 and are compared with the observed corresponding ultimate loads. From this table, it seems that the suggestions are reasonable for computing ultimate loads of brick aggregate R.C. deep beams (simply supported) when subjected to uniform loading. Yet it should be emphasized that the suggested change may be used only for an approximate estimate of the ultimate loads until extensive tests prove its applicability beyond doubt.

6.5 MOMENT CHARACTERISTICS OF TEST BEAMS

The moment capacity of test beams at different load levels (at diagonal cracking load and at ultimate load), and their computed flexural capacity and also the ratio of these two types of moment capacities are presented in Table 6.13. These include the maximum moment at initial diagonal cracking load designated as the maximum critical moment M_{cr} , the maximum moment at ultimate load M_u ,

Table 6.12 Comparison of Observed Ultimate Loads with Ultimate Loads Computed by Various Methods after Suggested Modifications

Beam mark	Observed ultimate load P_u (kip)	Computed ultimate load by suggested modified method					Ratios				
		ACI 318-89	Ray and Reddy	Ramkrishnan and Ananthanarayana	Selvan and Kuruville	Mau and Hsu	$\frac{P_{u1}}{P_u}$	$\frac{P_{u2}}{P_u}$	$\frac{P_{u3}}{P_u}$	$\frac{P_{u4}}{P_u}$	$\frac{P_{u5}}{P_u}$
		P_{u1} (kip)	P_{u2} (kip)	P_{u3} (kip)	P_{u4} (kip)	P_{u5} (kip)					
DB-P1	166.0	172.98	181.65	123.80	130.38	162.65	1.042	1.094	0.746	0.785	0.980
DB-P2	210.0	193.26	209.27	166.00	162.35	187.93	0.920	0.977	0.790	0.773	0.895
DB-P3	222.0	195.27	256.77	183.30	186.82	191.86	0.880	1.157	0.826	0.842	0.864
DB-P4	183.0	198.96	221.41	215.72	231.09	195.14	1.087	1.210	1.179	1.263	1.066
DB-P5	187.0	185.97	245.90	186.57	186.73	193.82	0.994	1.315	0.998	0.998	1.036
DB-P6	200.0	195.92	207.83	185.63	196.49	191.17	0.980	1.039	0.928	0.982	0.956
DB-P7	175.0	181.14	202.07	171.06	166.13	180.59	1.035	1.155	0.978	0.949	1.032
						Mean	0.991	1.138	0.921	0.942	0.976
						C	6.74%	8.71%	14.94%	16.59%	7.18%
DB-Q1	118.0	106.22	104.43	83.01	84.59	95.61	0.900	0.885	0.704	0.717	0.810
DB-Q2	150.0	126.01	133.95	114.17	122.13	138.96	0.840	0.893	0.761	0.814	0.926
DB-Q3	170.0	132.60	143.65	125.92	130.93	167.71	0.780	0.845	0.741	0.770	0.987
DB-Q4	136.0	129.39	116.83	142.42	147.59	126.20	0.951	0.859	1.047	1.085	0.928
DB-Q5	135.0	122.05	141.01	128.73	131.54	154.51	0.904	1.045	0.953	0.974	1.145
DB-Q6	133.0	119.13	113.84	124.61	127.96	118.01	0.896	0.856	0.937	0.962	0.887
DB-Q7	130.0	117.59	128.96	116.37	123.32	125.70	0.905	0.992	0.895	0.949	0.967
						Mean	0.882	0.911	0.863	0.896	0.950
						C	5.82%	7.83%	13.78%	13.58%	10.09%

C = Coefficient of variation.

and the flexural moment capacity M_{uf} , of the test beams. The flexural moment capacities of test beams M_{uf} , were calculated according to the ACI 318-89 Code⁽¹⁾ provisions for ultimate strength design of gravel aggregate concrete.

The ratio M_{tr}/M_{uf} is found to attain a mean value of about 0.37 for the beams of DB-P series and that for the beams of DB-Q series is about 0.39. However, it is perhaps suggestive to assume the maximum moment at initial diagonal cracking load to be about 37% of the flexural capacity for the beams of smaller span to depth ratios and subjected to uniformly distributed load.

From the table 6.13 it is seen that the average ultimate moment at failure is 79% of the flexural moment capacity for beams with $L/D=1.0$ while that for the other set of beams ($L/D=2.0$) appeared to be about 10% higher than the computed flexural capacity. From this it may be concluded that the deep beams subjected to uniform loading may or may not reach its maximum flexural capacity at failure. And this is in disagreement with the conclusion made by Kabir⁽⁵⁾.

6.6 LOAD DEFLECTION CHARACTERISTICS OF TEST BEAMS

The load deflection records of the test beams are presented graphically in figures 5.1 through 5.4. The deflection record represents the mid-span deflection with appropriate compensation made for support settlements. The usual linear relationship for shallow beams between load and deflection are found to be absent even in the lower range of loading prior to cracking. The corresponding deflections considering both flexure and shear were also computed and are furnished in these figures. The computations of deflections prior to flexural cracks were made using the formula for uncracked section (See Appendix-C)

$$\delta = \delta_m (1 + 2.208 D^2/L^2) \quad - - - - - (6.18)$$

Table 6.13 Moment Characteristics of Test Beams.

Beam mark	Maximum moment at		Computed flexural capacity, M_{uf} (K'')	Ratio $\frac{M_{cr}}{M_{uf}}$	Ratio $\frac{M_u}{M_{uf}}$
	Diagonal cracking load, M_{cr} (K'')	Ultimate load M_u (K'')			
1	2	3	4	5	6
Series DB-P : L/D=1.0					
DB-P1	210.00	435.75	549.64	0.382	0.793
DB-P2	236.25	551.25	601.93	0.392	0.916
DB-P3	288.75	582.75	869.62	0.332	0.670
DB-P4	236.25	480.38	554.49	0.425	0.865
DB-P5	236.25	490.88	870.41	0.272	0.564
DB-P6	236.25	525.00	554.88	0.426	0.946
DB-P7	210.00	459.38	600.46	0.350	0.765
			Mean	0.368	0.788
			C	13.86%	16.04%
Series DB-Q : L/D=2.0					
DB-Q1	165.00	354.00	302.64	0.545	1.170
DB-Q2	150.00	450.00	430.51	0.348	1.045
DB-Q3	150.00	510.00	475.42	0.316	1.073
DB-Q4	150.00	408.00	308.39	0.486	1.323
DB-Q5	240.00	405.00	475.42	0.505	0.852
DB-Q6	90.00	399.00	308.39	0.292	1.294
DB-Q7	90.00	390.00	425.53	0.212	0.917
			Mean	0.386	1.096
			C	30.16%	15.07%

C = Coefficient of variation.

where, δ = total deflection at mid-span,

δ_m = mid-span deflection due to bending only

$$= (5wL^2)/(384E_cI)$$

and, $E_c = 40000/\sqrt{f'_c}$ (For brick aggregate concrete, Ref.26)

After the formation of flexural cracks, the mid span deflections were computed using effective moment of inertia I_e and effective concrete area A_g , by the formula (See Appendix-C)

$$\delta = \frac{5PL^3}{384E_cI_e} \left[1 + 26.496 \times \frac{I_e}{A_gL^2} \right] \quad \text{--- (6.19)}$$

where, $I_e = I_{cr} + \left(\frac{M_{cr}}{M_a} \right)^3 (I_g - I_{cr})$

I_{cr} = Moment of inertia of cracked transformed section
 $= 0.5b(kd)^2(kd/6 + 1) + nA_g(d - kd)^2$

I_g = Moment of inertia of gross concrete section
 $= (bD^3)/12$

M_{cr} = Cracking moment = $(f_r I_g)/Y_t$

f_r = Modulus of rupture
 $= 8.3/\sqrt{f'_c}$ (For brick aggregate concrete, Ref.26)

$Y_t = D/2$

M_a = Maximum moment at the section considered
 $= wL^2/8 = PL/8$

$A_g = (12b^2 I_g)(2/3)$

$E_c = 40000/\sqrt{f'_c}$

It is seen that the actual deflections were significantly larger than the computed deflections. This was also observed by Kabir⁽⁵⁾; and also by Manuel, Slight, and Suter⁽¹⁵⁾ during their tests on deep beams. The shearing stresses, being considerably high in deep beams, appear to have significant effect on the deflections of such beams. Also the deviations of the observed deflections from the computed deflections are found to be more

pronounced in case of relatively deeper beams ($L/D=1$) compared to the other set with $L/D=2$.

6.7 CRACKING PATTERN AND MODE OF FAILURE

During the test programme the crack pattern and the mode of failure of each test beam were carefully observed and recorded. The crack pattern of each test beam was drawn during the testing operation and the photographs of the cracked surface of the beam were taken afterwards. The systems of crack patterns and the modes of failure of test beams are discussed in the following articles.

6.7.1 Cracking Pattern

Figures 5.5 through 5.18 show the cracks at failure of beams together with the loads at which each crack was first observed and the extent of the crack at that load.

Table 6.14 shows the diagonal cracking loads, the flexural cracking loads and the ultimate loads of all the test beams. From this table it is seen that the diagonal cracks develop first for the beams of DB-P series (except for DB-P6) and the mean values of P_{cr}/P_u and P_f/P_u are 0.47 and 0.54 respectively. On the other hand the flexural cracks appear before the diagonal cracks for the beams of DB-Q series (except for DB-Q7) and the mean values of P_{cr}/P_u and P_f/P_u are 0.36 and 0.31 respectively. Therefore it can be concluded that the deeper beam faces the diagonal cracks before the flexural cracks and can have greater values of the mean values of P_{cr}/P_u and P_f/P_u .

In all of the beams of DB-P and DB-Q series, it was observed that diagonal cracks propagated initially at higher rate but this rate of propagation decreases with the increase of load applied.

Table 6.14 Cracking Load Characteristics of Test Beams.

Beam mark	Diagonal cracking load, P_{cr} (kip)	Flexural cracking load, P_f (kip)	Ultimate load, P_u (kip)	Ratio $\frac{P_{cr}}{P_u}$	Ratio $\frac{P_f}{P_u}$
1	2	3	4	5	6
Series DB-P : L/D=1.0					
DB-P1	80	90	166	0.482	0.542
DB-P2	90	120	210	0.429	0.571
DB-P3	110	120	222	0.495	0.541
DB-P4	90	100	183	0.492	0.546
DB-P5	90	100	187	0.481	0.535
DB-P6	90	80	200	0.450	0.400
DB-P7	80	110	175	0.457	0.629
			Mean	0.469	0.538
			C	4.85%	11.86%
Series DB-Q : L/D=2.0					
DB-Q1	55	40	118	0.466	0.339
DB-Q2	50	50	150	0.333	0.333
DB-Q3	50	50	170	0.294	0.294
DB-Q4	50	40	136	0.368	0.294
DB-Q5	80	50	135	0.593	0.370
DB-Q6	30	30	133	0.226	0.226
DB-Q7	30	40	130	0.231	0.308
			Mean	0.359	0.309
			C	34.16%	13.70%

C = Coefficient of variation.

Flexural cracks penetrated the distances about 0.262D, 0.221D, 0.321D, 0.231D, 0.231D, 0.345D, 0.079D, 0.534D, 0.390D, 0.415D, 0.488D, 0.488D 0.531D, 0.437D in beams DB-P1, DB-P2, DB-P3, DB-P4, DB-P5, DB-P6, DB-P7, DB-Q1, DB-Q2, DB-Q3, DB-Q4, DB-Q5, DB-Q6, DB-Q7 respectively. The average value of these penetrations is 0.241D for the beams of DB-P series and that for the DB-Q beams is 0.469D. It is seen that even at ultimate load level, flexural cracks remain within the lower half of the beam depth.

6.7.2 Mode of Failure

All of the beams of DB-P series failed due to diagonal tension. Here concrete splitting occurred along the line of propagation of main inclined cracks. The concrete strut, formed between two approximately parallel diagonal cracks, were observed in some of the beams, e.g. DB-P2, DB-P5, Db-P7, DB-Q3, DB-Q4, DB-Q6. But the destruction of the strut by crushing of concrete described as " Shear Proper" by de Paiva and Siess⁽¹²⁾ was never found to occur during the tests. Possibly the presence of the adequate web reinforcements inhibited such failure.

Flexural failure was not the final mode of failure in any of the test beams though flexural cracks developed first in almost all of the beams of DB-Q series.

Leonhardt⁽¹³⁾ has reported that crushing of concrete at bearing blocks was the principal cause of failure he has encountered in the very deep beams ($L/D < 2$) of his test. Such crushing of concrete was not observed during our test programme. Obviously the width of the bearing blocks provided were sufficient to prevent such occurrences.

CHAPTER 7

CONCLUSIONS AND RECOMMENDATIONS FOR FUTURE STUDY

7.1 CONCLUSIONS

The conclusions are based on the study of structural behavior and shear strength of fourteen reinforced brick aggregate concrete beams having span to overall depth ratio (L/D) of 1 and 2 and subjected to uniformly distributed load at the top (compression face) only. The findings pertain to the simply supported single span beams.

From the test results the following tentative conclusions may be drawn. It may be emphasized here that further investigations are necessary to confirm these findings.

- (1) Tied arch-action initiate at an applied load of 50% of the ultimate load capacity for beams of span to depth ratio of 1 ($L/D=1$) and that is 70% of the ultimate load capacity for the beams of $L/D=2$.
- (2) Diagonal cracks develop first in relatively deeper beams ($L/D=1$) and flexural cracks develop first in the shallower beams ($L/D=2$) provided the beams have sufficient reinforcements.
- (3) ACI 318-89 Recommendations underestimates the shear stress causing diagonal cracking in deep beams.
- (4) The increase in flexural reinforcement or, horizontal web reinforcement alone has no significant influence upon the diagonal cracking shear stress of deep beam subjected to uniform loading.

- (5) The upper limit of the diagonal cracking shear stress of simply supported brick aggregate RC deep beam subjected to uniform loading may be taken as $4\sqrt{f'_c}$.
- (6) The de Cosio equation (Eqn. 6.2) may be used quite reliably to predict the shear stress at initial diagonal cracking.
- (7) The increase in ultimate load capacity of deep beams depend upon the increase in both the flexural and horizontal web reinforcements. Either the flexural or, the horizontal web reinforcement alone has no significant influence upon the ultimate load capacity.
- (8) The upper limit of the ultimate shear stress of simply supported brick aggregate RC deep beam subjected to uniformly distributed load may be taken as $8.5\sqrt{f'_c}$ and $11\sqrt{f'_c}$ for beams of span to depth ratio of 1 and 2 respectively.
- (9) The principal mode of failure in deep beams having adequate reinforcements is diagonal tension cracking. The concrete 'strut' between two parallel diagonal cracks may sometimes be formed but, in general, the failure of a deep beam was not due to the compression failure by crushing of such a 'strut'.
- (10) Singh, Ray, and Reddy⁽⁹⁾ method of computing ultimate load capacity of deep beams under four point loading can be used effectively by considering the average resisting shear along the critical load path II (as suggested by them) (Eqn.6.8 and Eqn.6.9).
- (11) Ultimate loads in shear of deep reinforced concrete beams can be estimated with a fair degree of accuracy by

Ramakrishnan and Ananthanarayana⁽¹⁰⁾ method by taking into consideration the contribution of reinforcements along with that of concrete (Eqn. 6.10 through Eqn. 6.12).

(12) Selvam and Kuruvilla⁽¹⁹⁾ method can also be effectively used in computing the ultimate load capacity of deep beams under uniform loading by considering the contributions of reinforcements along with that of concrete (Eqn. 6.13 through Eqn. 6.15).

(13) For correct estimation of ultimate load of deep beams by the Mau and Hsu⁽²⁰⁾ formula, the ratio of resisting shear stress to concrete crushing strength (v/f'_c) should be modified as in Eq. 6.17 .

7.2 RECOMMENDATIONS FOR FUTURE STUDY

The conclusions stated above were limited by the scope of the tests. It is believed that a wider area in this field remains unexplored in order to develop the guidelines for laying out a proper code of practice for designers. It should, therefore, be mentioned that the investigation on the effect of longitudinal reinforcements upon the strength of deep reinforced brick aggregate concrete beams should be continued and all the possible variables should be studied. The following recommendations are made for further research in brick aggregate reinforced concrete deep beams:

- (1) Influence of span to depth ratio (L/D) and shear span to depth ratio (a/D) on the cracking strength and ultimate strength of brick aggregate R C beams.
- (2) Influence of different types of loading on the strength of deep beams.

- (3) Effect of cyclic and sustained loading on the shear strength of deep beams.
- (4) Influence of the dimensions of reaction blocks and loading block/blocks on the load carrying capacity of deep reinforced brick aggregate concrete beams.
- (5) Behavior of brick aggregate reinforced concrete deep T-beams.
- (6) Influence of end anchorage plates and standard hooks on the performance of deep beams.
- (7) Influence of deformed bars (both flexural and web steel) on the ultimate load capacity of deep beams.
- (8) Behavior of R C deep beams with different end conditions.
- (9) Effect of different bar size used as web reinforcement on the strength of deep beams.
- (10) Influence of openings in the web of reinforced brick aggregate deep beams on the strength of such beams.
- (11) Influence of compression steel on the behavior of deep beams.
- (12) Effect of beam width upon the strength of deep beams.

LIST OF REFERENCES

1. ACI Standard, "Building Code Requirements for Reinforced Concrete (ACI 318-89)", 1st Printing, November, 1989, Detroit, U.S.A.
2. Comite Europeen du Beton-Federation Internationale de la Precontrainte, International Recommendations for the Design and Construction of Concrete Structures, Appendix 3, 1st ed., June, 1970. Published by the Cement and Concrete Association, London.
3. "The Shear Strength of Reinforced Concrete Members", by the joint ASCE-ACI Committee on Shear and Diagonal Tension of the Committee on Masonry and Reinforced Concrete of Structural Division, James G. MacGregor, Chmn., Journal of the Structural Division, ASCE, V.99, No.ST6 Proc., Paper 9791, June, 1973, pp.1091-1187.
4. ACI-ASCE Committee 426, "Shear and Diagonal Tension", ACI Journal Proceedings V.59, No.1, Jan.,1962, pp.1-30, No.2, Feb.,1962, pp.277-340, No.3, Mar.,1962, pp.353-396.
5. Kabir, A., "Shear Strength of Deep Reinforced Concrete Beam", Master's Thesis submitted to the Department of Civil Engineering, BUET, Dhaka, Oct., 1982.
6. Ali, G., "Study of Stress Distribution in Deep Reinforced Concrete Beams", Master's Thesis submitted to the Department of Civil Engineering, BUET, Dhaka, Sept., 1984.
7. Diaz de Cosio, R., and Siess, C.P. " Behavior and Strength in Shear of Beams and Frames without Web Reinforcement", Journal of the American Concrete Institute, Vol.56, Feb., 1960 pp.695-735.

8. ACI Standard, "Building Code Requirements for Reinforced Concrete (ACI 318-77)", 1st Printing, Dec., 1977, Detroit, U.S.A.
9. Singh, R., Ray, S.P., and Reddy, C.S., "Some Tests on Reinforced Concrete Deep Beams with and without Opening in the Web", Journal of the American Concrete Institute, vol.54, No.7, July, 1980, pp.189-194.
10. Ramakrishnan, V., and Ananthanarayana, Y., "Ultimate Strength of Deep Beams in Shear", Journal of the American Concrete Institute, Proceedings Vol. 65, No. 2, Feb., 1968, pp. 87-98.
11. Holmes*, M., and Meson, P.M., "Stresses in Deep Beams", Building Science, Vol. 7, pp.225-232, Pergamon Press, 1972.
12. de Paiva, H.A.R., and Siess, C.P., "Strength and Behavior of Deep Beams", ASCE Proc. Vol. 91, ST. 5, Oct, 1965, pp.19-41.
13. Leonhardt, F., "Strength and Behavior of Deep Beams in Shear", ASCE Proc., Vol. 92, ST. 2, April, 1966, pp.427-432.
14. Kong, F.K., Robins, P.J., and Cole, D.F., "Web Reinforcement Effects on Deep Beams", ACI Journal Proc., Vol. 67, No. 12, Dec., 1970, pp.1010-1017.
15. Manuel, R.F., Slight, B.W., and Suter, G.T., "Deep Beam Behavior Affected by the Length and Shear Span Variations", ACI Journal, Vol. 68, No. 12, Dec., 1971, pp.954-958.
16. Smith, K.N., and Vantsiotis, A.S., "Shear Strength of Deep Beams", ACI Journal, Vol.79, No.3, May-June, 1982, pp.201-213.
17. Berry, J.E., and Heino Ainsso, "Single Span Deep Beams", ASCE Journal Proc., Vol. 109, No. 3, March, 1983, pp.646-663.

18. Rogosky, D.M., Macgregor, J.G., and Ong, S.Y., "Tests of Reinforced Concrete Deep Beams", ACI Journal, Vol. 83, No.4, July-August, 1986, pp.614-623.
19. Manicka Selvam, V.K., and Kuruvilla, T., "Shear Strength of Concrete Deep Beams", The Indian Concrete Journal, August, 1987, Vol. 61, pp.219-222.
20. Mau, S.T., and Hsu, T.C., "Formula for the Shear Strength of Deep Beams", ACI Structural Journal, Vol. 86, No. 5, Sept-Oct., 1989, pp.516-523.
21. Park, R., and Paulay, T., "Reinforced Concrete Structures", John Willey and Sons, New York, 1974, pp.700-713, pp.286.
22. Raju, N.K., "Advanced Reinforced Concrete Design", CBS publishers & Distributors, Delhi, India, 1st Edition, 1988, pp.299-313.
23. Coker, E.G., and Filon, L.N.G., A Treatise on Photoelasticity, Cambridge University Press, London, 2nd Edition, 1957, pp.458-461.
24. Winter, G., and Nilson, A.H., "Design of Concrete Structures", McGraw-Hill Book Company, 10th Edition, 2nd Printing 1987, pp.138-146.
25. "Annual Book of ASTM Standard", Vol. 04.02, Printed at Easton, MD, 1988, U.S.A.
26. Ali A. Akhtaruzzaman, and Abul Hasnat, " Properties of Concrete Using Crushed Brick as Aggregate ", Concrete International Design & Construction, Vol.5, No.2, February, 1983, pp. 58-63.

APPENDIX - A

1. DESIGN OF TEST BEAM DB-P1

There is no method for designing brick aggregate R.C. deep beams. Here the test beams were designed according to ACI Building Code (ACI 318-89) recommendations. Beams DB-P1 and DB-Q1 were designed according to ACI Code. For all other beams, the amount of either the flexural or the horizontal web reinforcement or both were increased in relation to those of first beam of the corresponding series. Sample calculations for the design of test beam, DB-P1, to fail in shear as per ACI 318-89 Code provision is presented here.

Given Data for Beam DB-P1 :

Effective span of beam	: $L = l_n = 21''$
Nominal width of beam	: $b = 6''$
Overall depth of beam	: $D = 21''$
Effective depth of beam	: $d = (D - 1.5) = 19.5''$
Distance of critical section from the support center line	: $X_c = \{1.5 + 0.15 \times 21\} = 4.65''$
Area of flexural reinforcement	: $A_s = 2 \times 0.294 = 0.588 \text{ in.}^2$
Nominal concrete strength	: $f'_c = 2510 \text{ psi}$
Yield strength of flexural steel	: $f_y = 51000 \text{ psi}$
Yield strength of web steel	: $f_{wy} = 33000 \text{ psi}$
Area of web steel bar	: $A_v = A_{vh} = 0.054 \text{ in.}^2$

CALCULATIONS :

$$\text{Spacing of vertical stirrups, } s_{\max} = (0.054 \times 2) / (0.0015 \times 6) \\ = 12'' > d/5 (=3.9'')$$

So, selected spacing, $s = 3.5''$

$$\text{Spacing of horizontal stirrups, } (s_2)_{\max} = (0.054 \times 2) / (0.0025 \times 6) \\ = 7.2'' > d/3 (=6.5'')$$

So, selected spacing, $s_2 = 6''$

$$\begin{aligned} \text{Flexural steel ratio, } p &= (0.294 \times 2)/(6 \times 19.5) \\ &= 0.00503 \end{aligned}$$

From fig. A.1 we get, $M_u/V_u = (1.81P)/(0.2786P) = 6.50$

$$\text{Now, } v_c = \left(3.5 - 2.5 \times \frac{M_u}{V_u d} \right) \left(1.9/f_c' + 2500 \times \frac{p V_u d}{M_u} \right) \quad \text{--- (A.1)}$$

$$= \left(3.5 - 2.5 \times \frac{6.50}{19.5} \right) \left(1.9/2510 + 2500 \times \frac{0.00503 \times 19.5}{6.50} \right)$$

$$= 2.667 \times 132.915$$

$$= 2.5 \times 132.915 \quad \left[\left(3.5 - 2.5 \frac{M_u}{V_u d} \right) \leq 2.5 \right]$$

$$= 332.29 \text{ psi}$$

But $v_c \leq 6/f_c' \quad (= 6/2510 = 300.60 \text{ psi})$

So, $V_c = v_c b d = (300.60 \times 6 \times 19.5) \text{ lbs.} = 35.17^k$

$$\text{Now, } V_s = \left[\frac{A_v}{12 s} \left(1 + \frac{l_n}{d} \right) + \left(\frac{A_{vh}}{12 s_2} \left(11 - \frac{l_n}{d} \right) \right) \right] \times f_{wy} \times d \quad \text{--- (A.2)}$$

$$\text{or, } V_s = \left[\frac{0.054 \times 2}{12 \times 3.5} \left(1 + \frac{21}{19.5} \right) + \frac{0.054 \times 2}{12 \times 6} \left(11 - \frac{21}{19.5} \right) \right] \times 33 \times 19.5$$

$$= 13.01^k$$

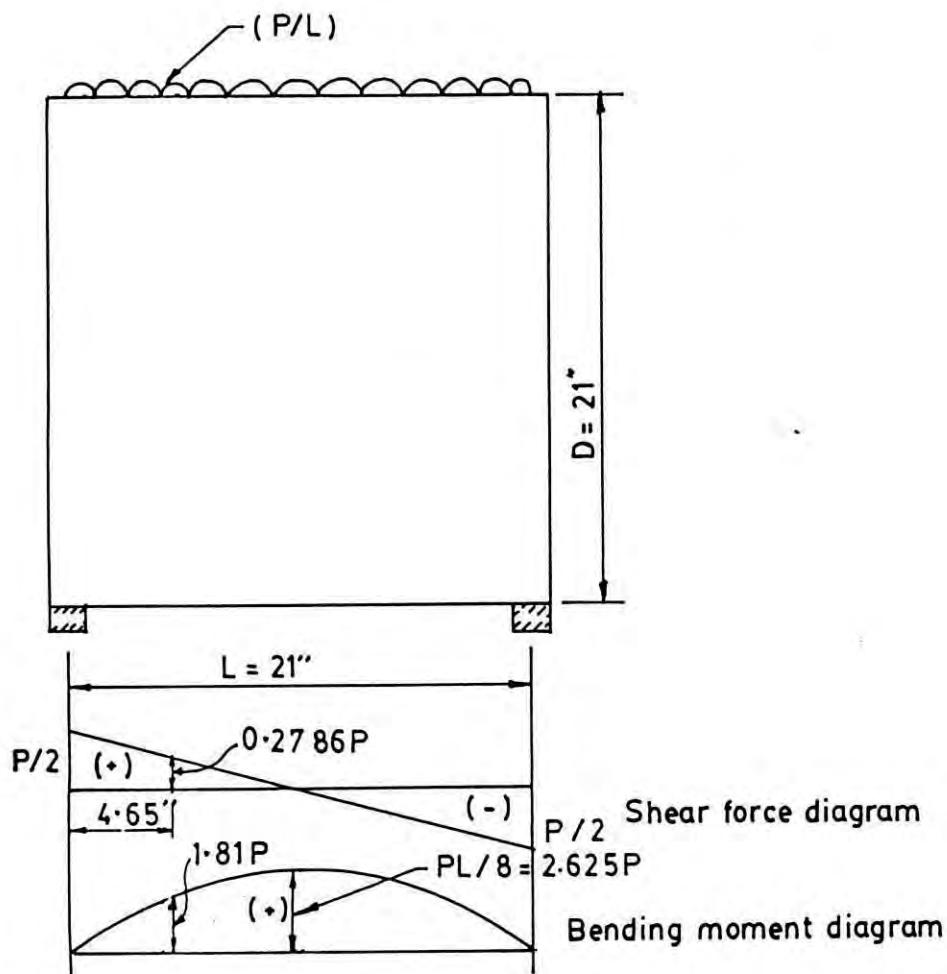


Fig. A-1 Simply supported beam of DB-P Series .

$$V_u = V_c + V_s = (35.17 + 13.01)^k = 48.18^k$$

$$\text{But } V_u \leq 8/f_c b d = (8/2510 \times 6 \times 19.5) \text{ lbs.} = 46.89^k$$

$$\text{So, } V_u = 46.89^k$$

$$\text{Now, critical shear, } 0.2786P = V_u = 46.89$$

$$\text{or, } P = 168.30^k$$

$$\text{Maximum moment, } M_{us} = PL/8 = [(168.30 \times 21)/8] \text{ k"} = 441.79 \text{ k"}$$

$$\text{Again, } M_{uf} = A_s f_y (d - a'/2) \quad \text{---(A.3)}$$

$$\text{here, } a' = \frac{A_s f_y}{0.85 f_c b} = \frac{(0.294 \times 2) \times 51}{0.85 \times 2.51 \times 6} = 2.343''$$

$$\text{So, } M_{uf} = (0.294 \times 2) \times 51 \times \left(19.5 - \frac{2.343}{2} \right) \text{ k''}$$

$$\text{or, } M_{uf} = 549.64 \text{ k''} > M_{us} (= 441.79 \text{ k''}) \quad \text{O.K.}$$

APPENDIX - B

SAMPLE CALCULATIONS FOR ULTIMATE LOAD CAPACITY OF TEST BEAM DB-P1BY VARIOUS METHODS

Data given are :

$$\begin{aligned} b &= 6", & D &= 21", \\ L &= 21", & f'_c &= 2510 \text{ psi}, \\ f'_{sp} &= 240 \text{ psi}, & f_y &= 51000 \text{ psi}, \\ f_{wy} &= 33000 \text{ psi}. & & \text{(5/8" dia bar)} \\ & & & \text{(1/4" dia bar)} \end{aligned}$$

Here, the different letters indicate their usual meaning.

1. ACI⁽¹⁾ APPROACH :

Let the total ultimate load capacity of beam DB-P1 = P kip.

So, the applied load per unit length = (P/21) k/in.

According to the Code, the distance of critical section from the nearest support center

$$= (1.5 + 0.15 \times 21)" = 4.65"$$

So, at the critical section -

Shear force, $V_u = \{(P/2) - (P/21)(4.65)\}^k = 0.27857P^k$

and bending moment, $M_u = \{(P/2)(4.65) - (P/21)(4.65^2/2)\} k"$
 $= 1.81018P k"$

So, the ratio, $M_u/(V_u d) = 1.81018P/(0.27857P \times 19.5) = 0.3332$

We know,

$$v_c = (3.5 - 2.5 \times \frac{M_u}{V_u d}) (1.9/f'_c + 2500 \times \frac{P V_u d}{M_u}) \quad \text{--- (B.1)}$$

$$\begin{aligned}
 v_c &= (3.5 - 2.5 \times 0.3332) \{ 1.9/f'_c + 2500 \times (p V_u d)/M_u \} \\
 &= 2.6667 \{ 1.9/f'_c + 2500 \times (p V_u d)/M_u \} \\
 &= 2.5 \{ 1.9/f'_c + 2500 (p V_u d)/M_u \} \quad [(3.5 - 2.5 M_u/V_u d) \leq 2.5]
 \end{aligned}$$

So, the shear in the critical section due to concrete contribution is -

$$\begin{aligned}
 V_c &= (2.5 \times 1.9/f'_c) b d \\
 &= \{ (2.5 \times 1.9/2510) 6 \times 19.5 \} \text{ lbs.} \\
 &= 27.843^k
 \end{aligned}$$

Hence, the concrete contribution in ultimate load capacity is

$$\begin{aligned}
 &= (27.843/0.27857)^k \\
 &= 99.94^k
 \end{aligned}$$

But, $v_c = 2.5 \{ 1.9/f'_c + (2500 p V_u d / M_u) \} \leq 6/f_c$
or, $(2500 p V_u d / M_u) \leq 0.5/f_c$

[Here, $(2500 \times 0.00503 / 0.3332) = 37.703 > 0.5/f_c (= 25.05)$]

So, the shear in critical section due to flexural steel contribution is -

$$\begin{aligned}
 V_f &= (2.5 \times 0.5/f'_c) b d \\
 \text{or, } V_f &= \{ (2.5 \times 0.5/2510) 6 \times 19.5 \} \text{ lbs.} \\
 &= 7.327^k
 \end{aligned}$$

Therefore, the flexural steel contribution in ultimate load is

$$\begin{aligned}
 &= (7.327/0.27857)^k \\
 &= 26.30^k
 \end{aligned}$$

Again, $V_s = \left[\frac{A_v}{s} \left(\frac{1 + l_n/d}{12} \right) + \frac{A_{vh}}{s_2} \left(\frac{11 - l_n/d}{12} \right) \right] f_{wy} d \quad \text{---(B.2)}$

Here, the contribution of vertical web steel in shear is

$$\begin{aligned}
 V_{sv} &= \left[\frac{A_v}{s} \left(\frac{1 + l_n/d}{12} \right) \right] f_{wy} d \\
 &= \left[\left\{ \frac{0.054 \times 2}{3.5} \left(\frac{1 + 21/19.5}{12} \right) \right\} 33 \times 19.5 \right]^k \\
 &= 3.437^k
 \end{aligned}$$

Hence, the contribution of vertical web steel in ultimate load is

$$\begin{aligned}
 &= (3.437 / 0.27857)^k \\
 &= 12.34^k
 \end{aligned}$$

Similarly, the contribution of horizontal web steel in ultimate load is, (from eqn. B.2)

$$\begin{aligned}
 &= \left[\frac{1}{0.27857} \left\{ \frac{0.054 \times 2}{6.0} \left(\frac{11 - 21/19.5}{12} \right) \right\} 33 \times 19.5 \right]^k \\
 &= \left[\frac{1}{0.27857} \times 9.578 \right]^k \\
 &= 34.39^k
 \end{aligned}$$

2. SINGH, RAY and REDDY⁽⁹⁾ APPROACH :

For uniformly distributed load, the critical load path II should be considered (i.e. $\beta = \beta_2$)

Nominal shear span of beam, $X_n = (1.5 + 0.5 + 3.5 + 1.0 + 1.75)''$
 $= 8.25''$

Effective shear span of beam, $X = (0.5 + 3.5 + 1.0)'' = 5.0''$

Cohesion of concrete, $c = \frac{\sqrt{f'_c} \times \sqrt{f'_{sp}}}{2}$

$$\text{or, } c = \frac{\sqrt{2510} \times \sqrt{240}}{2} \text{ psi} = 0.388 \text{ ksi}$$

Tangent of the angle of internal friction(ϕ) of concrete is

$$\begin{aligned} \tan\phi &= \frac{f'_c - f'_{sp}}{2 \times \sqrt{f'_c} \times \sqrt{f'_{sp}}} \\ &= \frac{2510 - 240}{2 \times \sqrt{2510} \times \sqrt{240}} = 1.462 \end{aligned}$$

Angle of inclination of critical load path with the horizontal is

$$\beta = \tan^{-1} (D/X) = \tan^{-1} (21/5) = 76.608^\circ$$

$$\tau_1 = \left(1 - \frac{X_n}{3D}\right) = \left(1 - \frac{8.25}{3 \times 21}\right) = 0.869$$

Therefore, the contribution of concrete in ultimate load capacity is-

$$\begin{aligned} &= 4 \times P_c \times \tau_1 = 4 \times \frac{c b D}{\sin\beta \cos\beta (\tan\beta + \tan\phi)} \times \tau_1 \\ &= \left[4 \times \frac{0.388 \times 6 \times 21}{\sin 76.608^\circ \cos 76.608^\circ (\tan 76.608^\circ + 1.462)} \times 0.869\right]^k \\ &= 133.20^k \end{aligned}$$

Contribution of flexural steel in ultimate load capacity is

$$= 4 \times P_s \times \mu_s = 4 \times (A_s \times f_y) \times \frac{\tan\beta \tan\phi - 1}{\tan\beta + \tan\phi} \times \mu_s$$

$$= [4 \times (2 \times 0.294 \times 51) \times \frac{4.2 \times 1.462 - 1}{4.2 + 1.462} \times 1] \text{ kip} \quad [\mu_s = 1]$$

$$= 108.92^k$$

Contribution of vertical web steel in ultimate load capacity is

$$= 4 \times P_{wv} \times \mu_w = 4 \times (F_{wv} \times \frac{\tan\phi}{\tan\beta + \tan\phi}) \times 0.5 \quad [\mu_w = 0.5]$$

$$= [4 \times (2 \times 0.054 \times 33 \times \frac{1.462}{4.2 + 1.462}) \times 0.5]^k \quad [F_{wv} = \Sigma(A_{wv} \times f_{wy})]$$

$$= 1.84^k$$

Contribution of horizontal web steel in ultimate load capacity,

$$= 4 \times P_{wh} \times \mu_w = 4 \times (F_{wh} \times \frac{\tan\beta \tan\phi - 1}{\tan\beta + \tan\phi}) \times 0.5$$

$$= [4 \times (3 \times 2 \times 0.054 \times 33 \times \frac{4.2 \times 1.462 - 1}{4.2 + 1.462}) \times 0.5]^k \quad [F_{wh} = \Sigma(A_{wh} \times f_{wy})]$$

$$= 19.44^k$$

3. RAMAKRISHNAN and ANANTHANARAYANA⁽¹⁰⁾ APPROACH :

Total ultimate load capacity of the beam is,

$$P_c = 2 \times k \times f_{sp} \times b \times D \quad \text{--- (B.3)}$$

$$= [2 \times 1.12 \times 240 \times 6 \times 21] \text{ lbs.}$$

$$= 67.74^k$$

4. SELVAM and KURUVILLA⁽¹⁹⁾ APPROACH :

Ultimate load capacity of the beam is,

$$P_u = [2.2 \alpha^{0.1} + 1.1 \beta^{0.2}] \times \epsilon^{0.5} \times f_{sp} \times b \times d \quad \text{--- (B.4)}$$

Here, $\alpha = a/D = (1.5 + 0.5 + 1.75)/21 = 0.1786$

$$\beta = D/L = 21/21 = 1.0$$

and, $\epsilon = \frac{f_y \text{ (ksi)}}{35.55} = \frac{51.0}{35.55} = 1.4346$

Therefore,

$$P_u = [(2.2 \times 0.1786^{0.1} + 1.1 \times 1.0^{0.2}) \times 1.4346^{0.5} \times 240 \times 6 \times 21] \text{ lbs.}$$

$$= 106.92^k$$

5. MAU and HSU⁽²⁰⁾ APPROACH :

According to this method,

$$\frac{v}{f_c} = 0.5 [K(w_h + 0.030) + \sqrt{\{K^2(w_h + 0.03)^2 + 4(w_h + 0.03)(w_v + 0.03)\}}] \leq 0.30 \quad \text{--- (B.5)}$$

For test beam,

$$K = (2 d_v)/D = \{2 \times (19.5 - 1.0)\}/21 = 1.714$$

$$w_h = P_h \times \frac{f_y}{f_c} = 0.0078 \times \frac{51.0}{2.51} = 0.1585 < 0.26 \quad \text{O.K.}$$

$$w_v = p_v \times \frac{f_y}{f'_c} = 0.0051 \times \frac{33.0}{2.51} = 0.0671 < 0.12 \quad \text{O.K.}$$

Hence, from eqn.(B.5), we get

$$\frac{v}{f'_c} = 0.5 [1.714 (0.1585 + 0.03) + \sqrt{\{1.714^2 (0.1585 + 0.03)^2 + 4(0.1585 + 0.03)(0.0671 + 0.03)\}}]$$

$$\text{or, } v/f'_c = 0.3727 \quad [\text{ But } v/f'_c \leq 0.30]$$

$$\text{Therefore, } v/f'_c = 0.30$$

$$\text{or, } v = (0.30 \times 2.51) \text{ ksi} = 0.753 \text{ ksi}$$

$$\text{Now, } V_h = v b d_v = [0.753 \times 6 \times (19.5 - 1.0)]^k = 81.324^k$$

Hence, the ultimate load capacity of the beam is

$$P_u = 2 V_h = (2 \times 81.324)^k = 162.648^k$$

APPENDIX - C

DERIVATION OF FORMULA FOR DEFLECTION :

There are no special methods for computation of deflection in deep beams. Here the formula for computation of deflection in ordinary beam considering the effect of shear is derived.

Deflection at any point within the span is given by -

$$\delta = \int \left\{ \frac{M(x) m(x)}{E I} dx \right\} + K_{\phi} \int \left\{ \frac{V(x) v(x)}{G A} dx \right\} \quad \text{--- (C.1)}$$

where,

$M(x), V(x)$ = bending moment and shear force due to actual load (fig. C.1),

$m(x), v(x)$ = bending moment and shear force caused by unit load at the point where deflection is required (fig. C.1),

K_{ϕ} = shape factor = 1.2 for rectangular section.

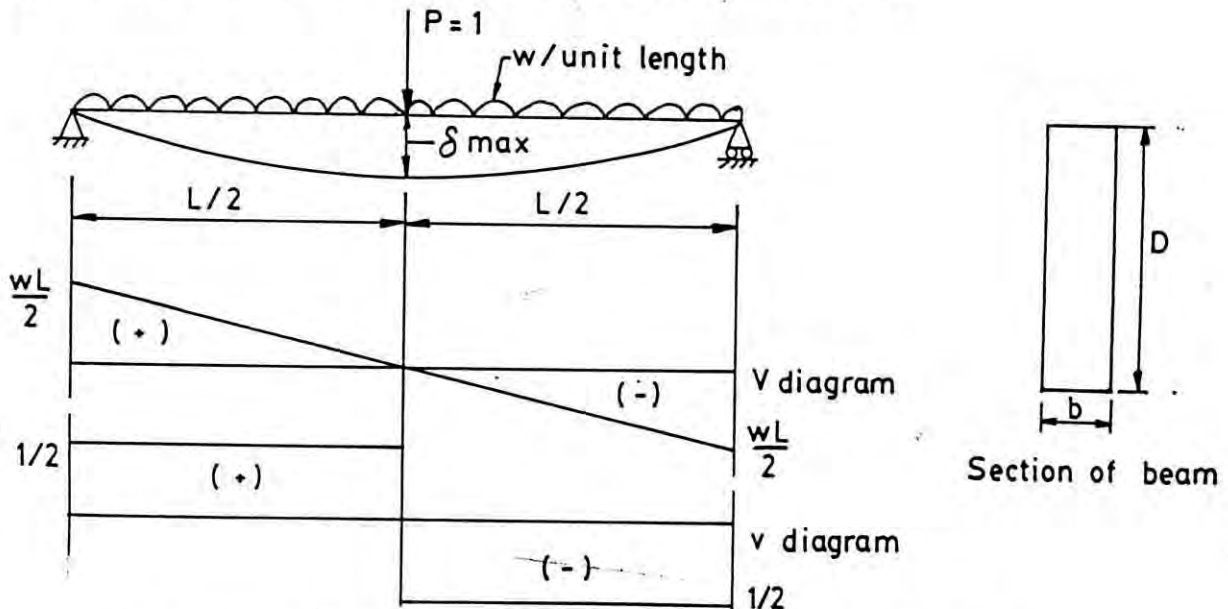


Fig. C.1 An uniformly distributed loaded beam.

Now,

$$\delta_{\max} = \delta_m + \delta_v \quad \text{--- (C.2)}$$

where,

δ_m = contribution of moment on deflection, and

δ_v = contribution of shear on deflection.

$$\text{Here, } \delta_m = \frac{5wL^4}{384E_c I} \quad \text{--- (C.3)}$$

$$\text{and, } \delta_v = 2 \times \frac{K_\phi}{GA} \left(\frac{1}{2} \times \frac{wL}{2} \times \frac{L}{2} \times \frac{1}{2} \right) = K_\phi \times \frac{wL^2}{8GA} \quad \text{--- (C.4)}$$

$$\text{Again, } E_c/G = 2(1 + \nu)$$

[ν = poisson's ratio

= 0.15 for concrete]

$$\text{Therefore, } \delta_{\max} = \frac{5wL^4}{384E_c I} + \frac{K_\phi wL^2}{8GA} \quad \text{[From eqns.C.2, C.3 and C.4]}$$

$$= \frac{5wL^4}{384E_c I} \left(1 + K_\phi \frac{48E_c I}{5GAL^2} \right)$$

$$\text{or, } \delta_{\max} = \frac{5wL^4}{384E_c I} \left(1 + 9.6 K_\phi \frac{E_c}{G} \times \frac{I}{AL^2} \right) \quad \text{--- (C.5)}$$

(i) UNCRACKED SECTION :

For a rectangular section of size $b \times D$,

$$\frac{I}{AL^2} = \frac{b D^3}{12 \times bDL^2} = \frac{D^2}{12L^2}$$

Therefore, putting the values of K_{ϕ} , (E_c/G) , and (I/AL^2) in eqn.(C.5),

$$\begin{aligned}\delta_{\max} &= \frac{5wL^4}{384E_c I} \left(1 + 2.208 \frac{D^2}{L^2} \right) \\ &= \delta_m \left(1 + 2.208 \frac{D^2}{L^2} \right) \quad \text{--- (C.6)}\end{aligned}$$

(ii) CRACKED SECTION :

After the formation of flexural cracks the effective concrete area A_e , and the effective moment of inertia I_e should be used for the computation of deflections.

Hence eqn.(C.5) reduces to

$$\begin{aligned}\delta_{\max} &= \frac{5PL^3}{384E_c I_e} \left(1 + 9.6 \times 1.2 \times 2.3 \times \frac{I_e}{A_e L^2} \right) \\ &= \frac{5PL^3}{384E_c I_e} \left(1 + 26.496 \times \frac{I_e}{A_e L^2} \right) \quad \text{--- (C.7)}\end{aligned}$$

Table C.1 Computed maximum deflections (in mm) at midspan of Test Beams at different load levels.

Beam mark	Load level	0 ^k	20 ^k	40 ^k	60 ^k	80 ^k	100 ^k	120 ^k	140 ^k	160 ^k	180 ^k	200 ^k	222 ^k
Series DB-P : L/D = 1.0													
DB-P1	0.0	0.0212	0.0423	0.0635	0.0942	0.1344	0.1734	0.2109	0.2468	0.2574	---	---	---
DB-P2	0.0	0.0196	0.0392	0.0588	0.0784	0.1177	0.1526	0.1860	0.2184	0.2499	0.2807	0.2959	---
DB-P3	0.0	0.0194	0.0388	0.0582	0.0776	0.1080	0.1353	0.1616	0.1872	0.2123	0.2372	0.2643	---
DB-P4	0.0	0.0190	0.0380	0.0571	0.0781	0.1160	0.1539	0.1907	0.2263	0.2656	---	---	---
DB-P5	0.0	0.0192	0.0384	0.0576	0.0783	0.1068	0.1341	0.1602	0.1858	0.2108	0.2195	---	---
DB-P6	0.0	0.0193	0.0386	0.0580	0.0804	0.1189	0.1564	0.1937	0.2293	0.2637	0.2974	---	---
DB-P7	0.0	0.0199	0.0398	0.0597	0.0840	0.1201	0.1550	0.1886	0.2236	0.2448	---	---	---
Series DB-Q : L/D = 2.0													
DB-Q1	0.0	0.0776	0.1994	0.3105	0.4177	0.5239	0.6190	---	---	---	---	---	---
DB-Q2	0.0	0.0733	0.1624	0.2475	0.3314	0.4148	0.4980	0.5811	0.6227	---	---	---	---
DB-Q3	0.0	0.0742	0.1485	0.2227	0.2969	0.3711	0.4454	0.5196	0.5938	0.6310	---	---	---
DB-Q4	0.0	0.0704	0.1833	0.2906	0.3931	0.4941	0.5941	0.6742	---	---	---	---	---
DB-Q5	0.0	0.0710	0.1419	0.2129	0.2838	0.3548	0.4258	0.4790	---	---	---	---	---
DB-Q6	0.0	0.0708	0.1849	0.2931	0.3964	0.4981	0.6000	0.6644	---	---	---	---	---
DB-Q7	0.0	0.0733	0.1607	0.2444	0.3270	0.4093	0.4914	0.5324	---	---	---	---	---

Deflections are computed considering the cracked sections (after formation of diagonal cracks) and using $E_c = 40000/f_c'$ (Ref.26)

APPENDIX - D

Table D.1 Observed strain values (in micro strain) in reinforcements of beam DB-P1 at different load levels

Gauge no.	Load level at which strain was measured																	
	0 ^k	10 ^k	20 ^k	30 ^k	40 ^k	50 ^k	60 ^k	70 ^k	80 ^k	90 ^k	100 ^k	110 ^k	120 ^k	130 ^k	140 ^k	150 ^k	160 ^k	166 ^k
1	0	17	32	51	72	96	123	154	197	305	409	539	678	786	918	1050	1179	1239
2	0	16	32	52	74	103	147	188	237	398	535	687	825	936	1069	1199	1332	1382
3	0	6	12	19	31	50	75	126	285	510	639	785	932	1074	1269	1462	1725	2037
4	0	3	4	8	14	21	28	40	47	65	85	97	124	184	295	439	598	644
5	0	11	21	32	48	71	95	172	474	662	795	820	931	1030	1183	1336	1411	2777
6	0	1	0	1	4	7	9	15	28	32	50	101	223	378	556	731	854	937
7	0	0	-4	0	0	8	10	26	50	141	232	344	388	428	495	537	473	117
8	0	-16	-36	-60	-80	-99	-122	-147	-195	-248	-272	-259	-197	-116	-2	147	429	829
9	0	-10	-22	-36	-50	-63	-79	-86	-13	20	33	48	52	63	86	100	126	194

Strain corresponding to yield stress of flexural reinforcement = 1532 MS (micro strain)

Strain corresponding to yield stress of web reinforcement = 1118 MS

Table D.2 Observed strain values (in micro strain) in reinforcements of beam DB-P2 at different load levels.

Gauge no.	Load level at which strain was measured																					
	0 ^k	10 ^k	20 ^k	30 ^k	40 ^k	50 ^k	60 ^k	70 ^k	80 ^k	90 ^k	100 ^k	110 ^k	120 ^k	130 ^k	140 ^k	150 ^k	160 ^k	170 ^k	180 ^k	190 ^k	200 ^k	210 ^k
1	-	-	-	-	-	-	-	-	-	-	-	-	-	-	-	-	-	-	-	-	-	-
2	0	31	52	74	79	101	126	170	221	260	331	396	492	568	642	718	808	892	950	1040	1149	1186
3	0	-1	-1	-1	25	27	32	36	40	55	133	216	297	355	424	493	582	676	767	918	1214	1253
4	0	7	14	21	29	36	45	54	64	73	73	72	95	135	265	385	506	603	672	731	758	801
5	0	6	12	20	26	33	42	52	64	90	401	594	741	837	948	1043	1176	1307	1492	2128	3253	3253
6	0	3	7	11	16	21	29	39	51	70	113	155	328	477	575	683	809	918	998	989	1032	1149
7	0	4	8	12	17	20	24	29	33	43	100	148	350	448	564	656	792	906	1007	1116	1362	2555
8	0	-5	-7	-7	-8	-11	-8	-10	-12	-15	-10	-12	-14	-15	-16	-16	-16	-17	-15	-16	-18	-18
9	0	-11	-24	-35	-51	-66	-81	-99	-119	-140	-173	-224	-258	-294	-334	-370	-415	-444	-445	-441	-429	-285

Strain corresponding to yield stress of flexural reinforcement = 1417 MS (micro strain)

Strain corresponding to yield stress of web reinforcement = 1118 MS

Table D.3 Observed strain values (in micro strain) in reinforcements of beam DB-P3 at different load levels.

Gauge no.	Load level at which strain was measured																						
	0 ^k	10 ^k	20 ^k	30 ^k	40 ^k	50 ^k	60 ^k	70 ^k	80 ^k	90 ^k	100 ^k	110 ^k	120 ^k	130 ^k	140 ^k	150 ^k	160 ^k	170 ^k	180 ^k	190 ^k	200 ^k	210 ^k	222 ^k
1	0	15	14	-38	23	232	248	-38	94	149	371	226	519	606	508	583	662	805	931	1059	948	835	1103
2	0	-7	43	61	92	110	126	144	153	241	217	305	336	438	465	557	647	675	697	760	873	938	956
3	0	7	23	18	18	24	55	74	105	147	232	321	441	447	591	582	641	758	851	961	976	1010	1301
4	-	-	-	-	-	-	-	-	-	-	-	-	-	-	-	-	-	-	-	-	-	-	-
5	0	-3	22	32	48	61	91	134	218	343	677	970	1083	1219	1356	1498	1643	1829	2018	2309	2676	3039	3306
6	0	-51	-42	-23	-4	-23	-6	-17	-30	5	-20	-6	-10	-18	-23	2	19	17	68	40	61	92	167
7	0	15	8	-1	6	-5	3	25	63	190	505	809	940	1090	1226	1389	1543	1679	1830	1902	2030	2024	2357
8	0	-49	-65	-77	-68	-116	-123	-163	-190	-173	-306	-303	-327	-348	-363	-432	-388	-301	-409	-321	-195	-26	961
9	0	-149	-32	-116	-61	13	-51	-99	-132	-30	-115	-15	138	41	257	59	171	275	183	241	89	138	346

Strain corresponding to yield stress of flexural reinforcement = 1382 MS (micro strain)

Strain corresponding to yield stress of web reinforcement = 1118 MS

Table D.4 Observed strain values (in micro strain) in reinforcements of beam DB-P4 at different load levels.

Gauge no.	Load level at which strain was measured																			
	0 ^k	10 ^k	20 ^k	30 ^k	40 ^k	50 ^k	60 ^k	70 ^k	80 ^k	90 ^k	100 ^k	110 ^k	120 ^k	130 ^k	140 ^k	150 ^k	160 ^k	170 ^k	180 ^k	183 ^k
1	-	-	-	-	-	-	-	-	-	-	-	-	-	-	-	-	-	-	-	-
2	0	3	14	22	28	39	47	68	74	91	110	130	149	166	193	212	227	248	257	239
3	-	-	-	-	-	-	-	-	-	-	-	-	-	-	-	-	-	-	-	-
4	0	2	5	10	15	20	28	32	36	36	39	43	45	47	50	50	49	50	40	22
5	0	3	4	6	9	10	14	16	20	22	15	-2	-6	-10	-10	4	6	39	57	81
6	0	-2	-3	5	10	13	26	29	35	31	37	7	-16	-49	-70	-59	-52	-51	-50	-59
7	0	1	4	8	12	14	19	24	31	40	57	68	81	117	186	281	303	321	371	403
8	0	-1	-36	-4	-6	-10	-14	-19	-22	-33	4	30	46	59	80	90	103	142	302	499
9	0	-5	-7	-8	-10	-12	-12	-15	-18	-23	-33	-39	-45	-50	-55	-54	-46	-47	-63	-76

Strain corresponding to yield stress of flexural reinforcement = 1532 MS (micro strain)

Strain corresponding to yield stress of web reinforcement = 1118 MS

Table D.5 Observed strain values (in micro strain) in reinforcements of beam DB-P5 at different load levels.

Gauge no.	Load level at which strain was measured																			
	0 ^k	10 ^k	20 ^k	30 ^k	40 ^k	50 ^k	60 ^k	70 ^k	80 ^k	90 ^k	100 ^k	110 ^k	120 ^k	130 ^k	140 ^k	150 ^k	160 ^k	170 ^k	180 ^k	187 ^k
1	0	17	35	55	72	100	136	167	204	250	324	407	474	543	642	689	784	842	938	1007
2	0	11	29	48	65	99	127	153	190	227	314	389	459	514	610	657	756	826	935	1017
3	0	9	20	36	57	81	113	150	203	287	381	464	525	589	698	754	869	933	1077	1256
4	-	-	-	-	-	-	-	-	-	-	-	-	-	-	-	-	-	-	-	-
5	0	14	51	65	85	100	126	226	387	595	719	836	975	1008	1103	1290	1359	1561	1583	1652
6	0	-7	1	-9	0	-12	-78	-122	-123	-94	123	211	359	430	543	652	718	780	947	1174
7	0	11	12	14	16	20	25	32	46	67	52	68	87	121	250	373	643	759	895	1007
8	0	-28	-58	-85	-100	-118	-100	-126	-159	-211	-176	-238	-303	-282	-275	-262	-196	-78	185	454
9	0	-3	-4	-5	-7	-8	-11	-9	-8	-9	-10	-11	-13	-14	-14	-15	-13	-15	-14	-14

Strain corresponding to yield stress of flexural reinforcement = 1382 MS (micro strain)

Strain corresponding to yield stress of web reinforcement = 1118 MS

Table D.6 Observed strain values (in micro strain) in reinforcements of beam DB-P6 at different load levels.

Gauge no.	Load level at which strain was measured																				
	0 ^k	10 ^k	20 ^k	30 ^k	40 ^k	50 ^k	60 ^k	70 ^k	80 ^k	90 ^k	100 ^k	110 ^k	120 ^k	130 ^k	140 ^k	150 ^k	160 ^k	170 ^k	180 ^k	190 ^k	200 ^k
1	-	-	-	-	-	-	-	-	-	-	-	-	-	-	-	-	-	-	-	-	-
2	0	0	8	15	22	27	38	53	62	66	73	130	151	118	120	144	159	169	189	191	294
3	-	-	-	-	-	-	-	-	-	-	-	-	-	-	-	-	-	-	-	-	-
4	0	5	2	-3	-11	7	14	30	-6	2	16	25	28	33	38	62	63	65	76	69	112
5	0	11	15	20	30	34	31	33	44	48	51	41	39	36	23	41	25	17	6	2	37
6	0	6	-50	-42	-35	-29	-24	-19	0	4	7	-52	-57	-59	-67	-3	-78	-73	-78	-107	-90
7	0	5	8	11	15	16	17	19	21	23	-85	-80	-79	-73	-68	-64	50	47	52	47	404
8	0	-10	-20	-32	-37	-48	-22	-12	-41	-20	-90	-20	-5	27	101	122	112	110	158	113	707
9	0	-156	-84	-46	37	22	30	35	48	-87	173	335	344	296	235	217	151	189	242	327	434

Strain corresponding to yield stress of flexural reinforcement = 1532 MS (micro strain)

Strain corresponding to yield stress of web reinforcement = 1118 MS

Table D.7 Observed strain values (in micro strain) in reinforcements of beam DB-P7 at different load levels.

Gauge no.	Load level at which strain was measured																		
	0 ^k	10 ^k	20 ^k	30 ^k	40 ^k	50 ^k	60 ^k	70 ^k	80 ^k	90 ^k	100 ^k	110 ^k	120 ^k	130 ^k	140 ^k	150 ^k	160 ^k	170 ^k	175 ^k
1	0	22	39	62	86	97	150	183	235	338	430	501	578	648	727	813	897	966	978
2	0	19	40	67	96	113	170	204	247	325	394	457	524	590	666	751	849	931	949
3	0	3	4	4	4	5	20	73	182	295	407	523	613	704	807	961	1206	1342	1362
4	0	9	15	25	32	37	52	64	75	80	80	90	146	249	362	428	533	632	684
5	0	14	26	41	53	57	91	143	313	677	856	1025	1135	1248	1391	1452	1439	1502	1639
6	0	-6	-3	3	15	0	4	17	42	67	87	113	177	235	324	404	451	606	718
7	0	-5	-8	-7	-6	-5	-6	-7	-8	-9	-9	-10	-11	-10	-11	-10	-11	-11	-13
8	0	-28	-44	-57	-70	-74	-104	-108	-108	-65	-30	20	50	79	108	86	137	427	591
9	0	-23	-41	-58	-77	-78	-109	-135	-166	-210	-254	-305	-338	-346	-311	-204	-58	145	344

Strain corresponding to yield stress of flexural reinforcement = 1417 MS (micro strain)

Strain corresponding to yield stress of web reinforcement = 1118 MS

Table D.8 Observed strain values (in micro strain) in reinforcements of beam DB-Q1 at different load levels.

Gauge no.	Load level at which strain was measured												
	0 ^k	10 ^k	20 ^k	30 ^k	40 ^k	50 ^k	60 ^k	70 ^k	80 ^k	90 ^k	100 ^k	110 ^k	118 ^k
1	0	24	131	204	356	536	737	890	972	1144	1396	1573	1778
2	0	108	107	241	430	558	841	801	1001	1061	1367	1368	1466
3	0	116	43	87	222	381	625	839	952	1139	1416	1557	1462
4	0	-29	-3	-11	180	424	548	706	802	939	1019	1290	2165
5	0	22	34	5	65	198	350	269	289	237	274	495	599
6	0	-227	-34	-174	-243	-199	-132	-33	-206	-76	-43	419	737
7	0	-9	-74	10	10	-46	-141	-22	-7	33	-20	233	350
8	0	125	16	20	120	256	280	191	312	223	320	525	562
9	0	48	54	63	40	-34	-44	-17	-23	66	123	490	447

Strain corresponding to yield stress of flexural reinforcement = 1417 MS (micro strain)

Strain corresponding to yield stress of web reinforcement = 1118 MS

Table D.9 Observed strain values (in micro strain) in reinforcements of beam DB-Q2 at different load levels.

Gauge no.	Load level at which strain was measured															
	0 ^k	10 ^k	20 ^k	30 ^k	40 ^k	50 ^k	60 ^k	70 ^k	80 ^k	90 ^k	100 ^k	110 ^k	120 ^k	130 ^k	140 ^k	150 ^k
1	0	33	73	146	251	358	442	548	643	724	809	906	1015	1126	1332	1475
2	0	38	78	150	264	372	454	570	689	789	886	979	1074	1181	1358	1504
3	0	13	19	21	50	84	104	164	249	339	422	516	616	727	889	1166
4	0	14	25	44	84	137	169	217	265	301	337	374	417	453	493	556
5	0	7	10	13	19	26	50	151	282	377	471	556	641	736	858	992
6	0	-1	-7	-6	10	53	80	117	149	175	197	226	308	395	522	887
7	0	2	-1	-6	-8	-11	-8	-6	11	71	118	199	342	449	563	624
8	0	-13	-40	-6	-7	-7	14	85	144	199	230	233	232	217	175	139
9	0	1	-8	-17	-22	-26	-40	-51	-66	-70	-82	-102	-121	-126	-104	-40

Strain corresponding to yield stress of flexural reinforcement = 1382 MS (micro strain)

Strain corresponding to yield stress of web reinforcement = 1118 MS

Table D.10 Observed strain values (in micro strain) in reinforcements of beam DB-Q3 at different load levels.

Gauge no.	Load level at which strain was measured																	
	0 ^k	10 ^k	20 ^k	30 ^k	40 ^k	50 ^k	60 ^k	70 ^k	80 ^k	90 ^k	100 ^k	110 ^k	120 ^k	130 ^k	140 ^k	150 ^k	160 ^k	170 ^k
1	0	44	91	163	277	368	457	539	622	692	768	846	900	972	1040	1077	1080	1241
2	0	44	82	146	263	366	461	543	627	702	790	880	964	1062	1148	1252	1386	1434
3	0	-8	-4	1	5	28	64	98	164	246	302	345	378	414	443	481	519	562
4	0	10	27	58	172	283	433	512	573	623	672	727	771	816	853	903	950	1009
5	0	18	26	35	40	60	62	73	133	276	471	629	732	830	916	1009	1092	1136
6	0	-11	-18	-14	10	46	129	166	201	222	237	254	268	285	292	307	326	407
7	0	2	3	6	7	14	21	34	78	102	362	497	596	696	798	917	1022	1165
8	0	6	4	2	1	7	42	61	111	233	233	238	264	272	294	322	347	338
9	0	27	6	0	-9	-17	-36	-48	-37	-29	214	369	466	545	606	640	642	527

Strain corresponding to yield stress of flexural reinforcement = 1112 MS (micro strain)

Strain corresponding to yield stress of web reinforcement = 1118 MS

Table D.11 Observed strain values (in micro strain) in reinforcements of beam DB-Q4 at different load levels.

Gauge no.	Load level at which strain was measured														
	0 ^k	10 ^k	20 ^k	30 ^k	40 ^k	50 ^k	60 ^k	70 ^k	80 ^k	90 ^k	100 ^k	110 ^k	120 ^k	130 ^k	136 ^k
1	0	46	84	240	331	440	523	595	686	786	884	979	1103	1229	1291
2	0	45	81	242	339	461	555	660	759	858	961	1067	1175	1301	1357
3	0	24	44	82	124	291	417	577	714	832	942	1069	1139	1208	1254
4	0	25	43	162	236	339	394	439	494	552	609	674	746	823	888
5	0	-7	5	23	47	154	256	395	536	654	776	826	945	1094	1286
6	0	17	18	37	74	216	263	298	327	378	398	467	512	552	630
7	0	11	18	34	44	59	103	202	285	340	355	391	460	670	881
8	0	-14	-23	-19	-28	1	52	128	202	269	359	461	539	706	881
9	0	-18	-43	-69	-94	-118	-112	-51	19	97	186	308	426	783	991

Strain corresponding to yield stress of flexural reinforcement = 1417 MS (micro strain)

Strain corresponding to yield stress of web reinforcement = 1118 MS

Table D.12 Observed strain values (in micro strain) in reinforcements of beam DB-Q5 at different load levels.

Gauge no.	Load level at which strain was measured														
	0 ^k	10 ^k	20 ^k	30 ^k	40 ^k	50 ^k	60 ^k	70 ^k	80 ^k	90 ^k	100 ^k	110 ^k	120 ^k	130 ^k	135 ^k
1	0	43	99	201	274	349	430	525	613	696	783	875	956	1051	1084
2	-	-	-	-	-	-	-	-	-	-	-	-	-	-	-
3	0	19	43	70	106	186	316	424	506	576	649	735	817	918	1023
4	0	0	17	48	93	144	180	222	263	313	352	393	438	540	838
5	0	14	30	52	86	158	267	409	491	572	602	695	819	1106	1379
6	0	-22	-44	-62	-80	-85	-69	-79	-100	-122	-146	-161	-133	193	375
7	0	-11	-25	-32	-41	-46	-61	-75	-51	32	118	238	413	733	1079
8	0	-4	-19	-27	-28	-20	28	93	107	24	-92	-289	-425	-1011	-1327
9	0	-42	-67	-85	-126	-119	-72	18	98	152	202	244	366	549	698

Strain corresponding to yield stress of flexural reinforcement = 1112 MS (micro strain)

Strain corresponding to yield stress of web reinforcement = 1118 MS

Table D.13 Observed strain values (in micro strain) in reinforcements of beam DB-Q6 at different load levels.

Gauge no.	Load level at which strain was measured															
	0 ^k	10 ^k	20 ^k	30 ^k	40 ^k	50 ^k	60 ^k	70 ^k	80 ^k	90 ^k	100 ^k	110 ^k	120 ^k	130 ^k	133 ^k	
1	0	30	72	249	368	485	580	670	763	849	954	1033	1127	1162	1120	
2	0	37	78	260	461	648	807	963	1101	1224	1340	1439	1463	1557	1582	
3	0	27	75	175	388	554	693	811	913	991	1061	1122	1172	1200	1194	
4	0	33	88	154	345	462	553	613	663	716	761	825	863	860	768	
5	0	35	47	81	241	393	500	595	739	813	889	1075	1216	1338	1522	
6	0	-79	-122	-118	-97	-95	-61	-23	55	112	179	202	268	353	443	
7	0	-10	-23	-21	-20	-2	18	112	272	439	616	831	1077	1206	1327	
8	0	-1	-21	-3	53	125	189	228	269	334	383	425	502	667	724	
9	0	-24	-52	-55	-74	-50	-11	39	82	109	137	151	181	291	317	

Strain corresponding to yield stress of flexural reinforcement = 1417 MS (micro strain)

Strain corresponding to yield stress of web reinforcement = 1118 MS



Table D.14 Observed strain values (in micro strain) in reinforcements of beam DB-Q7 at different load levels.

Gauge no.	Load level at which strain was measured													
	0 ^k	10 ^k	20 ^k	30 ^k	40 ^k	50 ^k	60 ^k	70 ^k	80 ^k	90 ^k	100 ^k	110 ^k	120 ^k	130 ^k
1	0	40	80	233	380	480	581	658	755	836	920	1010	1105	1193
2	0	35	73	174	316	411	511	597	701	789	882	978	1080	1173
3	0	23	85	200	352	493	592	663	747	812	887	968	1076	1239
4	0	35	25	48	70	109	163	216	275	331	381	426	472	545
5	0	19	43	165	304	490	596	670	675	721	793	916	1126	1467
6	0	-17	-31	-29	-5	21	40	52	70	92	168	247	375	482
7	0	-17	-21	-38	-43	-17	65	65	74	110	165	266	438	691
8	0	-24	30	106	141	230	292	333	375	391	401	425	493	577
9	0	-35	94	134	218	221	236	267	301	339	389	460	579	681

Strain corresponding to yield stress of flexural reinforcement = 1382 MS (micro strain)

Strain corresponding to yield stress of web reinforcement = 1118 MS